

The Analysis of Brn3a and Thy1-CFP as Potential Markers of Retinal
Ganglion Cells after Optic Nerve Injury in Mice

by

Julie M. Levesque

Submitted in partial fulfilment of the requirements
for the degree of Master of Science

at

Dalhousie University
Halifax, Nova Scotia
May 2013

DALHOUSIE UNIVERSITY

DEPARTMENT OF PHYSIOLOGY & BIOPHYSICS WITH NEUROSCIENCE

The undersigned hereby certify that they have read and recommend to the Faculty of Graduate Studies for acceptance a thesis entitled “THE ANALYSIS OF BRN3A AND THY1-CFP AS POTENTIAL MARKERS OF RETINAL GANGLION CELLS AFTER OPTIC NERVE INJURY IN MICE” by Julie M. Levesque in partial fulfilment of the requirements for the degree of Master of Science.

Dated: May 28, 2013

Supervisor: _____
Readers: _____

DALHOUSIE UNIVERSITY

DATE: May 28, 2013

AUTHOR: Julie M. Levesque

TITLE: The Analysis of Brn3a and Thy1-CFP as Potential Markers of Retinal Ganglion Cells after Optic Nerve Injury in Mice

DEPARTMENT OR SCHOOL: Department of Physiology & Biophysics with Neuroscience

DEGREE: MSc CONVOCATION: October YEAR: 2013

Permission is herewith granted to Dalhousie University to circulate and to have copied for non-commercial purposes, at its discretion, the above title upon the request of individuals or institutions. I understand that my thesis will be electronically available to the public.

The author reserves other publication rights, and neither the thesis nor extensive extracts from it may be printed or otherwise reproduced without the author's written permission.

The author attests that permission has been obtained for the use of any copyrighted material appearing in the thesis (other than the brief excerpts requiring only proper acknowledgement in scholarly writing), and that all such use is clearly acknowledged.

Signature of Author

Dedication

*I would like to dedicate this thesis to my parents
who's love, support and guidance have been instrumental
in achieving this degree.*

TABLE OF CONTENTS

LIST OF FIGURES	ix
LIST OF TABLES	xi
ABSTRACT	xii
LIST OF ABBREVIATIONS USED	xiii
ACKNOWLEDGMENTS	xvi
CHAPTER 1: INTRODUCTION	1
1.1 Rationale	1
1.2 Gross anatomy of the mouse visual system	2
1.3 The retina	4
1.4 Current methods of labeling retinal ganglion cells	6
1.4.1 Retrograde labeling	7
1.4.1.1 Fluoro-Gold (FG)	7
1.4.1.2 1,1'-dioctadecyl-3,3,3',3'-tetramethylindocarbocyanine (DiI)	8
1.4.1.3 Rhodamine-B-isothiocyanate (RITC)	9
1.4.2 Immunohistochemistry	9
1.4.2.1 Gamma-synuclein (γ -synuclein)	11
1.4.2.2 RNA binding protein with multiple splicing (RBPMS)	12
1.4.2.3 Thy1	13
1.4.2.4 Brain-specific homeobox/POU domain protein 3A (Brn3a)	14
1.4.3 Thy1 Transgenic mice	17
1.4.3.1 Thy1-CFP transgenic mice	18

1.4.3.2 Thy1-YFP mice	19
1.5 Models of ON injury	19
1.6 Mechanisms of RGC death	20
1.6.1 Excitotoxicity	21
1.6.2 Neurotrophic factors	21
1.7 Research objectives and experimental design	22
1.8 Hypotheses	25
CHAPTER 2: MATERIALS AND METHODS	28
2.1 Experimental design	28
2.2 Animal care	33
2.3 Thy1-CFP genotyping	34
2.4 Surgical procedures	35
2.4.1 Retrograde labeling of the superior colliculus	35
2.4.2 Experimental models of ON injury	36
2.5 Wholemout preparation	37
2.5.1 Wholemout tissue preparation	37
2.5.2 Brn3a immunohistochemistry	38
2.5.3 Thy1-CFP transgenic mice	39
2.6 Cross sectional analysis	39
2.6.1 Cross section tissue preparation	39
2.6.2 Choline acetyltransferase (ChAT) immunohistochemistry	39
2.7 Image acquisition	40
2.7.1 Wholemout image acquisition	40

2.7.2 Cross sectional image acquisition	42
2.8 Image analysis	43
2.9 Western blotting	44
2.9.1 Protein extraction	44
2.9.2 Western blotting	44
2.9.3 Quantitation	46
2.10 Statistical analysis	46
CHAPTER 3: RESULTS	48
3.1 Characterization of RITC as a retrograde tracer	50
3.2 Brn3a as a potential RGC cell density marker after ONC and ONT	55
3.3 Brn3a+/RITC+ cell densities after ONC and ONT	60
3.4 Thy1-CFP expression after ONC and ONT	68
3.5 Thy1-CFP+/RITC+ cells in control and ON injured mice	74
CHAPTER 4: DISCUSSION	83
4.1 RITC as a neuronal tracer of RGCs	85
4.1.1 - RITC labeling in uninjured control mice	85
4.1.2 - RITC labeling after ON injury	87
4.2 Brn3a labeling of cells in the GCL	89
4.2.1 Brn3a+ cell density in control retinas	89
4.2.2 Brn3a+ cell density in ON injured mice	90
4.3 Thy1-CFP expression in cells of the GCL	95
4.3.1 Thy1-CFP+ cell density in control retinas	95
4.3.2 Thy1-CFP+ cell density in ON injured retinas	97

4.4 Limitations	100
4.4.1 Cell counting	100
4.4.2 ON injury	101
4.4.3 Retrograde labeling	101
4.4.4 Animal variance	102
4.5 Future work	102
4.6 Significance	103
4.7 Conclusion	104
BIBLIOGRAPHY	106
APPENDIX A : SUPPLEMENTARY FIGURE	122
APPENDIX B : COPYRIGHT PERMISSIONS	124

LIST OF FIGURES

Figure 1.1	Cross section of the mouse eye and visual system	3
Figure 1.2	Retinal anatomy	5
Figure 1.3	Indirect immunohistochemistry	10
Figure 2.1	Experimental design of Brn3a ⁺ GCL cell density analysis	30
Figure 2.2	Experimental design for the investigation of Brn3a retinal expression in control and ONT mice	31
Figure 2.3	Experimental design of Thy1-CFP ⁺ GCL cell density analysis	32
Figure 2.4	Experimental design for the detection of Thy1-CFP expressing cholinergic amacrine cells in Thy1-CFP transgenic mouse retinas	33
Figure 2.5	Wholemout image acquisition	42
Figure 3.1	Wholemout images of RITC labeling in control mice	51
Figure 3.2	RITC ⁺ cell density in control mice	52
Figure 3.3	Wholemout images of RITC ⁺ labeling after ON injury	53
Figure 3.4	RITC ⁺ cell density after ON injury	54
Figure 3.5	Wholemout images of Brn3a ⁺ cells in control and ON injured retinas	56
Figure 3.6	Brn3a ⁺ cell density after ON injury	59
Figure 3.7	Brn3a protein expression after ONT	60
Figure 3.8	Brn3a ⁺ /RITC ⁺ retinal wholemount images of control and ONC C57BL/6 mice	63
Figure 3.9	Brn3a ⁺ /RITC ⁺ retinal wholemount images of control and ONT C57BL/6 mice	64
Figure 3.10	Brn3a ⁺ /RITC ⁺ cell density after ON injury	66

Figure 3.11	Venn diagrams of RGCs expressing Brn3a	67
Figure 3.12	Venn diagrams of Brn3a ⁺ confirmed RGCs	68
Figure 3.13	Wholemout images of Thy1-CFP ⁺ in control and ON injured retinas	71
Figure 3.14	Thy1-CFP ⁺ cell density after ON injury in Thy1-CFP transgenic mice	73
Figure 3.15	Thy1-CFP ⁺ /RITC ⁺ retinal wholemount images of control and ONC Thy1-CFP transgenic mice	77
Figure 3.16	Thy1-CFP ⁺ /RITC ⁺ retinal wholemount images of control and ONT Thy1-CFP transgenic mice	78
Figure 3.17	Thy1-CFP ⁺ /RITC ⁺ cell density after ON injury in Thy1-CFP transgenic mice	79
Figure 3.18	Venn diagrams of Thy1-CFP expressing RGCs	80
Figure 3.19	Venn diagrams of Thy1-CFP confirmed RGCs	81
Figure 3.20	Cross sections of Thy1-CFP mouse retinas labeled with ChAT	82
Figure A.1	Cytoplasmic expression of Thy1-CFP in Thy1-CFP transgenic wholemount retina	123

LIST OF TABLES

Table 1.1:	Percentage of nuclei in the GCL of the mouse retina that are immunopositive for Brn3a, Brn3b, Brn3c and various double labeling combinations	15
Table 1.2:	Population of Brn3a immunopositive nuclei and FG positive cells of the uninjured and injured retinas of the rat	16
Table 3.1:	RITC ⁺ and Brn3a ⁺ cell densities of control, ONC and ONT C57BL/6 mouse retinas	57
Table 3.2:	Brn3a ⁺ /RITC ⁺ cell densities of control, ONC and ONT C57BL/6 mouse retinas	65
Table 3.3:	RITC ⁺ and Thy1-CFP ⁺ cell densities of control, ONC and ONT Thy1-CFP transgenic mouse retinas	72
Table 3.4:	Thy1-CFP ⁺ /RITC ⁺ cell densities of control, ONC and ONT Thy1-CFP transgenic mouse retinas	76

ABSTRACT

Purpose: Retinal ganglion cell (RGC) loss is a measure of the progression of many visual disorders. It is important to identify RGCs with good specificity, so RGC numbers can be reliably analyzed. The purpose of this study was to analyze the effectiveness of two current RGC markers: Brn3a immunohistochemistry and the expression of Thy1-CFP in the Thy1-CFP transgenic mouse.

Methods: Rhodamine- β -isothiocyanate (RITC) retrograde labeling, immunohistochemistry, wholemount retinal imaging, western blot, cross sectional analysis and cell densities in uninjured control animals and 3, 5, 7 and 14 days post-optic nerve crush (ONC) or transection (ONT) were tabulated.

Results: Brn3a positive (Brn3a⁺) cell density was significantly less than RITC positive (RITC⁺) cell density in control mice. After ON injury, Brn3a⁺ cell density did not decrease at the same rate as RITC⁺ cell density. The density of RGCs that express Brn3a was significantly less than the individual Brn3a⁺ and RITC⁺ cell density at all experimental time points. Thy1-CFP positive (Thy1-CFP⁺) cell density was significantly less than RITC⁺ in control mice and significantly more than RITC⁺ cell density 14 days after ON injury. Thy1-CFP co-localized with ChAT positive (ChAT⁺) cells 7 days after ONT.

Conclusion: Brn3a and Thy1-CFP are not reliable markers of RGCs. Retrograde labeling remains one of the most reliable methods of labeling RGCs in mice.

LIST OF ABBREVIATIONS USED

γ-synuclein	Gamma synuclein
ARVO	Association for Research in Vision and Ophthalmology
BDNF	Brain derived neurotrophic factor
Brn3a	Brain-specific homeobox/POU domain protein 3A
Brn3a⁺	Brain-specific homeobox/POU domain protein 3A positive cells
Brn3b	Brain-specific homeobox/POU domain protein 3B
Brn3c	Brain-specific homeobox/POU domain protein 3C
BSA	Bovine serum albumin
ChAT	Choline acetyltransferase
cSLO	Confocal scanning laser ophthalmoscope
DiI	1,1'-dioctadecyl-3,3,3',3'-tetramethylindocarbocyanine
DMSO	Dimethyl sulfoxide
FG	Fluoro-Gold
FG⁺	Fluoro-Gold positive cells
GCL	Ganglion cell layer
INL	Inner nuclear layer
IPL	Inner plexiform layer
LGN	Lateral geniculate nucleus
LSD	Least significant difference
MANOVA	Multivariate analysis of variance
NDS	Normal donkey serum
NFL	Nerve fibre layer

NGF	Nerve growth factor
NMDA	N-Methyl-D-aspartic acid
OCh	Optic chiasm
OHSt	Hydroxystilbamidine methanesulfonate
OHSt⁺	Hydroxystilbamidine methanesulfonate positive cells
ON	Optic nerve
ONC	Optic nerve crush
ONT	Optic nerve transection
ONL	Outer nuclear layer
OPL	Outer plexiform layer
OPN	Olivary pretectal nucleus
Otr	Optic nerve tracts
PBS	Phosphate buffered saline
PFA	Paraformaldehyde
PMSF	Phenylmethanesulfonyl fluoride
POU	Derived from three transcription factors: Pituitary specific Pit-1, Octamer transcription factor and Unc-86
PVDF	Polyvinylidene fluoride
RBPMS	RNA binding protein with multiple splicing
RBPMS⁺	RNA binding protein with multiple splicing positive cells
RGC	Retina ganglion cell
RITC	Rhodamine-B-isothiocyanate
RITC⁺	Rhodamine-B-isothiocyanate positive cells
SC	Superior colliculus

SCN	Superchiasmatic nucleus
SDS	Sodium dodecyl sulphate
SDS-PAGE	Sodium dodecyl sulphate-polyacrilimide gel electrophoresis
TBST	Tris-buffered saline with tween-20
Thy1-CFP⁺	Thy1-CFP positive cells
TrkA	Neurotrophic tyrosine kinase receptor type 1
To-Pro⁺	To-Pro positive cells

ACKNOWLEDGMENTS

When I first started my research, I came to the realization that I knew very little about the retina. As I started to read books and articles dealing with the retina, I was sparked and motivated to learn more on retinal ganglion cells. With further investigation into the subject, my enthusiasm bubbled over as I shared some ideas with colleagues and friends.

Although writing this thesis has been an exciting challenge, I get a more enthusiastic charge from speaking to people about what I have learned throughout this experience. I fully understand that it is more difficult for me to spread excitement through the written word than it is to talk about my findings. So as you read this thesis, try to picture a young person bubbling with enthusiasm about her topic, gesturing with her hands and walking around the room, because she is too charged up to stand behind a podium. I have tried to write this thesis in a tone to make it easy and enjoyable to read. It is hoped that I have succeeded my goal.

I would like to thank my supervisor **Dr. Balwantray Chauhan** whose terrific ideas and experience contributed greatly to my learning. I admire your knowledge and hope someday to mentor someone as I have been mentored by you. I would like to thank **Michele Archibald** who fixed my goofy writing errors and gave me just the perfect editing recommendations. **Corey Smith** who gave

me excellent, invaluable advice on my early drafts. Several people have had especially profound influence on my thinking over the course of my research: **Dr. Xu Wang, Andrea Nuschke, Kelly Stevens, Dr. William Baldrige, Dr. Francois Tremblay, Dr. James Fawcett.** The influence of their work and thought on my own thinking has been immeasurable.

CHAPTER 1: INTRODUCTION

1.1 Rationale

In Canada, the direct cost of vision loss to the health care system is 8.6 billion dollars per year, ranking it as the most expensive health condition.¹ Many forms of vision loss and ocular neuropathies are the result of the death of a particular type of retinal neuron: the retinal ganglion cell (RGC). RGC death is a trademark of many retinal and optic nerve diseases.²⁻⁵ The progress of ocular neuropathies is often measured by the loss of RGCs, however the identification of these cells has proven difficult. The proper identification of RGCs with animal disease models has been of great importance in understanding the physiological progression of RGC death.

Mice are used commonly in experimental vision research, likely due to its ease of use, low cost and the availability of transgenic strains which can be customized for specific research objectives.⁶⁻⁹ The proper identification of RGCs with markers may be used to determine disease progression. An ideal marker for the identification of RGCs would be minimally invasive, clearly label all RGCs, would not label other cells, continue to only label RGCs following injury and solely label viable RGCs. This thesis will evaluate current methods of RGC identification in both healthy mouse retinas and those damaged by optic nerve crush (ONC) and optic nerve transection (ONT).

1.2 Gross anatomy of the mouse visual system

The first tissue which light must cross when entering the mouse visual system is the cornea (Figure 1.1 A). The cornea is a transparent avascular collagenous tissue which refracts approximately 2/3 of light into the lens. The lens is responsible for the remainder of light refraction and focuses it on the retina. The pupil limits the quantity of light entering the eye by pupillary light reflex. The retina is a thin sheet of neural tissue that transduces light into an electrochemical signal, which is then transmitted to the brain via the optic nerve (ON).^{10, 11}

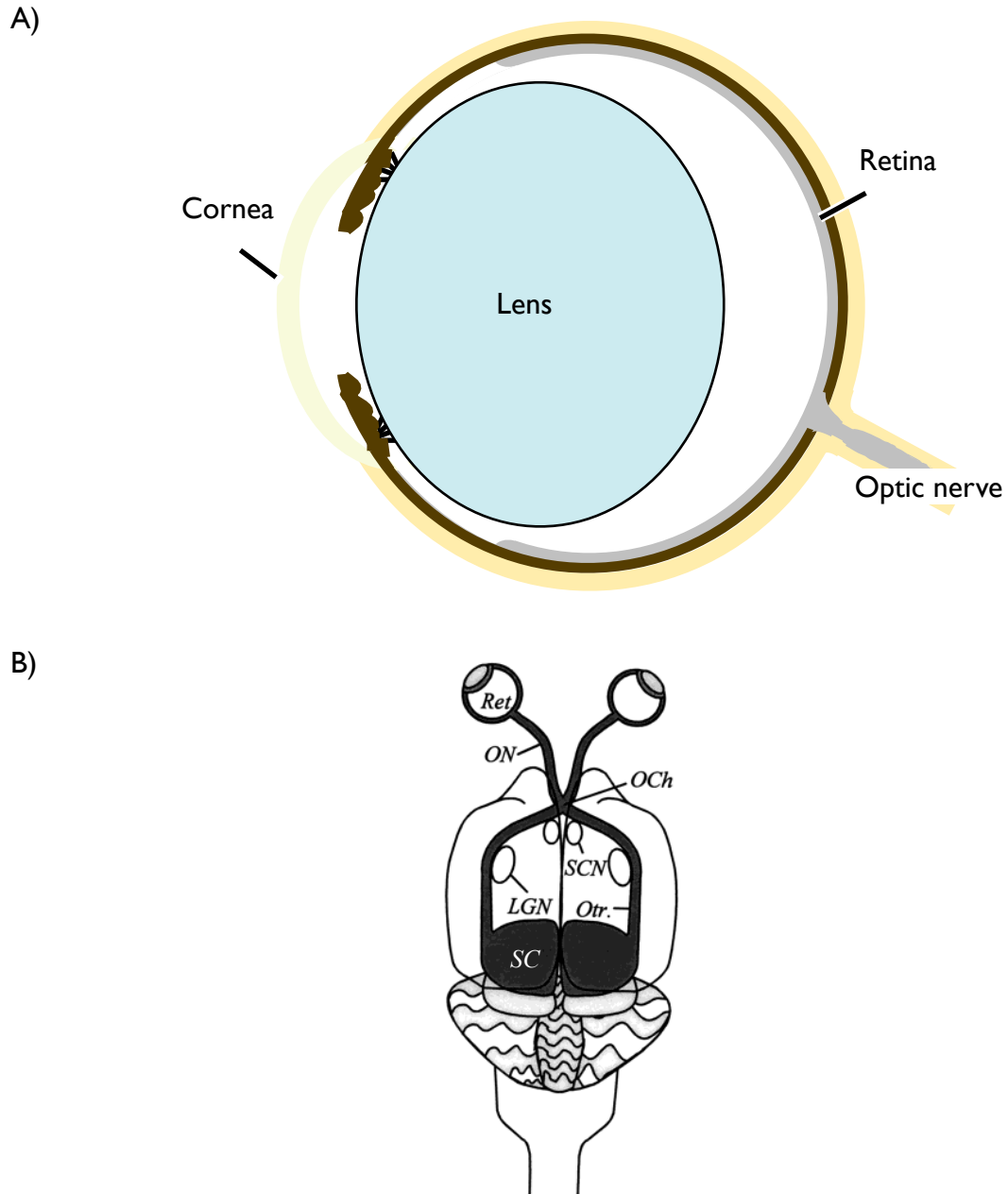


Figure 1.1 - Cross section of the mouse eye and visual system

A) Cross section of the mouse eye. Light passes through the cornea and lens where it is refracted onto the retina. B) An electrochemical signal from the retina (Ret) is transmitted through the optic nerve (ON) crossing over at the optic chiasm (OCh) where the ON now becomes ON tracts (Otr). Most axons project to the superior colliculus (SC), but some project to the lateral geniculate nucleus (LGN) and superchiasmatic nucleus (SCN). Panel B from Bodueutsh N, Thanos S. (2000) published in GLIA with approval from John Wiley and Sons.

The long axons of RGCs, extending from their cell bodies in the ganglion cell layer (GCL) course along the retina, superficially forming the innermost retinal layer, the nerve fiber layer (NFL), and aggregate to form part of the ON. The ON courses from the eye towards the brain where most axons cross over at the optic chiasm to the contralateral side (Figure 1.1 B).^{11, 12} Post-chiasm, the ONs become optic tracts, where approximately 96% of RGC axons project to the superior colliculus (SC),¹³ while the remainder project to the superchiasmatic nucleus (SCN) of the hypothalamus,^{14, 15} the lateral geniculate nucleus (LGN)¹⁴, olivary pretectal nucleus (OPN)¹⁵ or intergeniculate leaflet of the ventral thalamus.^{14, 15}

1.3 The retina

The retina is a neural network of cells responsible for the detection and transmission of light signals to the brain. Light detection begins at the photoreceptor outer segments where photons are transduced to an electrochemical signal. Photoreceptors are divided into two subtypes: rods and cones. Rods detect stimuli of low intensities while cones are used at a higher level of adaptation where it subserves color vision. Photoreceptors synapse with bipolar cells, which relay information vertically and form post-synaptic connections onto RGCs. RGCs process information received from bipolar cells.

Horizontal and amacrine cells transmit information laterally within the retina forming lateral inhibition to create receptive fields.^{8, 11}

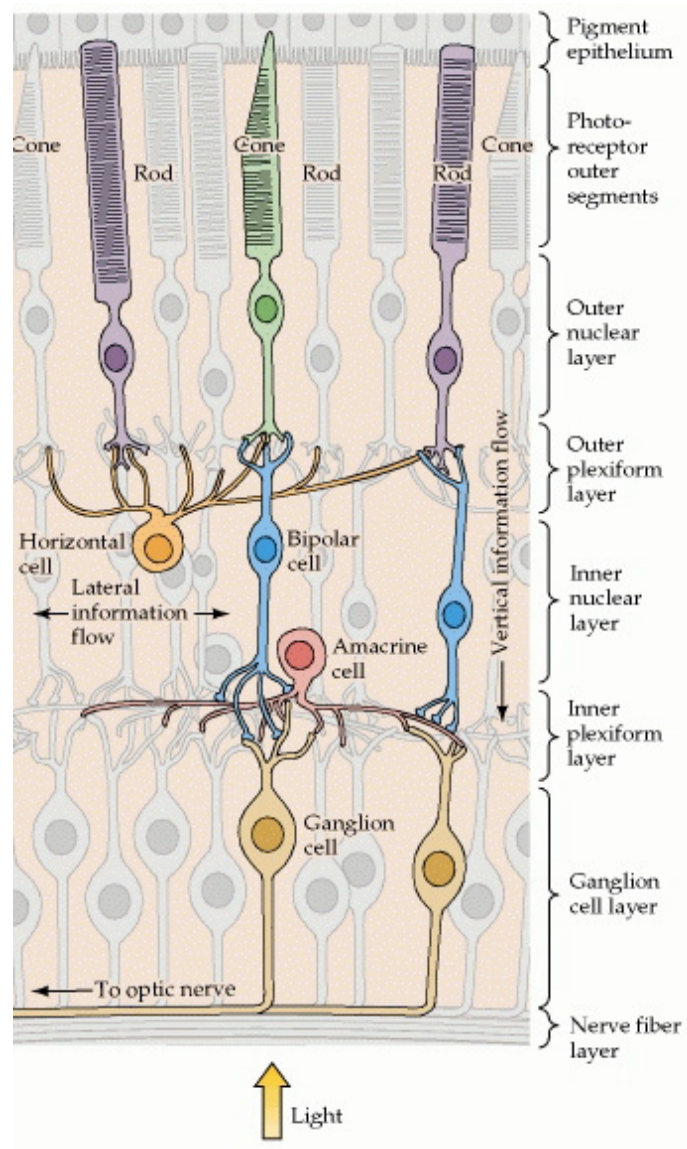


Figure 1.2 - Retinal anatomy

Light is detected by the photoreceptors in the outer retina. Photoreceptors synapse onto horizontal and bipolar cells, and then synapse onto amacrine cells and RGC. Horizontal cells transmit information laterally shaping receptive fields. RGC axons course along the surface of the retina, forming the NFL. Figure from Neuroscience. 2nd edition. Purves *et al.* with approval from Sinauer Associate, Inc.

The aforementioned cell types are organized into nuclear and plexiform layers (Figure 1.2). One of the outermost layers of the retina, the outer nuclear layer (ONL), is comprised of photoreceptor cell bodies. Photoreceptors form post-synaptic connections with horizontal cells and bipolar cells in the outer plexiform layer (OPL). Horizontal, bipolar and amacrine neuronal cell bodies make up the inner nuclear layer (INL), also the location of the cell bodies of Müller cell glia. Horizontal cells are found in the most distal part of the INL and form pre-synaptic connections with photoreceptors while amacrine cells are found in the proximal area and form post-synaptic connections with RGCs in the inner plexiform layer (IPL). There are nearly as many amacrine cells as RGCs cell bodies that populate the GCL, making the identification of RGCs a difficult task.^{8, 10, 11} In an uninjured mouse, there are approximately 40,000 RGCs in the GCL and the RGC cell density is highest at the ON head and decreases with eccentricity.^{8, 11, 16}

1.4 Current methods of labeling retinal ganglion cells

Techniques currently used for labeling RGCs include retrograde labeling, immunohistochemistry and the use of transgenic mice which express a fluorophore under a modified RGC specific promoter, Thy1 (e.g. Thy1-CFP, Thy1-YFP).

1.4.1 Retrograde labeling

Retrograde labeling is a classic technique of labeling RGCs. This technique takes advantage of the RGC axonal projections to the SC by surgically applying a neuronal tracer to the SC, which is retrogradely transported to RGC cell bodies in the retina.¹⁷ Bilateral retrograde labeling of the SC labels approximately 96% of all RGCs in the mouse retina¹³ and 98% of RGCs in the rat retina.¹⁸ The high degree of RGC labeling and specificity is the reason why retrograde labeling from the SC is one of the most reliable methods of labeling RGCs in rodents,¹⁹⁻²¹ however, SC labeling is invasive, since a portion of the cortex must be removed in order to apply the neuronal tracer to the SC, and is time-consuming, since time must be allotted for the transportation of the neuronal tracer to the cytoplasm of RGCs. SC labeling is performed commonly with either Fluoro-Gold (FG), 1,1'-dioctadecyl-3,3',3'-tetramethylindocarbocyanine (DiI) or rhodamine-B-isothiocyanate (RITC).

1.4.1.1 Fluoro-Gold (FG)

The most commonly used fluorescent neuronal tracer for RGC labeling is FG.^{6, 19, 22, 23} Weak bases, like FG, diffuse through the membranes of intracellular vesicles and are passively incorporated by pH-trapping at the axon terminals. Within the vesicle, the pH begins to increase to a more basic state due to the

diffusion of FG. With this shift in pH the vesicle membrane becomes impermeable, thus trapping the dye within the vesicle.^{24, 25} The vesicles can then be transported at speeds of up to 2 cm per day along the cytoskeleton of axons and dendrites.²⁶ FG can also seep through gap junctions, labeling a subset of amacrine cells in the INL within 9-13 weeks after FG labeling,²⁷ making FG unsuitable for long-term studies.²⁵ FG initially has a very strong signal, however this signal fades quickly in both *in vivo* and *ex vivo* applications due to photobleaching.^{24, 28-30}

1.4.1.2 1,1'-dioctadecyl-3,3,3',3'-tetramethylindocarbocyanine (DiI)

DiI is a carbocyanine dye that passively inserts into the cell membranes with its long lipophilic tails. During endocytosis, the DiI-labeled membrane enters the cell and becomes incorporated into vesicle membranes.²⁵ DiI remains in vesicular membranes for long periods of time and does not fade, making it a good candidate for long-term studies. However, vesicularized DiI also results in a granular appearance which can make identifying cells difficult. In fixed tissue, DiI diffuses laterally into membranes of surrounding cells, thus staining cell morphology in a non-RGC specific manner.³¹ This passive diffusion can vary with speeds of a few millimeters to a few centimeters per day, depending on temperature.²⁵

1.4.1.3 Rhodamine-B-isothiocyanate (RITC)

RITC is a non-toxic, hydrophilic neuronal tracer.^{25, 32} When compared to carbocyanines, RITC provides more uniform labeling of RGCs across the retina.^{32, 33} RITC is vesicularized and appears more granular than carbocyanines since it does not diffuse laterally once inside the vesicle. The granular appearance of RITC increases the need for a nuclear counterstain to aid in the identification of cells. RITC is taken up by axon terminals and is actively transported at approximately 5 mm per day.³² In rats, the number of labeled RGCs identified with RITC is similar at both 5 and 30 days post-SC surgery. This signifies that in the rat, RITC labeled all RGCs that project to the SC 5 days after SC labeling surgery and did not fade or leave RGCs up to 30 days post-surgery making it a reliable marker of RGCs for up to 30 days post-surgery.²⁰

1.4.2 Immunohistochemistry

Immunohistochemistry is a common technique used to identify a specific protein (antigen) in a tissue (Fig. 1.3). Primary antibodies specific for antigens of interest are raised in animals and purified into an antibody serum. In indirect immunohistochemistry, a secondary antibody is used. The secondary antibody, conjugated to a fluorophore or molecular probe, targets the animal host antigen

of the primary antibody. First, the tissue is incubated in the primary antibody serum resulting in antigen-specific binding of the primary antibody. To increase specificity by decreasing background noise, the secondary antibody, conjugated

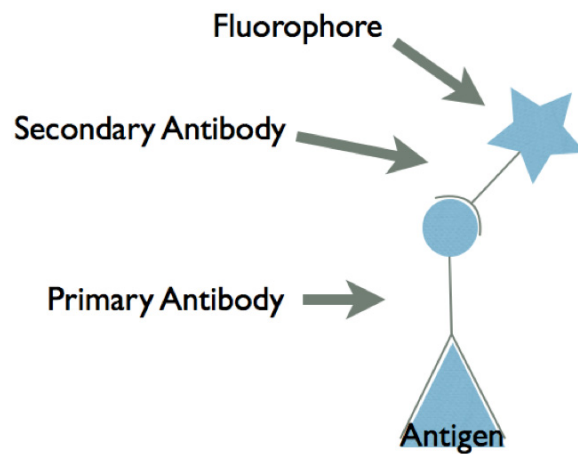


Figure 1.3 - Indirect immunohistochemistry

The immunohistochemical fluorescence complex is formed by detection of an antigen with a primary antibody. To increase specificity, a secondary antibody conjugated to a fluorophore is used to detect the primary antibody thus forming an antigen-specific fluorescence complex which can be detected under microscopy.

to a fluorophore or molecular probe, is incubated with the tissue. Together the primary and secondary antibodies form a fluorescent complex specific to the

antigen of interest. This complex can be detected under microscopy depicting localized protein expression in tissue and cells.

Protein targeting in the retina has the potential to label RGCs without the need to perform invasive surgeries, thus simplifying the identification of RGCs *ex vivo*. Proteins currently being used as candidates for RGC specific immunohistochemistry labeling include gamma-synuclein (γ -synuclein), RNA binding protein with multiple splicing (RBPMS), Thy1 and brain-specific homeobox/POU domain protein 3A (Brn3a).

1.4.2.1 Gamma-synuclein (γ -synuclein)

Synucleins are small soluble proteins expressed in neural³⁴ and some cancerous tissue.³⁵ There are 3 different types of synucleins: alpha (α), beta (β) and gamma (γ).³⁶ γ -synuclein is expressed in primary sensory neurons, sympathetic neurons, motor neurons,³⁷ the brain,³⁸ ovarian tumors,³⁵ olfactory tissue³⁹ and the retina.³⁴ The function of γ -synuclein is not well known, however it is hypothesized that γ -synuclein may have a chaperone-like function.⁴⁰ In 2008 Surgucheva *et al.* demonstrated in human retinas that γ -synuclein was expressed uniquely in Brn3a immuno-positive cells, another RGC marker.⁴¹ During mouse development, γ -synuclein is expressed specifically in RGCs.^{34, 42} Soto *et al.* have analyzed γ -synuclein as an RGC marker utilizing *in situ* hybridization with

uninjured DBA/2J mice, a transgenic mouse model of glaucoma. Their results indicate that $47\pm 3\%$ of the cells in the GCL were RGCs identified by the neuronal tracer FG that expressed γ -synuclein while $1.0\pm 0.5\%$ were γ -synuclein positive only.⁶ This means that only a small portion of γ -synuclein expressing cells are not confirmed RGCs.

1.4.2.2 RNA binding protein with multiple splicing (RBPMS)

RBPMS is part of the RNA recognition motif RNA binding protein family. This family is involved in the post-transcriptional regulation of mRNA: pre-mRNA processing, transport, localization, translational regulation and mRNA stability.²³ The precise function of RBPMS is still unknown. In an *in situ* hybridization study, Kwong *et al.* identified 99.5% of FG positive (FG⁺) cells as RBPMS positive (RBPMS⁺) and 97% of RBPMS⁺ cells as FG⁺ in uninjured Wistar rats. Since most RBPMS⁺ cells are also FG⁺ cells, this indicates that most RGCs that project to the SC of the rat express RBPMS. RBPMS could be identified mostly in the nucleus, but was also present in the cytoplasm of RBPMS positive cells. Kwong *et al.* also compared RBPMS to other RGC markers - β -tubulin, neurofilament-heavy and Thy-1 - and identified 97%, 95% and 96% overlap, respectively.²³ A further study by Kwong *et al.* using Wistar rats and immunohistochemistry of RBPMS demonstrated ~96% of RBPMS cells were also

FG⁺ 4 weeks after ONC,⁴³ indicating that RBPMS continues to label RGCs after ON injury.

1.4.2.3 *Thy1*

Thy1 is a surface immunoglobulin,⁴⁴ that can be found in neurons,⁴⁵⁻⁴⁷ astrocytes⁴⁸ and fibroblasts.⁴⁹ In an *in situ* hybridization analysis of *Thy1* mRNA expression in mice after an ON injury, *Thy1* mRNA expression was not affected until 7 days after injury at which point only 20% of cells that expressed *Thy1* mRNA remained and by 14 days post-injury no cells expressed *Thy1* mRNA. These results did not follow the same trend as the nuclear stained DAPI cells, which were still present 21 days after ONC. Therefore it was concluded that *Thy1* mRNA expressing cells stop expressing *Thy1* mRNA before RGC cell death, suggesting that *Thy1* may be an early indicator of RGC stress.⁵⁰ Previously, researchers believed *Thy1* was unique to RGCs,^{49, 51, 52} however *Thy1* expression has been identified in astrocytes of rat ON culture⁴⁸, in Müller cell endfeet and other cells of the INL presumably amacrine or bipolar cells which are also present in the GCL and could be unintentionally identified when using *Thy1* as an RGC marker.^{49, 53}

1.4.2.4 Brain-specific homeobox/POU domain protein 3A (*Brn3a*)

The POU (derived from three transcription factors: Pituitary specific Pit-1, Octamer transcription factor and Unc-86) domain of transcription factors is composed of three nearly identical members *Brn3a*, brain-specific homeobox/POU domain protein 3b (*Brn3b*) and brain-specific homeobox/POU domain protein 3c (*Brn3c*).⁵⁴ In the mouse, *Brn3a*, *Brn3b* and *Brn3c* are expressed in 35%, 36% and 15% of cells, respectively, in the GCL layer (Table 1.1). Double labeling of *Brn3a* and *Brn3b* labels 37% of cells in the GCL. Since double labeling of *Brn3a* and *Brn3b* is very similar to their individual labeling percentages of 35% and 36%, it is thought that most cells that express *Brn3a* also express *Brn3b*. Double labeling of *Brn3c* with *Brn3a* labeled 36% of the cells in the GCL, since the individual labeling with only *Brn3a* resulted in 35% of the labeling of cells within the GCL, it was concluded that most cells that express *Brn3a* also express *Brn3c*. Double labeling of *Brn3c* with *Brn3b* labeled 36% of the cells in the GCL. Since the individual labeling of *Brn3b* is 36% of the cells in the GCL, it was concluded that cells that express *Brn3b* also express *Brn3c*. Therefore, *Brn3c* labels a small subset of *Brn3a* and *Brn3b* immunopositive cells.⁵⁴

While *Brn3a* and *Brn3b* are, for the most part, present in the same cells, it is *Brn3a* that has been primarily used as an RGC marker for retinal research. *Brn3a* plays an important role in dendritic stratification and determining the

Table 1.1 - Percentage of nuclei in the GCL of the mouse retina that are immunopositive for Brn3a, Brn3b, Brn3c and various double labeling combinations

Experiment 1 n=700-900

Anti-Brn3a	36%
Anti-Brn3b	35%
Anti-Brn3a and anti-Brn3b	37%

Experiment 2 n=700-800

Anti-Brn3a	35%
Anti-Brn3b	36%
Anti-Brn3c	15%
Anti-Brn3a and Anti-Brn3c	36%
Anti-Brn3b and Anti-Brn3c	36%

Sections were counted stained with DAPI, a nuclear stain, to determine the total amount of nuclei in each section. n, total number of nuclei counted per slide. Attained from Xiang M, Zhou L, Macke JP, Yoshioka T, Hendry SHC, Eddy RL, Shows TB, Nathans J (1995).

ratio of monostратified:bistratified RGC in the retina during the development of mouse RGCs.⁵⁵ Brn3a positive (Brn3a⁺) cells have been shown to project directly to the SC and LGN of mice.⁵⁶ In the uninjured rat, Brn3a⁺ cells were quantified per retina with automated cell counting, revealing ~83 000 Brn3a⁺ RGCs compared to ~80 000 FG⁺ RGCs (Table 1.2). Of these cell counts, 92.2% were FG⁺ and Brn3a⁺, 4.4% were only Brn3a⁺ and 3.4% were only FG⁺.¹⁹ This signifies that in the rat, Brn3a is expressed in most RGCs that project the SC and only a small subset of cells are not confirmed as RGCs. In the rat, Brn3a is expressed in

significantly fewer cells than FG⁺ cells 2, 5 and 14 days after ONT. Similarly, after ONC in the rat, Brn3a expression is found in significantly less cells than FG⁺ cells 5 and 14 days post-injury. These findings indicate that Brn3a protein expression is down regulated prior to RGC death after ONC and ONT in the rat.¹⁹

Table 1.2 - Population of Brn3a immunopositive nuclei and FG positive cells of the uninjured and injured retinas of the rat

Uninjured						
Brn3a ⁺	83 499 ± 4541					
FG ⁺	80 251 ± 2210					
ONC	Control (n=32)	2 days (n=8)	5 days (n=8)	9 days (n=8)	14 days (n=8)	
Brn3a ⁺	85 047 ± 3696	79 013 ± 8435	40 690 ± 6227 [†]	21 869 ± 7578	10 176 ± 2940 [†]	
FG ⁺	82 535 ± 2672	80 101 ± 3477	73 553 ± 3039	36 974 ± 7209	21 117 ± 5824	
ONT	Control (n=32)	2 days (n=8)	5 days (n=8)	9 days (n=8)	14 days (n=8)	
Brn3a ⁺	82 434 ± 4802	65 120 ± 6439 [†]	29 463 ± 5552 [†]	17 335 ± 7068	4778 ± 1332 [†]	
FG ⁺	82 078 ± 3283	80 899 ± 4406	68 943 ± 8370	25 299 ± 3989	10 598 ± 2785	

FG⁺RGCs were quantified using an automated system for the uninjured, control right eyes, at 2 days and 5 days post ONT or post ONC. Retinas processed at 9 and 14 days post-ONC and ONT labeled with FG were manually counted. Brn3a⁺RGCs were counted using an automated system for all time points. † Statistically significant when compared to the number of FG⁺RGCs at the corresponding time point. Attained from Nadal-Nicolás FM, Jiménez-López M, Sobrado-Calvo P, Nieto-López, Cánovas-Martínez I, Salinas-Navarro M, Vidal-Sanz M, Agudo M (2009).

A study by Galindo-Romero *et al.* compared the individual Brn3a⁺ cell density to the cell density of those labeled by hydroxystilbamidine methanesulfonate (OHSt), the active portion of FG, in mice following ONT. In the uninjured mouse retina, ~2500 Brn3a⁺ cells/mm² and ~2900 OHSt positive (OHSt⁺) cells/mm² were labeled. Five days after ONT, densities decreased to ~1100 Brn3a⁺ cells/mm² and ~1600 OHSt⁺ cells/mm². By day 21, only 300 Brn3a⁺ cells/mm² and ~400 OHSt⁺ cells/mm² remained. Galindo-Romero *et al.* concluded that Brn3a was expressed in a similar number of cells to those labeled with OHSt in the mouse retina.⁵⁷ Although the quantification of Brn3a⁺ cells in the GCL is known, co-localization of Brn3a with a retrograde marker after injury remains uncharacterized. Therefore, the RGC cell specificity of Brn3a expression in the mouse retina post-injury has yet to be confirmed.

1.4.3 Thy1 Transgenic mice

The use of transgenic mice that express fluorescent proteins in the retina provides the opportunity to view RGC survival in a longitudinal manner, potentially providing a better understanding of how neuronal cells function and how RGCs react to injury.⁵⁸⁻⁶¹

The ability to view RGCs and their dendritic trees with transgenic mice has been possible since 2000.⁶²⁻⁶⁵ One protein that has made the *in vivo*

identification of RGCs possible is Thy1. In 2000 Feng *et al.* used the Thy1 promoter gene to produce 4 variants of transgenic mice, Thy1-GFP, Thy1-YFP, Thy1-CFP and Thy1-RFP.⁶⁵ Of these, Thy1-CFP and Thy1-YFP are the most frequently used in research to date.

1.4.3.1 Thy1-CFP transgenic mice

The Thy1-CFP transgenic mouse is currently utilized for *in vivo* and *ex vivo* studies of retinal damage.^{9, 58, 66, 67} Thy1-CFP positive (Thy1-CFP⁺) cells label approximately 73% of DiI-labeled cells, with only a small percentage (<4%) that solely express Thy1-CFP in uninjured mice.^{9, 66} Wang *et al.* identified 2778 ± 216 CFP⁺ cells/mm² and ~3200 FG⁺ cells/mm² in the uninjured Thy1-CFP transgenic mouse, with approximately 93% of Thy 1-CFP⁺ cells co-localizing with FG.⁷ In a study by Chauhan *et al.*, *in vivo* cell counts demonstrated 86%, 63%, 54%, 31%, 20% and 8% of Thy 1-CFP⁺ cells survived 3, 5, 7, 10, 14 and 21 days, respectively, after ONT.⁵⁸ This pattern of cell loss similarly corresponds to the loss of RGCs labeled with a retrograde tracer in the mouse^{19, 57} and rat^{68, 69} after ONT. In an *in vivo* imaging study using an ONC mouse model, 19%, 11%, 9%, 4%, and 3% of Thy 1-CFP⁺ cells survived 1, 2, 3, 10 and 50 weeks after injury. These findings suggest that Thy1-CFP expression in cells precedes the loss of RGCs after ONC in the mouse.⁵⁹

1.4.3.2 Thy1-YFP mice

Developed by Feng *et al.*, the Thy1-YFP mouse line expresses YFP in less than 1% of RGCs.^{60, 65, 70} This transgenic mouse is predominantly used for studies of RGC morphology and function. Leung *et al.* were able to identify six different types of RGCs that are Thy1-YFP⁺ in the Thy1-YFP transgenic mouse and were able to observe the rate of dendritic field shrinkage after ONC.⁶⁰ In an *in vivo* study by Liu *et al.*, Thy1-YFP mice were bred with transgenic mice that over-expressed brain derived neurotrophic factor (BDNF), an essential neurotrophin of RGCs, and concluded that BDNF accelerates laminar refinement, the synaptic pruning of RGC dendrites.⁶¹

1.5 Models of ON injury

Since the mechanisms of RGC death during disease in humans are still not fully understood, having an accurate animal model to study RGC loss is a continuing goal. Animal models of RGC damage can be divided into two categories: acute and chronic. Acute injuries include: the acute increase of intraocular pressure by cannulating the anterior chamber to a raised saline reservoir, thereby causing ischemia and mechanical damage to the retina and ON;⁷¹ and surgical methods to damage the ON, by either transecting⁵⁸ or crushing the nerve.⁶⁰ Chronic injuries include: the surgical implantation of an

osmotic minipump releasing low doses of endothelin-1 directly onto the ON, causing ischemic damage;⁷² the injection of magnetic microbeads into the anterior chamber;⁷³ laser damage to the trabecular meshwork;⁷⁴ and an injection of hypertonic saline into the episcleral veins,⁷⁵ the last three of which interfere with the outflow of aqueous humor from the eye, resulting in elevated intraocular pressure.

Damage of the ON by ONC and ONT causes RGC loss.⁷⁶ These techniques are relatively consistent and used by many in the ocular research field. In the ONC injury model, the ON is physically crushed by mechanically applied pressure to the ON. In the uninjured mouse, approximately 44% of RGCs survive 1 month after ONC.⁷⁷ In a complete ONT, the nerve is cut leaving the dura and adjacent vasculature intact. In the mouse, all RGCs survive approximately 2 days, after which RGC density significantly declines, leaving less than 20% cell survival by 14 days post-ONT.⁵⁷

1.6 Mechanisms of RGC death

The two main mechanisms of RGC death after injury are excitotoxic and neurotrophic. The increase in release of excitotoxic amino acids into the extracellular matrix is associated with the excitotoxic theory while the loss of neurotrophic factors is associated with the neurotrophic theory.⁷⁸

1.6.1 Excitotoxicity

Excitotoxicity due to an overstimulation of the ionotropic glutamate receptors triggered by physiological responses caused by an injury can result in RGC cell death.⁷⁹ Dreyer *et al.* have found elevated glutamate levels in the vitreous of glaucomatous patients.⁸⁰ The source of the excitotoxicity is thought to be through the N-Methyl-D-aspartic acid (NMDA) receptor, a glutamate receptor known for its function in synaptic plasticity.⁸¹⁻⁸³ The activation of the NMDA receptor results in an influx of calcium ions, which triggers a cascade leading to apoptosis.⁸²

1.6.2 Neurotrophic factors

Neurons are dependent on many peptide factors: growth factors, cytokines, and neurotrophic factors.⁷⁹ The most well-known neurotrophic factor that neurons require constantly over their cell cycle is BDNF. BDNF is produced at the SC of the mouse and retrogradely transported to the retina by RGCs.⁸⁴ BDNF is first released during development and becomes essential for cell survival in the adult rodent.⁸⁵ The removal of the SC in Wistar rats results in rapid death of RGCs and ONT can result in an ~80% RGC death.⁸⁶ Replacement with endogenous BDNF reduced the amount of cell death and promoted axonal

regeneration.⁸⁷ Some RGCs can express BDNF and this expression has been found to be upregulated by 54% after ONC in Sprague-Dawley rats.⁸⁸

1.7 Research objectives and experimental design

Although retrograde labeling does succeed in labeling ~96% of all RGCs, this method is time consuming and invasive therefore, the objective of this thesis is to analyze the viability of two currently used RGC markers: Brn3a, an immunohistochemical marker, and Thy1-CFP expression in the Thy1-CFP transgenic mouse. An ideal RGC marker would be one that can clearly and reliably label all RGCs in uninjured retinas and continue to do so after ON injury. To achieve this goal, the project was divided into two parts each with specific objectives.

Part I - Brn3a immunohistochemistry

- I. Does Brn3a label the same quantity of cells as RITC in uninjured control retinas?

RITC will be used as a retrograde marker to specifically and reliably label RGCs in uninjured control retinas. Brn3a immunohistochemistry will be performed on control retinas and Brn3a⁺

cell density will be compared to RITC positive (RITC⁺) cell density within the same retina

II. Does Brn3a label the same quantity of cells as RITC after ON injury?

Mice pre-labeled with RITC will undergo either an ONC or ONT surgery. Brn3a⁺ cell density will be compared to RITC⁺ cell density within the same retina at each experimental time point.

III. Is Brn3a expression unique to RGCs in control and ON injured retinas?

Co-localization of Brn3a and RITC will be analyzed to examine the RGC specificity of the Brn3a⁺ cell population. Cells that are labeled by RITC and express Brn3a represent RGCs that express Brn3a. Cells that express Brn3a that are not labeled by RITC could be non-RGC specific expression of Brn3a. Together this will demonstrate if Brn3a is expressed solely in RGCs of uninjured, ONC and ONT mice.

Part II - Thy1-CFP transgenic mice

- I. Does Thy1-CFP label the same quantity of cells as RITC in uninjured control retinas?

RITC will be used as a retrograde marker to specifically and reliably label RGCs in uninjured retinas. Thy1-CFP⁺ cell density will be compared to RITC⁺ cell density in the same retina.

- II. Does Thy1-CFP label the same quantity of cells as RITC after ON injury?

Thy1-CFP transgenic mice pre-labeled with RITC will undergo either an ONC or ONT surgery and the cell density of Thy1-CFP⁺ and RITC⁺ cells will be compared within the same retinas at each experimental time point.

- III. Is Thy1-CFP solely expressed in RGCs?

Co-localization of Thy1-CFP and RITC will demonstrate whether Thy1-CFP is an RGC specific marker. Cells that are identified by the neuronal tracer RITC and express Thy1-CFP represent RGCs that express Thy1-CFP. Cells that solely express Thy1-CFP and are not labeled by RITC could be non-RGC specific expression of Thy1-CFP. This will indicate

whether Thy1-CFP expression in the Thy1-CFP transgenic mouse is solely expressed in RGCs of uninjured, ONC and ONT mice.

Choline acetyltransferase (ChAT) is expressed in cholinergic amacrine cells and used as a marker to detect this subtype of amacrine cell. Cross sections of Thy1-CFP transgenic mouse eyes will be used to demonstrate if Thy1-CFP expressing cells co-localize with ChAT denoting whether Thy1-CFP is expressed in cholinergic amacrine cells.

1.8 Hypotheses

It is hypothesized that:

- I. After ONC or ONT in mice, RITC will label RGCs for a longer period of time than Brn3a immunohistochemistry will detect.

It would be expected that the protein expression of Brn3a would decrease prior to cell death since Brn3a is produced by the cells and protein expression changes in injured cells while RITC is not dependent on the health of the cell. Therefore, we expect RITC to label RGCs for a longer period of time than Brn3a immunohistochemistry will detect.

II. After ONC or ONT in the Thy1-CFP transgenic mouse, RITC will label RGCs for a longer period of time than Thy1-CFP expression in the Thy1-CFP transgenic mouse.

Thy1-CFP is produced within cells and is dependent on the health of the cell in order to be expressed while RITC, once inside the cytoplasm of cells, remains within cells until phagocytosed. Therefore, it is expected that Thy1-CFP expression reduces in RGCs prior to cell death.

III. Thy1-CFP will be expressed in cholinergic amacrine cells after ONT in the Thy1-CFP transgenic mouse retina.

Previous studies have shown expression of Thy1 in cholinergic amacrine cells.⁴⁹ Since Thy1-CFP is regulated under the Thy1 promoter, it is expected that Thy1-CFP is expressed in cholinergic amacrine cells.

IV. Brn3a⁺, Thy1-CFP⁺ and RITC⁺ cell density will decrease at a faster rate in the ONT mouse model than the ONC mouse model.

ONT and ONC are both acute injury models however ONT is the complete severing of the axons near the ON head while ONC is damaging the axons in the same region as ONT but crushes the axons which may not injure all axons. For these reasons, we hypothesize that cell density will decrease at a faster rate after ONT than ONC.

CHAPTER 2: MATERIALS AND METHODS

2.1 Experimental design

The neuronal tracer RITC was surgically applied to the SC of C57BL/6 (n=36) and Thy1-CFP transgenic (n=36; Thy1-CFP-H, C57BL/6 background) mice (Fig. 2.1 and 2.3) to identify ~96% of all RGCs of the retina. Each mouse underwent the surgical application of an ON injury either, ONC or ONT, 7 days after SC labeling surgery. Injured mice were euthanized at 3, 5, 7 or 14 days post-ONC or ONT.

2.1.1 Does Brn3a label the same quantity of cells as RITC in uninjured control retinas? Does Brn3a label the same quantity of cells as RITC after ON injury? Is Brn3a expression unique to RGCs in control and ON injured retinas?

The retinas of RITC labeled C57BL/6 ON injured mice underwent immunohistochemistry for the detection of Brn3a⁺ cells and To-Pro staining, a nuclear counterstain, in order to aid in the identification of all RITC⁺ RGCs. Imaging of retinas under confocal microscopy detected RITC⁺, Brn3a⁺ and To-Pro positive (To-Pro⁺) cells. These images were masked and analyzed by cell counting of all RITC⁺, Brn3a⁺ and Brn3a⁺/RITC⁺ cells. Cell densities were tabulated which allowed us to examine the effectiveness of Brn3a as an RGC marker since RITC is detected in most RGCs. Western blot analysis of Brn3a protein expression in the retina also aided in the evaluation of Brn3a expression and its reaction to injury (Fig 2.2). Protein from control and 3, 5, 7 or 14 days ONT C57BL/6 mouse retinas (n=20) was extracted. Since ONT and ONC cell densities yielded similar results only ONT protein levels were measured. Brn3a expression at all time points were quantitated from western blots demonstrating changes in Brn3a expression.

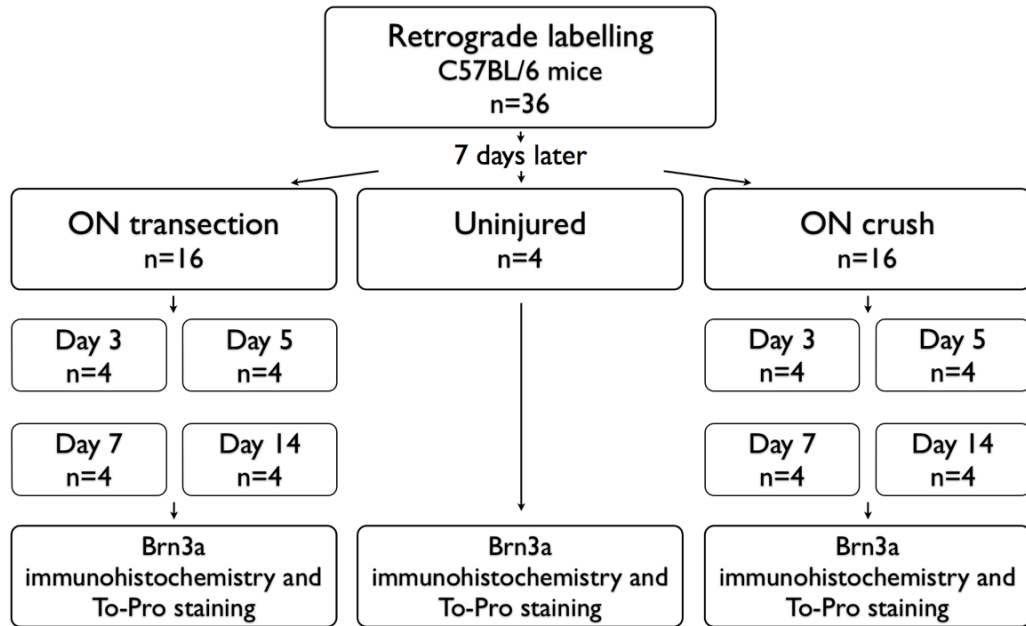


Figure 2.1 - Experimental design of Brn3a⁺ GCL cell density analysis

C57BL/6 mice were first labeled with RITC with SC labeling surgery. Seven days later, RITC labeled mice underwent a second surgery to cause an ON injury resulting in RGC loss. Mice were euthanized at 3, 5, 7 or 14 days after ON injury and Brn3a immunohistochemistry and To-Pro staining was performed on their retinas. Retinas were wholemounted and imaged with a confocal microscope. Acquired images were cell counted and cell densities were tabulated.

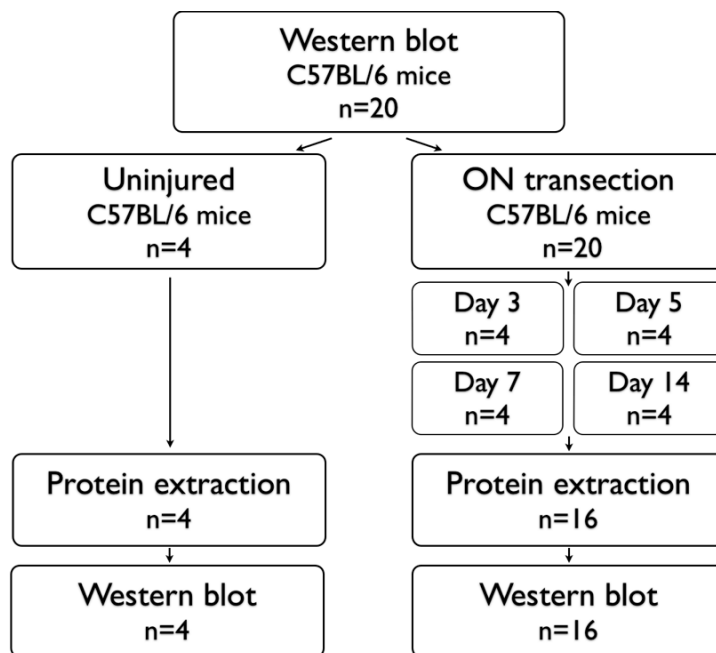


Figure 2.2 - Experimental design for the investigation of Brn3a retinal expression in uninjured and ONT mouse retinas

Protein from uninjured and ONT mouse retinas was extracted. To detect varying Brn3a protein levels during the experimental timeline, western blot analysis of the protein levels was performed.

2.1.2 Does Thy1-CFP label the same quantity of cells as RITC in uninjured control retinas? Does Thy1-CFP label the same quantity of cells as RITC after ON injury? Is Thy1-CFP solely expressed in RGCs?

Thy1-CFP retinas from RITC labeled Thy1-CFP transgenic mice were stained with To-Pro, wholemounted and imaged with confocal microscopy. Thy1-CFP⁺, RITC⁺ and Thy1-CFP⁺/RITC⁺ cells were cell counted from images. Cell densities were tabulated and analyzed to determine the effectiveness of Thy1-CFP as an RGC marker.

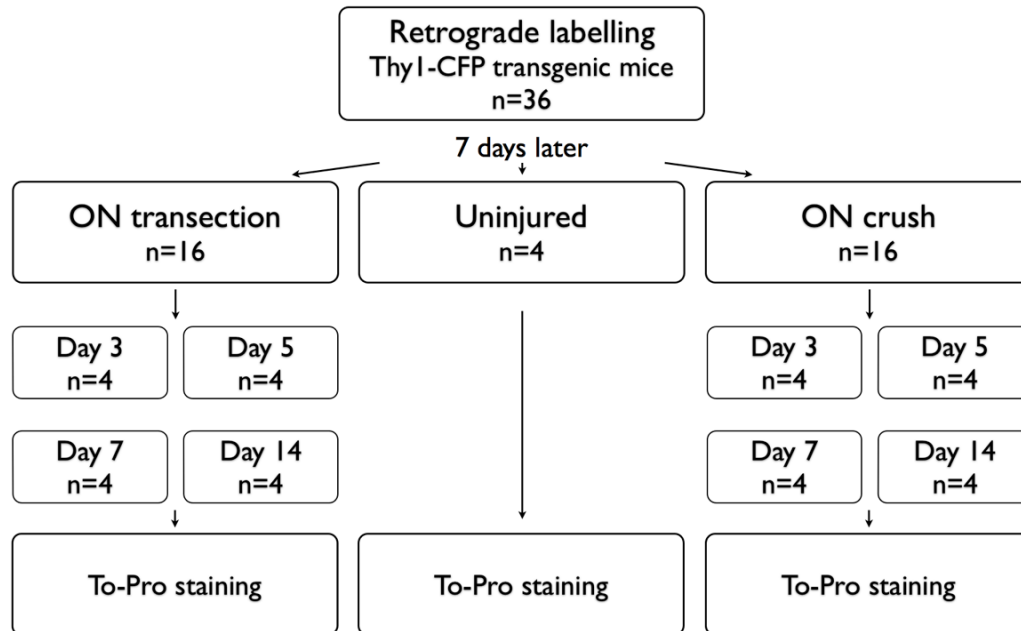


Figure 2.3 - Experimental design of Thy1-CFP⁺ GCL cell density analysis

Thy1-CFP transgenic mouse retinas were labeled with RITC by SC surgery. Seven days after SC labeling surgery, RITC labeled mice underwent either ONC or ONT surgery and were sacrificed at their appropriate experimental time point. Retinas underwent To-Pro staining, were wholemounted and imaged with confocal microscopy. Cell densities were tabulated by cell counting RITC⁺, Thy1-CFP⁺ and Thy1-CFP⁺/RITC⁺ cells in images from wholemounted retinas.

Thy1-CFP transgenic mice (n=4) were divided into an untreated control group and a 7 day post-ONT group (Fig. 2.4). Mice were euthanized at their appropriate time points. Untreated and 7 day post-ONT eyes were sectioned cross sectionally. ChAT immunohistochemistry was performed on Thy1-CFP cross sections to detect if Thy1-CFP is expressed in cholinergic amacrine cells.

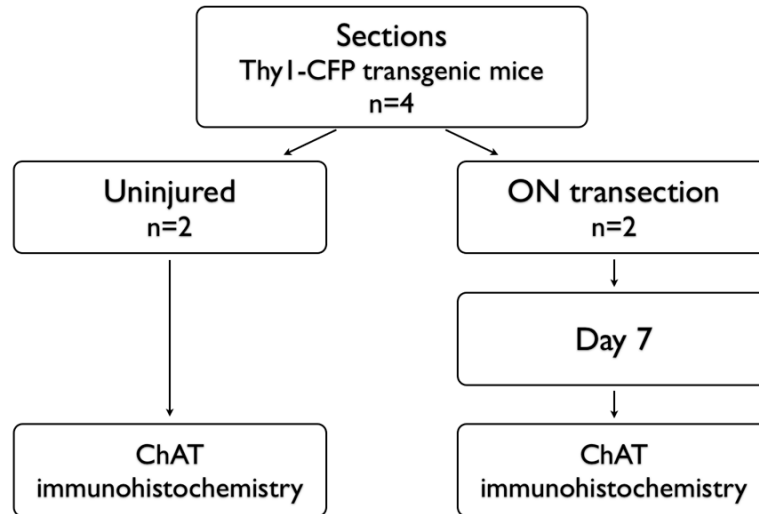


Figure 2.4 - Experimental design for the detection of Thy1-CFP expressing cholinergic amacrine cells in Thy1-CFP transgenic mouse retinas

Cross sections of uninjured (n=2) and 7 day ONT (n=2) Thy1-CFP transgenic mice were detected for ChAT expression by immunohistochemistry. Co-localization of Thy1-CFP and ChAT were detected under confocal microscopy.

2.2 Animal care

All experiments were performed on mice in compliance with the Association for Research in Vision and Ophthalmology (ARVO) Statement for the Use of Animals in Ophthalmic and Vision Research and with ethical approval from the Dalhousie University Committee on Laboratory Animals. Thy1-CFP heterozygous breeders were obtained from The Jackson Laboratory (Bar Harbour, ME, USA) and C57BL/6 18-20 g mice were obtained from Charles River Laboratories International Inc. (Wilmington, MA, USA). Mice were housed in

covered cages, fed standard rodent diet and water *ad libitum* in a 12-hour light-dark cycle environment.

Mice were anesthetized with 2-3 % isofluorane (Baxter International Inc., Alliston, Ontario) at an oxygen flow rate of 1 L / min. Buprenorphine (0.03 mg / kg; Temgesic®, Reckitt Benckiser Health (UK) Ltd., Hertfordshire, UK) was used as an analgesic drug and injected subcutaneously. Mice were euthanized with an intraperitoneal injection of sodium pentobarbital (240 mg / ml; Bimeda - MTC Animal Health Inc., Cambridge, Ontario).

Eyes were collected from mice for the wholemount, cross sectional and western blot analyses.

2.3 Thy1-CFP genotyping

Thy1-CFP transgenic mice have endogenous expression of CFP under a modified Thy1 promoter allowing them to be genotyped by visualizing these purported RGCs *in vivo* with a confocal scanning laser ophthalmoscope (cSLO) with special excitation bandpass (448 nm) and barrier (460 nm - 490 nm) filter sets.

2.4 Surgical procedures

2.4.1 Retrograde labeling of the superior colliculus

Animals were injected with buprenorphine prior to surgery and placed under isoflurane induced anesthesia. The surgical area was shaved, cleaned and sterilized with 10 % povidone-iodine topical solution USP (Purdue Pharma, Perkering, Ontario). Surgical tools were autoclaved prior to each surgery and sterilized with a bead sterilizer between surgeries. When sufficiently anesthetized, a small incision was made in the skin exposing the skull surface at the midbrain. Two small bilateral holes of approximately 1 mm in diameter were drilled into the skull at approximately 0.1 mm from bregma and directly on the edge of lambda, exposing the cortical surface. Fragments of bone and dura were removed and the cortex was suctioned to expose the underlying SC. After clearing excess blood from the surgical area, surgical gelfoam soaked in RITC solution (2.5 % RITC (Lot# MKBG2359V, Sigma-Aldrich Co., St. Louis, MO, USA), 2 % dimethyl sulfoxide (DMSO; Sigma-Aldrich Co.), dH₂O) was placed over the SC. The overlying skin was closed using 5-0 surgical suture with an intermittent stitch. The animal was removed from anesthetic isoflurane and placed in a cage on a regulated heating pad at 37 °C overnight along with a bowl

of mash to facilitate fast rehabilitation. Animals recovered from surgery for 7 days before the next procedure.

2.4.2 Experimental models of ON injury

Animals were injected with buprenorphine prior to surgery and placed under isoflurane anesthesia. The surgical area was prepared as described in 2.4.1. A small suture was made in the superior conjunctiva of the eye. The suture was pulled downwards, thus changing the orientation of the eye and later facilitate the visualization of the ON. An incision along the supraorbital ridge was made where the tissue was dissected and teased away from the supraorbital ridge until the eye was exposed. With the ON visible, the dura was carefully dissected exposing the ON. The ONT surgery was performed by severing the ON approximately 1 mm from the eye with two sharp forceps. ONC was achieved with a pair of self-closing forceps placed around the ON for approximately 3 seconds, 1 mm from the globe. The incision was sutured with a 5-0 surgical suture. The animal was recovered as described in section 2.4.1.

2.5 Wholemout preparation

2.5.1 Wholemout tissue preparation

Eyes were dissected maintaining orientation of the eye (superior, inferior, nasal and temporal) by keeping the pigmented *caruncula lachrymalis* attached to the eye. Eyes were pinned on a silicone based petri dish, the cornea and lens were removed with forceps and spring scissors and the remainder of the eye placed in 4 % paraformaldehyde (PFA; Thermo Fisher Scientific Inc., Rockford IL, USA) in phosphate buffered saline (PBS; Sigma-Aldrich Co.) at room temperature for 1 hour on a rocker. The eye cup was repinned in the silicone dish and a small cut was made with spring scissors between the nasal and superior retina to maintain retinal orientation. Retinas were dissected from the eye cup with two fine tipped forceps and placed in 4 % PFA for an additional 2 hours at room temperature with rocking. Thy1-CFP retinas were stained with To-Pro (Lot #507591, Invitrogen Molecular Probes, Eugene, OR, USA), a nuclear stain, while C57BL/6 retinas underwent Brn3a immunohistochemistry.

2.5.2 Brn3a immunohistochemistry

C57BL/6 retinas were permeabilized in PBS, 0.5 % Triton X-100 (Sigma-Aldrich Co.) by freezing at -80 °C for 15 minutes, and then rinsed in fresh PBS, 0.5 % Triton X-100 at room temperature for 10 minutes. The primary antibody of goat anti-Brn3a (Lot# C1407 and D1612; Santa Cruz Biotechnology Inc., Santa Cruz, CA, USA) was diluted in blocking buffer (PBS, 2 % bovine serum albumin (BSA; Sigma-Aldrich Co.) and 2 % Triton X-100) at a 1:100 dilution ratio and incubated with the retina overnight at 4 °C. After the incubation period was completed, three 20 minute washes in PBS were performed. The retina was incubated in Alexa-488-conjugated AffiniPure Donkey anti-goat IgG (H+L) secondary antibody (Lot# 103176 and 99929, Jackson ImmunoResearch Laboratories, Inc, Baltimore Pike, West Grove, PA, USA) in a 1:200 dilution ratio with blocking buffer for 2 hours at room temperature followed by three 20 minutes PBS washes at room temperature. To-Pro nuclear staining was performed at a 1:1000 dilution with PBS at room temperature for 15 minutes then the retinas were washed with PBS for 10 minutes at room temperature. Retinas were wholemounted in Vectashield mounting medium (Vector Laboratories Inc., Burlingame, CA, USA), covered with a no.0 coverslip and stored at 4 °C until they were imaged.

2.5.3 Thy1-CFP transgenic mice

Thy1-CFP retinas were incubated in a 1:1000 dilution of To-Pro in PBS at room temperature for 15 minutes then washed with PBS for 10 minutes at room temperature. Retinas were wholemounted in Vectashield mounting medium, covered with a no.0 coverslip and stored at 4 °C until they were imaged.

2.6 Cross sectional analysis

2.6.1 Cross section tissue preparation

Thy1-CFP mouse eyes were dissected and placed in 4 % PFA overnight at 4 °C, followed by 30 % sucrose (Thermo Fisher Scientific Inc.) for an additional night at 4 °C. Eyes were embedded and frozen in Tissue-Tek OCT compound (Sakura Finetek USA, Inc., Torrance, CA, USA). With a cryostat (Leica CM1850), 20 µm sections were taken (cross sectionally through the eye) and placed on superfrost slides to dry overnight.

2.6.2 Choline acetyltransferase (ChAT) immunohistochemistry

Sections were washed at room temperature with PBS for 3 minutes three times and incubated in permeabilization solution (0.4 % Triton X-100, PBS) for 30 minutes at room temperature. Whole eye sections were rinsed with PBS three

times for 3 minutes each at room temperature and incubated in blocking buffer (0.1 % Triton X-100, 3 % Normal donkey serum (NDS), PBS) for 1 hour at room temperature. Slides with retinal sections were incubated overnight at room temperature in primary antibody (goat anti-ChAT; Lot# LV1522609, Millipore, Billerica, MA, USA) at 1:100 dilution in blocking buffer. The omission of primary antibody served as a negative control for immunohistochemistry of sections. Eye sections were washed five times for 5 minutes each in PBS at room temperature and then incubated in secondary antibody (Alexa-488-conjugated AffiniPure Donkey anti-goat IgG (H+L); Lot# 103176 and 99929, Jackson ImmunoResearch Laboratories, Inc) in a 1:200 dilution with blocking buffer for 2 hours at room temperature. Sections were washed for 5 minutes five times with PBS at room temperature, mounted with Vectashield and a no.0 coverslip.

2.7 Image acquisition

2.7.1 Wholemout image acquisition

Each wholemounted retina was labeled with To-Pro, RITC and either Brn3a-Alexa 488 fluorescence complex or had endogenous expression of Thy1-CFP. Images of wholemounted retinas were acquired with confocal microscopy (E800; Nikon Canada Inc., Mississauga, ON). The filter set included

DAPI (435 - 485 nm), GFP (520 - 560 nm) and HYQ Cy5 (663 - 738 nm). Images were obtained in the following order: (1) RITC, since RITC is most vulnerable to photobleaching, (2) Thy1-CFP or Brn3a, (3) To-Pro. Each image was taken in a radial pattern from the ON head. Three areas were targeted for imaging in each quadrant (nasal, temporal, inferior, superior) at 0.416 mm, 1.25 mm, 2 mm from the ON center, resulting in a total of 12 areas that were imaged for each retina (Fig. 2.5). Areas were imaged with each laser individually to avoid bleed-through and inaccurate quantification. Each image was comprised of a z-stack of the GCL with 2 μ m between each step within the z-stack resulting in a 3D image of the GCL, thus imaging all labeled cells. Each step was averaged twice to reduce background noise. The averaged z-stack was then compressed into a single 2D image of the area and was used for cell counting.

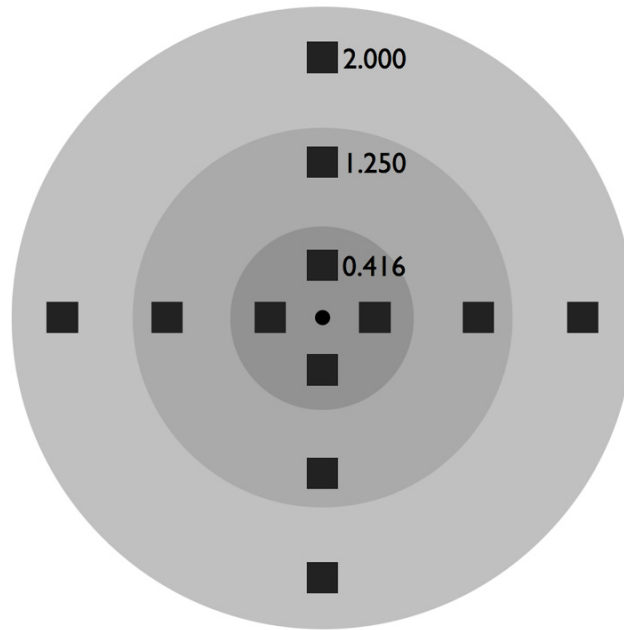


Figure 2.5 - Wholemount image acquisition

Wholemount retinas were imaged with confocal microscopy in a radial pattern beginning from the ON head. Images were acquired at approximately 0.416 mm, 1.25 mm and 2 mm from the ON head in all four quadrants (nasal, temporal, inferior and superior).

2.7.2 Cross sectional image acquisition

With confocal microscopy, images were selected from uninjured and injured sections. In order to have a good representation of cell density when comparing uninjured and injured sections, images were taken close to the optic nerve head. The GFP filter (520 -560 nm) was used to detect Thy1-CFP expression and the DAPI (435-485 nm) filter was used to detect ChAT immunohistochemistry.

2.8 Image analysis

Images were compressed and cells were counted in a masked fashion; images were renamed, reordered and mixed with different degrees of damage by an unbiased laboratory technician prior to cell counting by the author or experimenter. Each image was cell counted individually with imageJ (<http://rsbweb.nih.gov/ij/>) cell counting plug-in (<http://rsbweb.nih.gov/ij/plugins/cell-counter.html>) with To-Pro as a counterstain. With this plug-in, the experimenter clicks on RITC⁺, Brn3a⁺ or Thy1-CFP⁺ cells leaving a mark and automatically tallying every counted cell.

RITC, Brn3a and Thy1-CFP cell markings were saved with only To-Pro counterstain in the image to avoid any bias for double labeling counts. The corresponding images were then overlaid and cells that had both the RITC counting marker and the Brn3a or Thy1-CFP counting marker on the same To-Pro stained nuclei were counted, resulting in accurate unbiased counts of RGCs that express Brn3a and RGCs that express Thy1-CFP.

2.9 Western blotting

2.9.1 Protein extraction

Individual retinas were collected, and the fresh tissue was placed into microcentrifuge tubes on ice. Tissue was stored at -80 °C until protein extraction. Retinas were homogenized in RIPA buffer (1 % Triton X-100, 3.48 mM sodium dodecyl sulfate (SDS; Thermo Fisher Scientific Inc.), 150.07 mM NaCl (Millipore), 19.98 mM Tris-HCl Base (Sigma-Aldrich Co.), 12.74 mM deoxycholic acid (Thermo Fisher Scientific Inc.)) containing protease inhibitors (0.00729 mM pepstatin A (Sigma-Aldrich Co.), 0.012 mM leupeptin (Sigma-Aldrich Co.), 0.5 M phenylmethanesulfonyl fluoride (PMSF; Sigma-Aldrich Co.), 10.81 mM iodoacetamide (Sigma-Aldrich Co.)) and incubated on ice for 20 minutes. The homogenate was spun at 13,000 rpm at 4 °C for 15 minutes. The supernatant was removed and stored at -80 °C. Protein concentrations were determined by Pierce BCA Protein Assay Kit (Thermo Fisher Scientific Inc.).

2.9.2 Western blotting

20 ug of protein was loaded and subjected to a 10 % sodium dodecyl sulphate polyacrylamide gel electrophoresis (SDS-PAGE) at a current of 90 V for 20 minutes and 100 V for an additional 100 minutes. The protein was transferred

to immobilon polyvinylidene fluoride (PVDF) membrane at a current of 97 V for 1 hour. The membrane was blocked (5 % milk in (Bio-Rad Hercules, CA, USA) Tris-buffered saline with tween-20 (TBST; 0.14 M NaCl, 0.02 M Tris-HCl Base, 0.1 % Tween-20 (Sigma-Aldrich Co.))) for 2 hours and incubated in primary antibody (Goat anti-Brn3a; Lot#G1012, Santa Cruz Biotechnology) with blocking solution at 1:500 dilution ratio overnight at 4 °C. Three TBST washes were completed at room temperature for 20 minutes each followed by secondary antibody (Donkey anti-goat horseradish peroxidase, Lot# V1108, Vector) incubation at a 1:1000 dilution ratio in block for 1 hour at room temperature. The membrane was washed 3 times at room temperature for 20 minutes each with TBST and then the protein-antibody complex was detected with ECL Bio-Rad detection kit (Bio-Rad Laboratories (Canada) Ltd., Mississauga, Ontario). A 10 minute TSBT wash was completed at room temperature to remove any excess ECL and the membrane was incubated in rabbit anti-Actin (Lot# 090M4758, Sigma Aldrich) in a 1:1000 dilution ratio in block overnight at 4 °C. Three TBST 20 minutes washes were performed followed by incubation in secondary antibody (Preoxidase labeled anti-rabbit IgG (H+L); Lot# X0126, Vector) at a 1:10000 dilution in block for 1 hour at room temperature. The membrane was washed 3 times at room temperature for 20 minutes each with TBST and detected with ECL Bio-Rad detection kit.

2.9.3 Quantitation

Quantitation was calculated by densitometry of the film exposure. A scan of the film exposure was processed in image J with the “gels” option found in the analyze drop down menu (<http://rsb.info.nih.gov/ij/docs/menus/analyze.html#gels>). Each lane was selected, densitometry was analyzed and curves were plotted. With the freehand line tool, a line was made at the bottom of the curve to eliminate any background noise from the film. The total area underneath the curve was acquired. The area underneath the curve is a method of quantitating the amount of protein represented by the band on the film exposure. Once all densitometry of the band were tabulated, they were all normalized to the internal control, actin.

2.10 Statistical analysis

Statistical analysis was performed with IBM® SPSS® program v.21 (IBM corp., Armonk, NY, USA). All cell density data are expressed as mean \pm standard deviation. Significance of cell density changes after ONC or ONT of RITC, Brn3a and Thy1-CFP was determined by multivariate analysis of variance (MANOVA) with Fisher’s least significant difference (LSD) post-hoc testing. A paired-sample t-test was completed to compare Thy1-CFP⁺ or Brn3a⁺, RITC⁺, and Thy1-CFP⁺ /

RITC⁺ or Brn3a⁺/RITC⁺ labeling within each experimental time point. A paired-sample t-test was performed to compare the two types of mice, C57BL/6 and Thy1-CFP, at all experimental time points. Significance of RITC labeling at 7 and 21 day time points was assessed by two independent samples t-test. Significance of western blot densitometric values were analyzed by ANOVA with LSD post-hoc testing.

CHAPTER 3: RESULTS

We first analyzed RITC as a viable neuronal tracer that could identify 96% of all RGCs at all experimental time points. This was accomplished by identifying qualitative characteristics (e.g. cytoplasmic, nuclear) of the labeling. The cell density of RITC⁺ cells was then quantified at 7 days after SC surgery to assure that maximal labeling of all cells was achieved prior to the ON injury. We also quantified cells at a 21 day post-SC surgery time point because we allowed 7 days for the transport of RITC to the SC and our latest experimental time point was 14 days. This preliminary analysis of RITC assured that RITC labeling did not change for the duration of the experimental time points and that the cell loss identified at experimental time points were, in fact, due to cell loss and not the

loss of the neuronal tracer itself. RITC was then characterized in the ON injured retina by identifying qualitative characteristics and quantitative analysis of cell densities at 3, 5, 7 and 14 days after ONC and ONT.

Brn3a and Thy1-CFP expression were first described by analyzing the protein expression pattern of cells (e.g. cytoplasmic, nuclear) in control and ON injured retinas. Brn3a⁺ or Thy1-CFP⁺ cell densities were then tabulated and compared to RITC⁺ cell density. Brn3a⁺ and Thy1-CFP⁺ cell density rates of cell loss were reported and compared to RITC⁺ cell density rate of cell loss.

The expression pattern of cells labeled by both Brn3a⁺ and RITC⁺ (Brn3a⁺/RITC⁺), RGCs that express Brn3a, or Thy1-CFP⁺ and RITC⁺ (Thy1-CFP⁺/RITC⁺), RGCs that express Thy1-CFP, were identified. Brn3a⁺/RITC⁺ or Thy1-CFP⁺/RITC⁺ cell densities were tabulated and reported. The proportions of Brn3a⁺/RITC⁺ or Thy1-CFP⁺/RITC⁺ were compared to total Brn3a⁺ or Thy1-CFP⁺ cell densities, which identified the proportion of Brn3a⁺ or Thy1-CFP⁺ cells that were confirmed RGCs, thus identifying cell specificity of Brn3a and Thy1-CFP expression. The proportions of Brn3a⁺/RITC⁺ or Thy1-CFP⁺/RITC⁺ were also compared to total RITC⁺ cell densities, which identified the proportion of RGCs that express Brn3a or Thy1-CFP. This demonstrated whether all RGCs were identified with our experimental markers. Lastly, Thy1-CFP was analyzed for amacrine cell labeling in uninjured and ONT retinas.

3.1 Characterization of RITC as a retrograde tracer

In uninjured mice, RITC labeling of RGCs appeared as punctate labeling within the cytoplasm of cells in both 7 and 21 day time points after the application of RITC to the SC (Fig. 3.1). The intensity and density of RITC filled vesicles found within the cytoplasm was similar at both 7 and 21 day time points.

RITC⁺ cell densities of 7 and 21 post-SC labeling surgical time points mice were quantified to identify if RITC is a viable RGC marker and whether the invasiveness of the surgery affect RGC labeling (Fig. 3.2). There was no significant difference in RITC⁺ cell density at 7 days, 3003 ± 194 cells/mm² (mean \pm standard deviation), and 21 days, 3116 ± 215 cells/mm², after SC labeling (two independent sample t-test $P = 0.699$). These RITC⁺ cell densities were similar to previously published SC labeling RGC densities with FG.^{7, 13, 57}

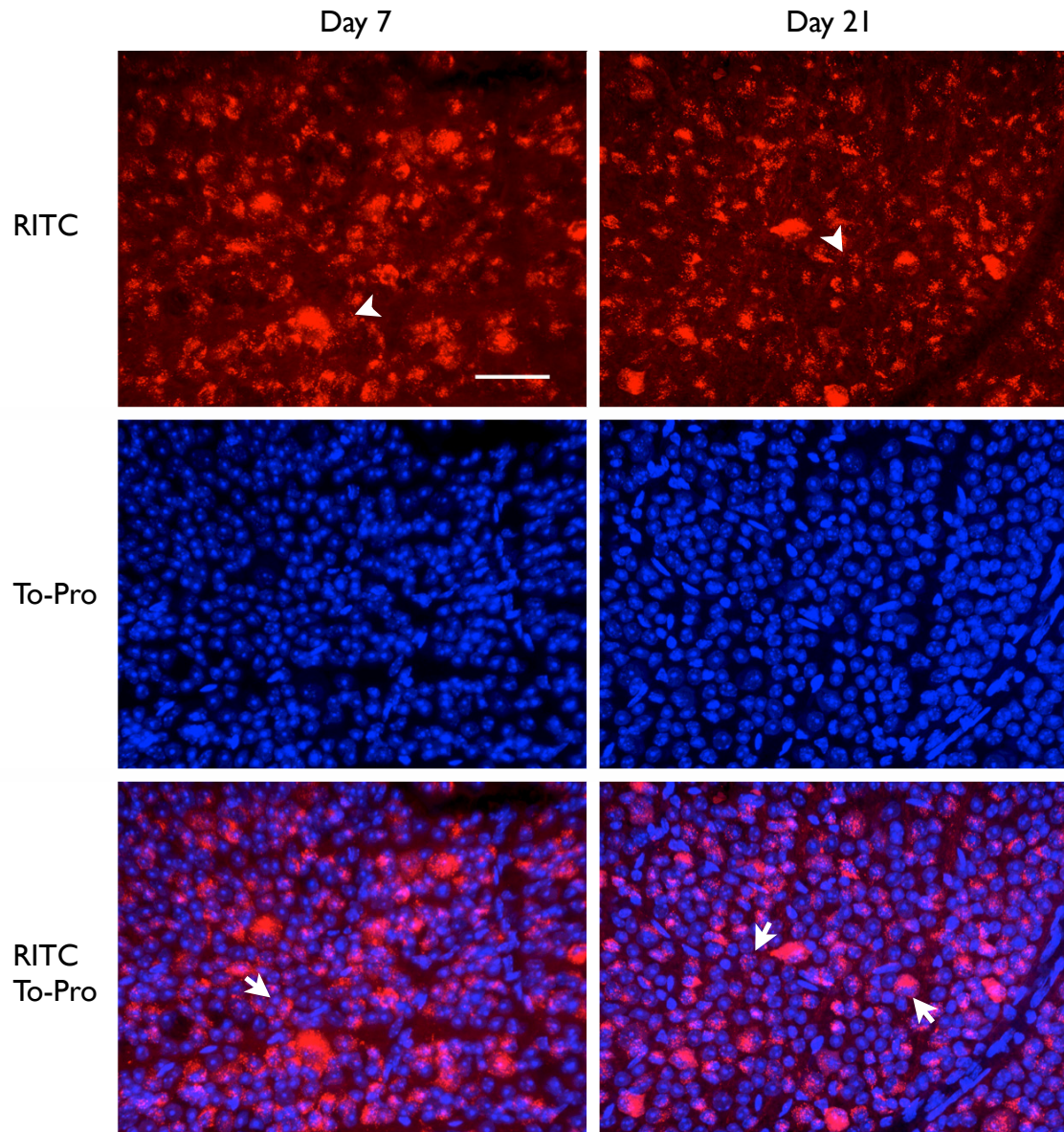


Figure 3.1 - Wholemout images of RITC labeling in control mice

RITC panels show punctate labeling of vesicularized RITC within the cytoplasm of RGCs while To-Pro panels depict all nuclei of cells in the ganglion cell layer (GCL). In the RITC⁺/To-Pro⁺ panels, RITC can be seen solely in the cytoplasm of cells, thus contouring To-Pro stained RGCs. Arrow head = punctate RITC labeling; Arrow = RITC cytoplasmic staining; Scale bar = 50 μ m

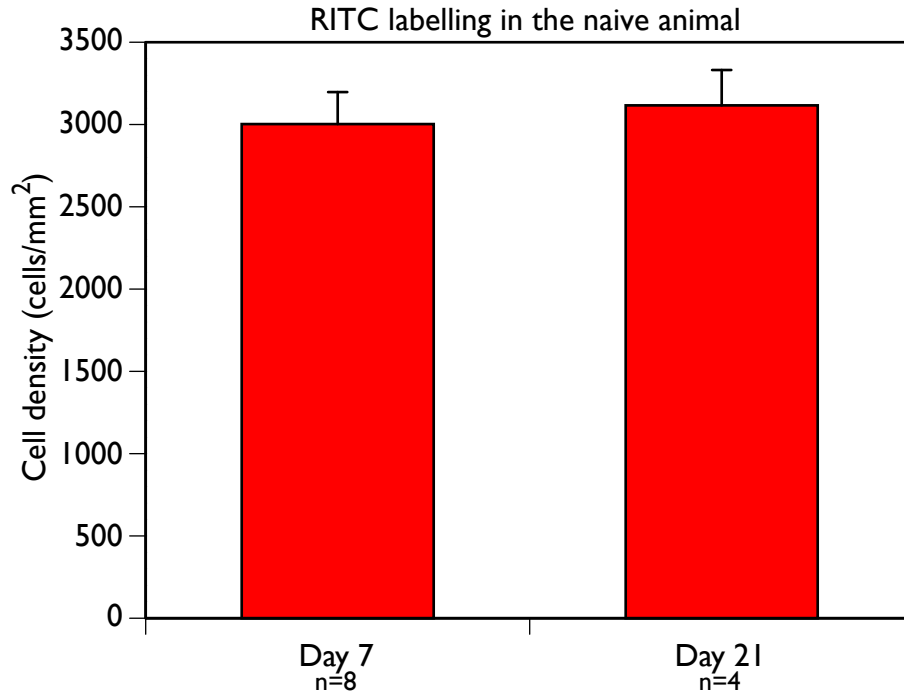


Figure 3.2 - RITC⁺ cell density in control mice

Cell densities of RITC in uninjured mice 7 and 21 days after labeling. There is no significant difference (two independent sample t-test $P = 0.699$) between the time points in the quantity of cells labeled.

After ONC and ONT, some RITC labeling remained vesicularized however in dead and damaged cells, RITC was no longer punctate and was replaced by debris and condensed cytoplasm (Fig. 3.3).

The RITC⁺ cell densities of C57BL/6 mice are stated in Table 3.1 and RITC⁺ cell densities of Thy1-CFP transgenic mice are stated in Table 3.3 . RITC⁺ cell density significantly decreased (Multivariate Analysis of Variance; MANOVA $P < 0.005$) at 3, 5, 7, and 14 days after ONC and ONT in C57BL/6 mice when compared to the uninjured retinal cell density (Fig. 3.4 A and B). RITC⁺ cell

density also significantly decreased (MANOVA $P < 0.005$) 3, 5, 7, and 14 days after ONC and 5, 7 and 14 days after ONT in Thy1-CFP transgenic mice when compared to the uninjured retinal cell density (Fig. 3.4 C and D). No statistically significant difference in response to ON injury between C57BL/6 and Thy1-CFP transgenic mice with RITC labeling was identified (paired-sample t-test $P > 0.05$).

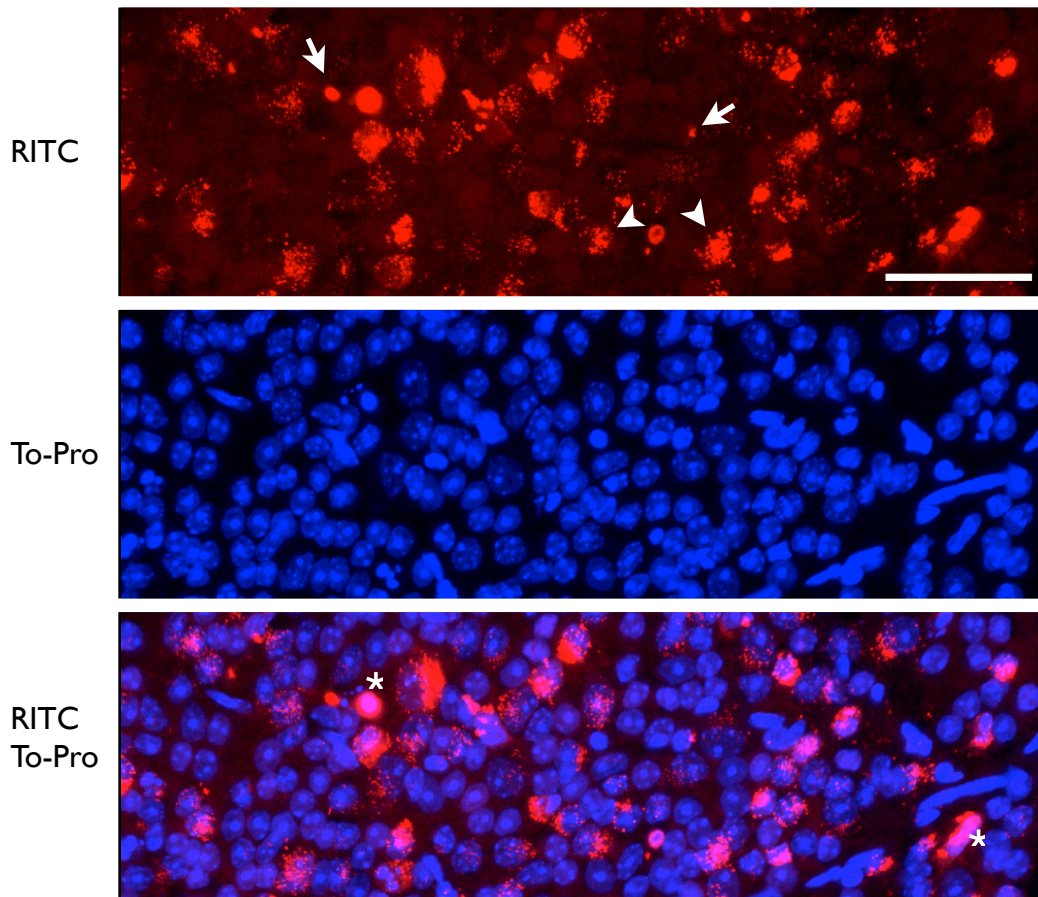


Figure 3.3 - Wholemount images of RITC⁺ labeling after ON injury
Five days after ONC, RITC can be viewed in vesicles within the cytoplasm (arrow head) and as debris (arrow) in RITC panel while To-Pro is depicting nuclei of all cells within the GCL. In the bottom panel, RITC labeling has condensed in some cells and is depicted as debris while the nuclei is still intact (star). Scale bar = 50 μm

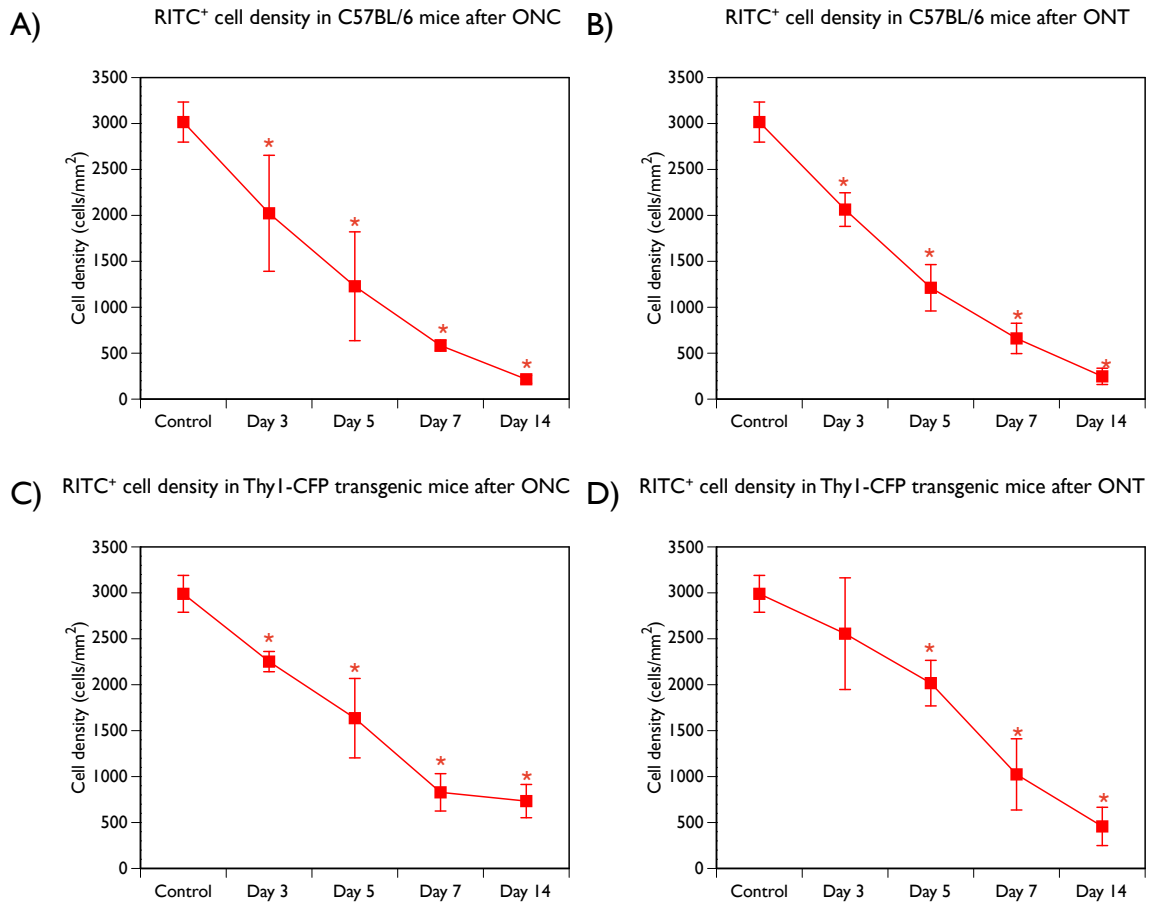


Figure 3.4 - RITC⁺ cell density after ON injury

These graphs show RITC⁺ cell density significantly decreases after ONC and ONT in C57BL/6 mice and Thy1-CFP transgenic mice. C57BL/6 and Thy1-CFP generally follow the same injury profile with ONC and ONT.

* Statistically significant when compared to the control group. MANOVA
 $P < 0.005$

In summary, RITC is a viable neuronal tracer used for RGC labeling. RITC labeling stays vesicularized within the cytoplasm of healthy cells for 21 days. After ONC and ONT, RITC⁺ cell densities gradually decrease and dead and dying cells are depicted as debris.

3.2 Brn3a as a potential RGC cell density marker after ONC and ONT

In control mouse retinas, Brn3a has clear nuclear expression of the protein, since all Brn3a expression co-localizes with the nuclear stain, To-Pro. However, cell morphology is not detected since Brn3a is not found in the cytoplasm. Brn3a continues to have clear nuclear labeling of cells and co-localizes with To-Pro after ONC and ONT (Fig. 3.5).

Brn3a⁺ cell densities were tabulated in control and 3, 5, 7 and 14 day ONC and ONT retinas to determine if Brn3a⁺ and RITC⁺ cell densities after ON injury were comparable (Table 3.1). No statistically significant difference between ONC and ONT injury models was identified in the C57BL/6 mouse (MANOVA $P > 0.05$).

Brn3a⁺ cell density remained unchanged from uninjured control to 3 days after ONC and ONT (Fig. 3.6, A and C). In controls, Brn3a⁺ cell density was 2137 ± 279 cells/mm² while 3 days after ONC and ONT it was 2119 ± 255 cells/mm² and 1842 ± 257 cells/mm², respectively. Western blot analysis showed a significant decrease in Brn3a expression 3 days after ONT (MANOVA $P < 0.005$, Fig. 3.7) however, Brn3a⁺ cell density only began to decrease significantly 5 days after ONC and ONT (MANOVA $P < 0.005$).

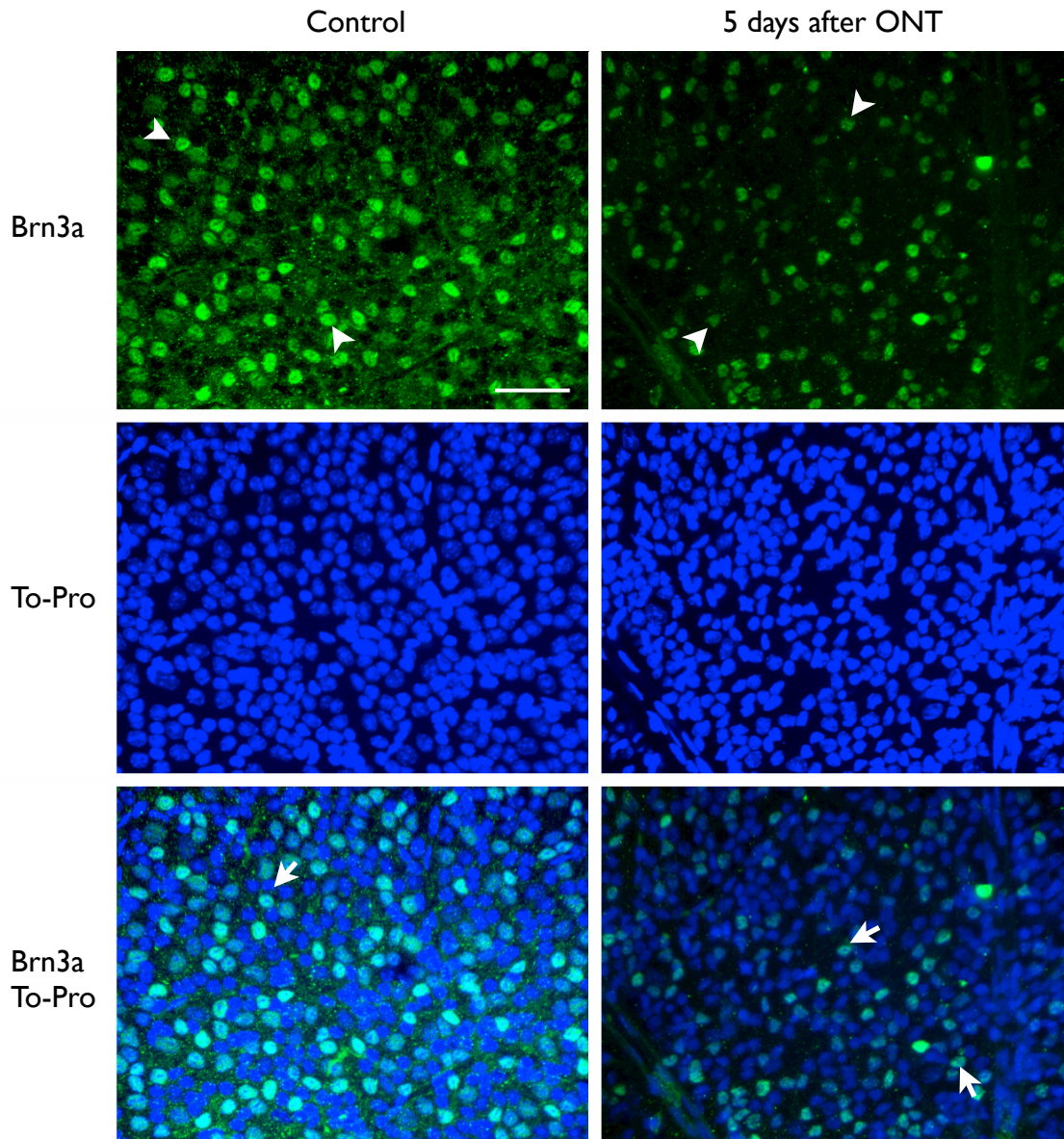


Figure 3.5 - Wholemout images of Brn3a⁺ cells in control and ON injured retinas

Brn3a cell expression intensity does not change after ON injury (arrow head). With To-Pro nuclear staining, Brn3a co-localizes with To-Pro in the control and ON injured retinas (arrow). Scale bar = 50 μ m

Table 3.1 - RITC⁺ and Brn3a⁺ cell densities of control, ONC and ONT C57BL/6 mouse retinas

Control (n=4)					
RITC ⁺ RGCs	3016 ± 218				
Brn3a ⁺ cells	2137 ± 279 [†]				
ONC	Day 3 (n=4)	Day 5 (n=4)	Day 7 (n=4)	Day 14 (n=4)	
RITC ⁺ RGCs	2023 ± 631*	1228 ± 592*	583 ± 61*	216 ± 43*	
Brn3a ⁺ cells	2119 ± 255	1326 ± 337*	503 ± 162*	259 ± 26*	
ONT	Day 3 (n=4)	Day 5 (n=4)	Day 7 (n=4)	Day 14 (n=4)	
RITC ⁺ RGCs	2063 ± 183*	1212 ± 252*	661 ± 165*	248 ± 89*	
Brn3a ⁺ cells	1842 ± 257	1406 ± 167*	568 ± 148*	334 ± 115 [†] *	

Cell densities (mean ± SD) of Brn3a expressing cells in the GCL and RITC labeled cells of the GCL. All cell densities were determined by manual counting of images of whole-mounted retinas.

* Statistically significant when compared to the control group. MANOVA $P < 0.05$

Brn3a⁺ cell density was significantly less than RITC⁺ cell density in control retinas (paired-sample t-test, $P = 0.007$). Although Brn3a⁺ cell density was similar to the RITC⁺ cell density after ON injury (paired-sample t-test $P > 0.05$, Fig. 3.6 A and C), Brn3a⁺ cells were more resilient to ONC and ONT than RITC⁺ cells since Brn3a⁺ cell density did not decrease significantly until 5 days after ON injury (MANOVA $P < 0.005$). Brn3a⁺ cell density decreased from ~100% to ~20% after ONC and ~90% to ~15% after ONT between 3 and 14 days after injury. RITC⁺ cell density decreased from ~70% to ~10% and ~70% to ~20% between 3 and 14 days after ONC and ONT, respectively (Fig. 3.6, B and D).

In summary, Brn3a⁺ cells are characterized by nuclear labeling of cells in control and injured retinas. Brn3a⁺ cell density is significantly lower than RITC⁺ cell density in control mice however Brn3a⁺ cell density is similar to RITC⁺ cell density after ONC and ONT. The reduction of Brn3a⁺ cell expression precedes the reduction in Brn3a⁺ cell density since Brn3a⁺ cell density does not significantly decrease until 5 days after the ON injury.

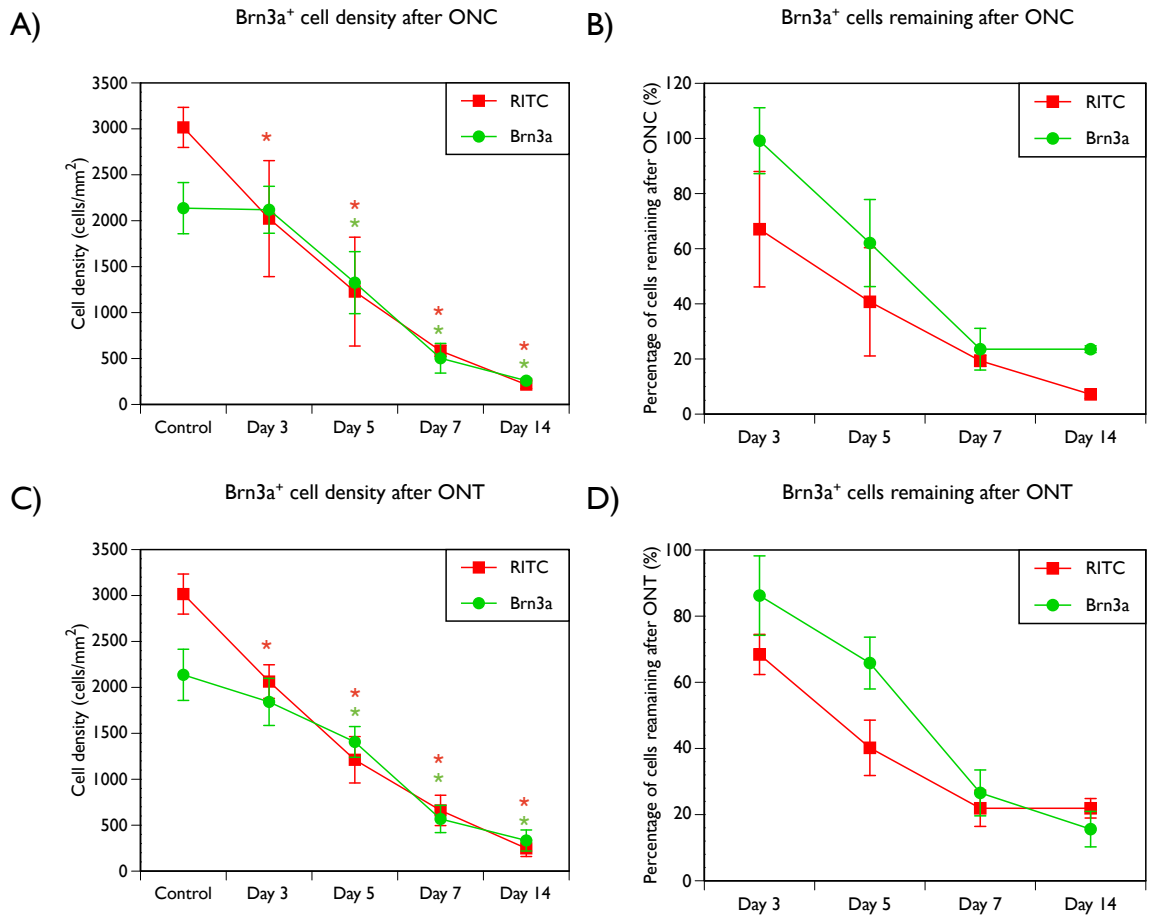
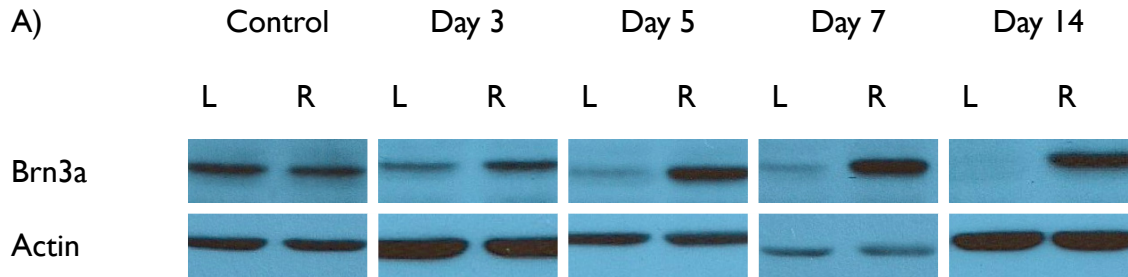


Figure 3.6 - Brn3a⁺ cell density after ON injury

Brn3a⁺ cell density does not significantly decrease until 5 days after A) ONC and C) ONT. However, Brn3a⁺ cell density is similar to RITC⁺ cell density after ONC and ONT. Since Brn3a⁺ cell density does not decrease significantly until 5 days after ONC and ONT, there is a proportion of Brn3a⁺ labeled cells remaining 3 and 5 days after B) ONC and D) ONT.

* Statistically significant when compared to the control group. MANOVA $P < 0.005$



B)

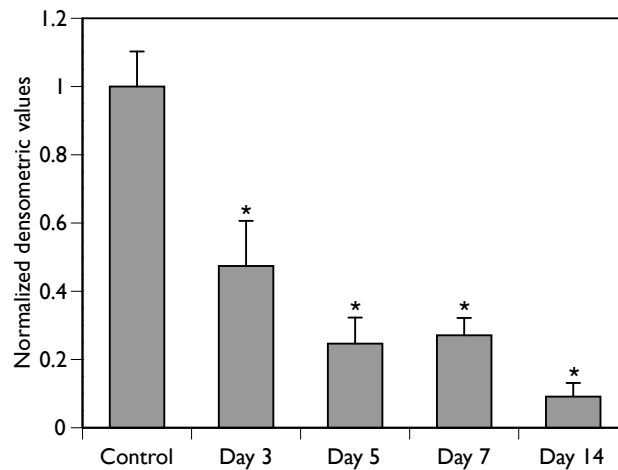


Figure 3.7 - Brn3a protein expression after ONT

A) Western blot gels representing a gradual decrease of Brn3a expression after ONT in mice. Left eye (L) = injured retina; Right eye (R) = control fellow eye

B) These bands were quantitated by densitometry of control and 3, 5, 7, and 14 days after ONT retinas. Brn3a cell expression significantly decreases 3 days after ONT.

* Significant decrease when compared to the uninjured control. ANOVA $P < 0.005$

3.3 Brn3a⁺/RITC⁺ cell densities after ONC and ONT

In control and ON injured mouse retinas, some cells were Brn3a⁺/RITC⁻, some were Brn3a⁻/RITC⁺, while others were Brn3a⁺/RITC⁺ (Fig. 3.8 and 3.9). A

decrease in the quantity of labeled cells was observed after ONC (Fig. 3.8) and ONT (Fig. 3.9).

Brn3a⁺/RITC⁻, Brn3a⁻/RITC⁺ and Brn3a⁺/RITC⁺ cell densities were quantified to identify whether Brn3a was only expressed in RITC⁺ cells, since RITC only labels RGCs (Table 3.2). In control mice, Brn3a⁺/RITC⁺ cell density was 1614 ± 260 cells/mm². This control cell density was significantly less than the individual RITC⁺ and Brn3a⁺ cell densities (paired-sample t-test, $P = 0.005$). As a general trend, Brn3a⁺/RITC⁺ cell density was significantly less than the individual RITC⁺ and Brn3a⁺ cell densities after ONC and ONT at all experimental time points (paired-sample t-test $P < 0.05$, Fig. 3.10, A and C). However after ONC and ONT, Brn3a⁺/RITC⁺ cell density gradually decreased at the same rate as the RITC⁺ cell density (Fig. 3.10, B and D). Approximately 80%, ~40%, ~30%, ~20% of Brn3a⁺/RITC⁺ and RITC⁺ cells remained 3, 5, 7 and 14 days after ON injury respectively.

Two methods were utilized to compare the double labeled cells. First, the proportion of RITC⁺ RGCs that express Brn3a were quantified. This comparison identified the population of RITC⁺ RGCs that expressed Brn3a. Secondly, we quantified the proportion of Brn3a⁺ cells that were RITC⁺ RGCs. This allowed us to identify if there were any Brn3a⁺ cells that were not co-identified with RITC neuronal tracer.

In uninjured control mice, ~54% of RITC⁺ cells were Brn3a⁺/RITC⁺ (Fig. 3.11). Approximately 61% of RITC⁺ cells were Brn3a⁺/RITC⁺ 3 days after ONC and gradually decreased to ~22% 14 days after injury. Three days after ONT, ~51% of RITC⁺ cells were Brn3a⁺/RITC⁺ and decreased to ~38% 14 days after ONT.

In uninjured control mice, ~76% of Brn3a⁺ cells were Brn3a⁺/RITC⁺ (Fig. 3.12). Approximately 58% of Brn3a⁺ cells were Brn3a⁺/RITC⁺ 3 days after ONC and decreased to ~18% 14 days after injury. After ONT, ~57% of Brn3a⁺ cells were Brn3a⁺/RITC⁺ 3 days after injury and decreased to ~28% 14 days after ON injury.

In summary, Brn3a⁺/RITC⁺ cell density was significantly lower than RITC⁺ and Brn3a⁺ cell densities at all time points. However, Brn3a⁺/RITC⁺ cell density decreased at the same rate as the RITC⁺ cell density after ONC and ONT. The proportion of RITC⁺ cells that were Brn3a⁺/RITC⁺ gradually decreased after ONC and ONT and the proportion of Brn3a⁺ cells that were Brn3a⁺/RITC⁺ also gradually decreased after ONC and ONT.

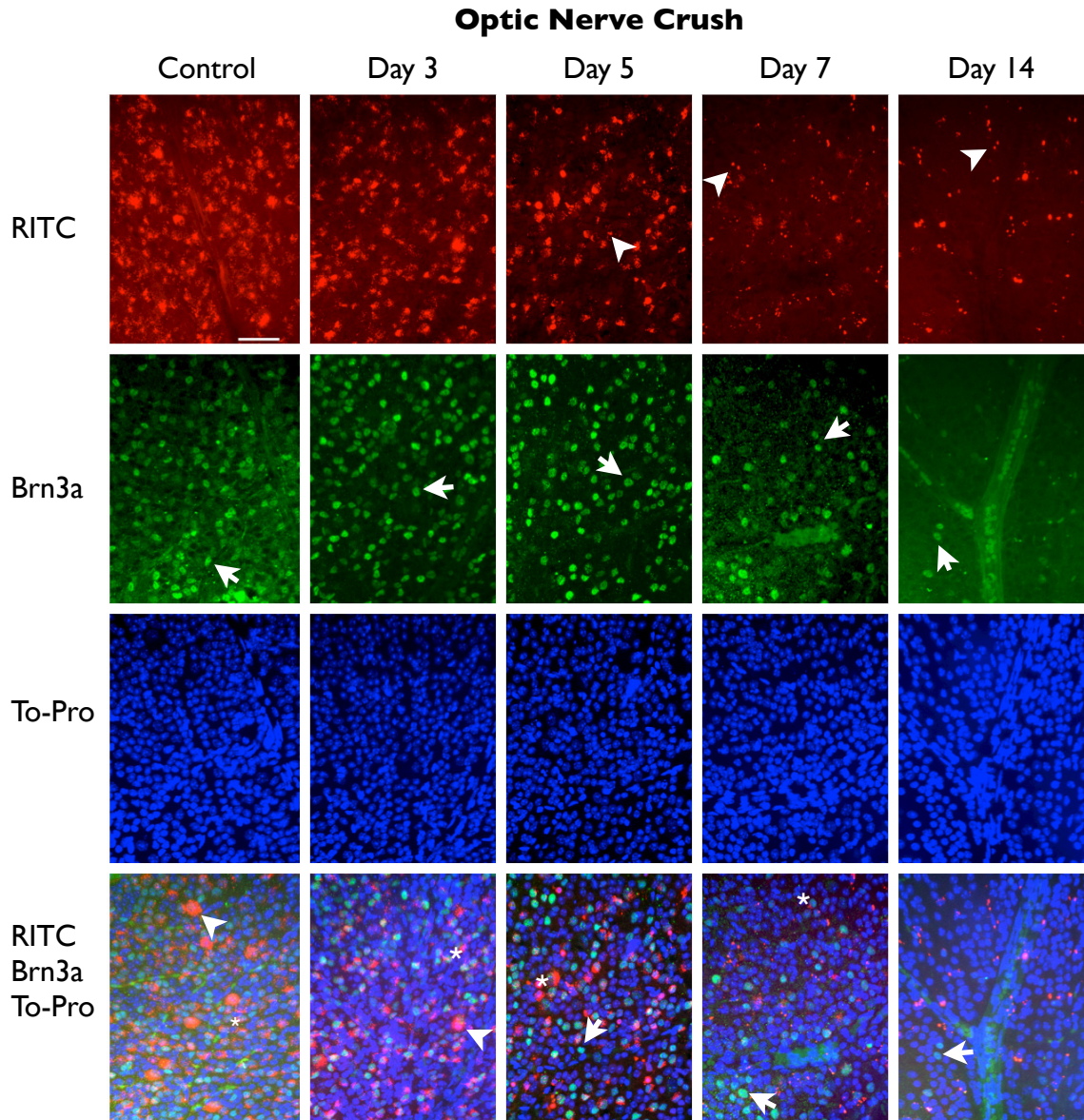


Figure 3.8 - Brn3a⁺/RITC⁺ retinal wholemount images of control and ONC C57BL/6 mice

Brn3a⁺ and RITC⁺ cell densities gradually decrease after ONC. After ONC, RITC (arrowhead) appears as punctate labeling in dead and dying cells while Brn3a (arrow) has clear nuclear labeling of cells at all experimental time points. The triple labeling panels show some cells were Brn3a⁺/RITC⁺ (star), some were Brn3a⁺/RITC⁻ (arrow) while others were Brn3a⁻/RITC⁺ (arrow head) in control and ON injured mice. Scale bar = 50 μm

Optic Nerve Transection

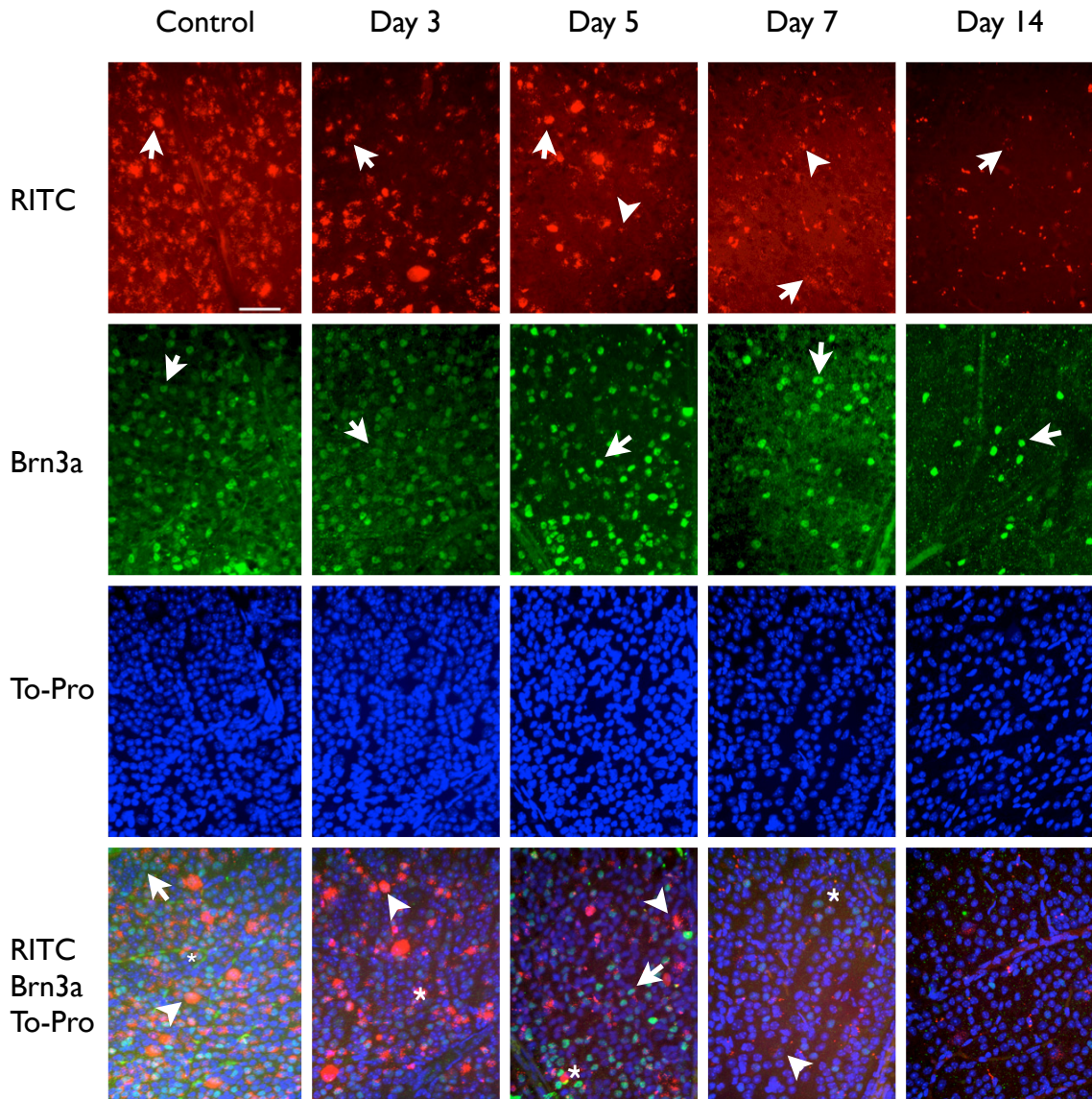


Figure 3.9 - Brn3a⁺/RITC⁺ retinal wholemount images of control and ONT C57BL/6 mice

RITC labeling of cells decreases after ONT. RITC appears in vesicles within the cytoplasm (arrow) in healthy cells while after ONT, RITC may appear as debris (arrow head). Brn3a cell density decreases after ONT but still clearly labels the nucleus of cells (arrow). In triple labeled images, some cells were Brn3a⁺/RITC⁺ (star), while others were Brn3a⁺/RITC⁻ (arrow) and Brn3a⁻/RITC⁺ (arrow head). Scale bar = 50 μm

Table 3.2 - Brn3a⁺/RITC⁺ cell densities of control, ONC and ONT C57BL/6 mouse retinas

Control (n=4)				
Brn3a ⁺ /RITC ⁺	1614 ± 260			
Brn3a ⁻ /RITC ⁺	1402 ± 263			
Brn3a ⁺ /RITC ⁻	523 ± 74			
ONC	Day 3 (n=4)	Day 5 (n=4)	Day 7 (n=4)	Day 14 (n=4)
Brn3a ⁺ /RITC ⁺	1226 ± 268*	641 ± 366*	145 ± 53*	47 ± 24*
Brn3a ⁻ /RITC ⁺	797 ± 377	587 ± 237	438 ± 34	169 ± 46
Brn3a ⁺ /RITC ⁻	893 ± 41	685 ± 300	358 ± 115	211 ± 26
ONT	Day 3 (n=4)	Day 5 (n=4)	Day 7 (n=4)	Day 14 (n=4)
Brn3a ⁺ /RITC ⁺	1045 ± 105*	668 ± 156*	152 ± 65*	93 ± 67*
Brn3a ⁻ /RITC ⁺	1018 ± 225	544 ± 104	509 ± 132	155 ± 25
Brn3a ⁺ /RITC ⁻	797 ± 162	739 ± 162	416 ± 202	240 ± 57

Brn3a⁺/RITC⁺, Brn3a⁻/RITC⁺ and Brn3a⁺/RITC⁻ cell densities (mean ± SD). All cell densities were determined by manual counting of retinal images of whole-mounted retinas.

* Statistically significant when compared to the control group. MANOVA test $P < 0.05$

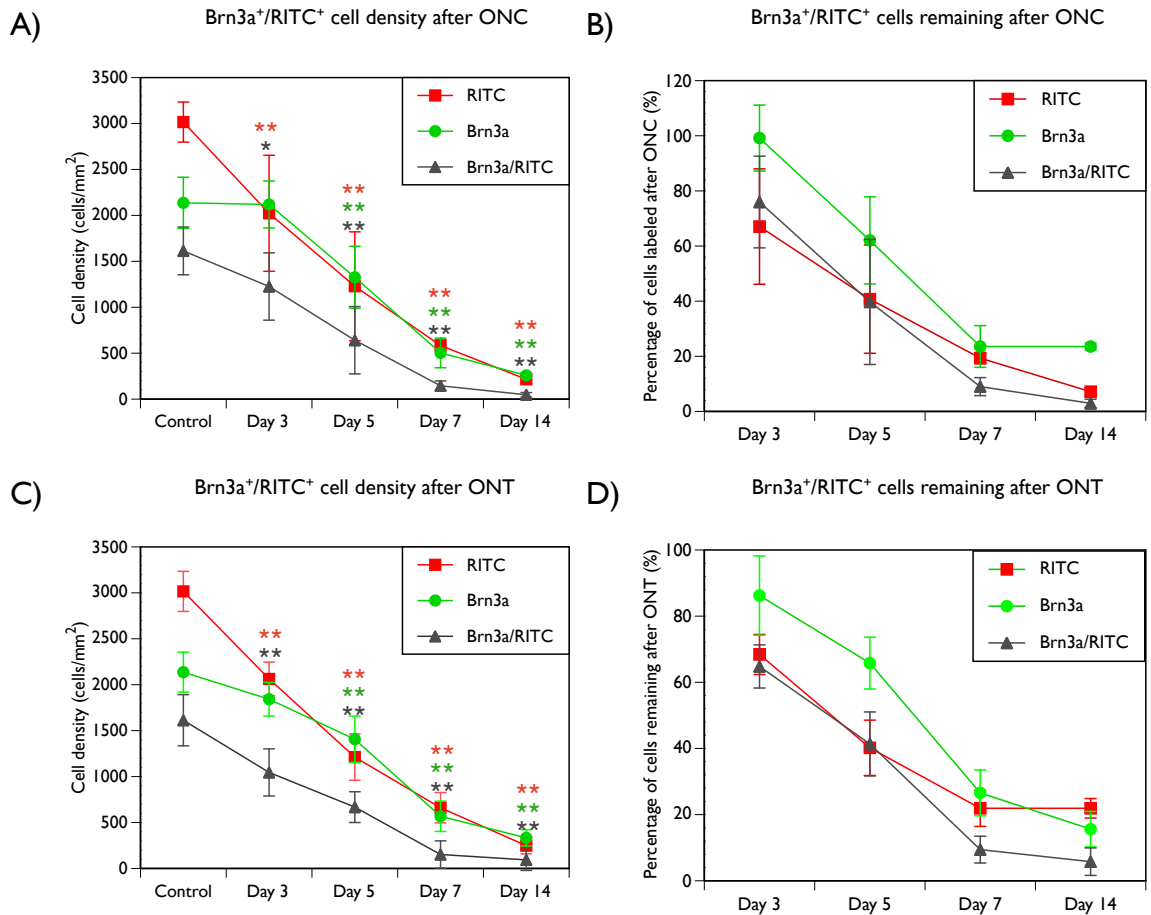
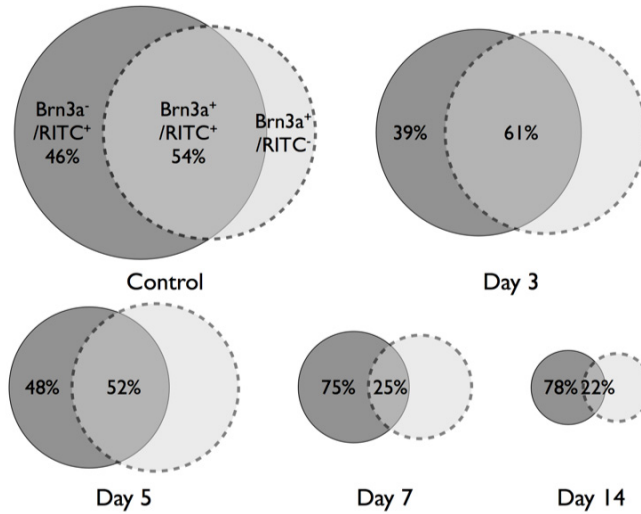


Figure 3.10 - Brn3a⁺/RITC⁺ cell density after ON injury

Brn3a does not have the same cell density as RITC in the control retinas but has similar cell densities to RITC after ONC and ONT. A) Cell densities of Brn3a⁺, RITC⁺ and Brn3a⁺/RITC⁺ in the control mice and 3, 5, 7 and 14 days after ONC. B) Percentage of remaining cells labeled 3, 5, 7, and 14 days after ONC. C) Brn3a⁺, RITC⁺ and Brn3a⁺/RITC⁺ cell densities in the control and 3, 5, 7, and 14 days after ONT. D) Percentage of remaining cells labeled 3, 5, 7, and 14 days after ONT.

Statistically significant when compared to the control group. MANOVA test
 * $P < 0.05$, ** $P < 0.005$

Optic Nerve Crush



Optic Nerve Transection

B)

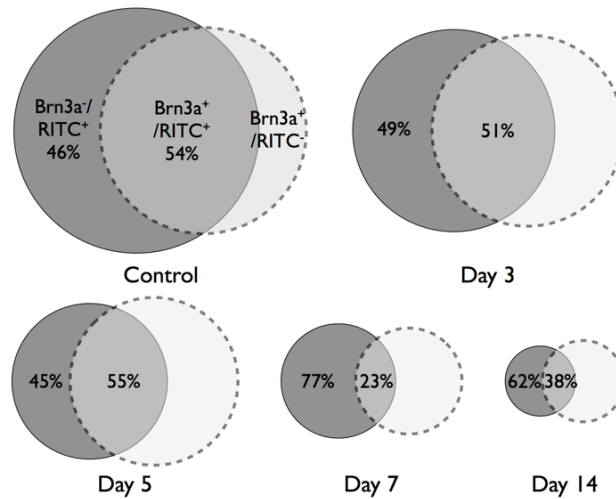
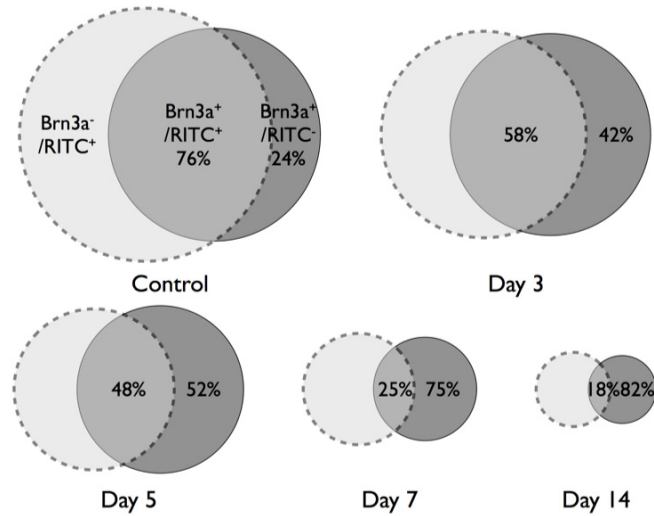


Figure 3.11 - Venn diagrams of RGCs expressing Brn3a

The area of these Venn diagrams are proportional to the total cell population labeled by RITC (dark circles) and Brn3a (light circles). The overlap between RITC⁺ and Brn3a⁺ cell density is representative of the Brn3a⁺/RITC⁺ cell density. As cell density decreases, the Venn diagrams also proportionally decrease when compared to the control cell population. After A) ONC and B) ONT, the proportion of RITC⁺ cells that express Brn3a decreases.

Optic Nerve Crush

A)



Optic Nerve Transection

B)

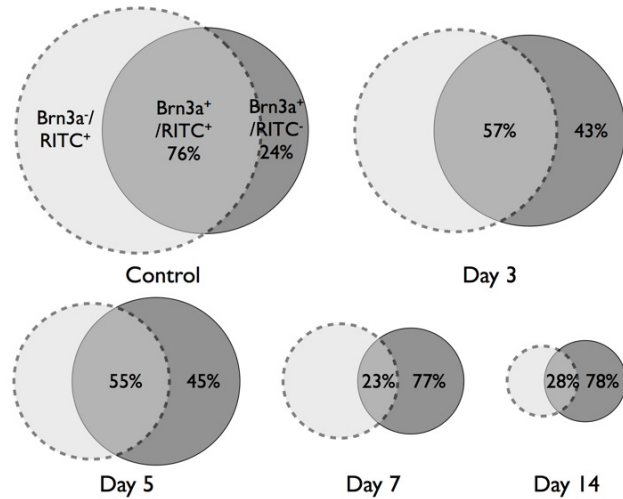


Figure 3.12 - Venn diagrams of Brn3a⁺ confirmed RGCs

The area of these Venn diagrams are proportional to the total cell population labeled by RITC (light circles) and Brn3a (dark circles). The overlap between RITC⁺ and Brn3a⁺ cell density is representative of the Brn3a⁺/RITC⁺ cell density. As cell density decreases, the Venn diagrams also proportionally decrease when compared to the control cell population. The proportion of Brn3a⁺ cells that are confirmed RGCs labeled by RITC decreases after A) ONC and B) ONT.

3.4 Thy1-CFP expression after ONC and ONT

In retinas of control mice, Thy1-CFP was characterized by clear cytoplasmic and nuclear expression since Thy1-CFP co-localized with To-Pro and contoured the nuclei of cells. Thy1-CFP cell expression changed after ON injury by being expressed solely in the cytoplasm of some cells since Thy1-CFP surrounded the To-Pro stained nuclei (Fig. 3.13 and A.1). In control and ON injured retinas, Thy1-CFP was expressed at various intensities and cell morphologies. Axonal blebbing could also be visualized with Thy1-CFP expression 5 to 14 days after ONC and ONT.

Thy1-CFP⁺ cell densities were determined in control and 3, 5, 7, and 14 days after ONC and ONT mice (Table 3.3). No statistically significant difference between ONC and ONT injury models was identified in the Thy1-CFP transgenic mouse (MANOVA $P > 0.05$). Thy1-CFP⁺ cell density did not significantly change over time until 7 days after ONC and ONT (MANOVA $P > 0.05$; Fig. 3.14, A and C).

While RITC⁺ cell density gradually decreased after ONC and ONT, Thy1-CFP⁺ cell density remained relatively the same. Thy1-CFP⁺ cell density was significantly lower than RITC⁺ cell density in uninjured control mice. In contrast, Thy1-CFP⁺ cell density was significantly higher than RITC⁺ cell density 14 days after ON injury (paired-sample t-test; ONT $P=0.007$; ONC $P=0.019$). Fourteen

days after ONC and ONT, Thy1-CFP labeled approximately 60% of cells when compared to its control Thy1-CFP cell density while RITC⁺ labeled 20% of the control RITC cell density (Fig. 3.14, B and D).

To summarize, Thy1-CPF expression changes from cytoplasmic and nuclear to solely cytoplasmic in some cells after ONC and ONT. Thy1-CFP⁺ cell density was significantly lower than RITC⁺ cell density in control mice while Thy1-CFP⁺ cell density was significantly higher in 14 day ON injured mice. 60% of the total Thy1-CFP cell density and ~20% of the total RITC population remained 14 days after ON injury.

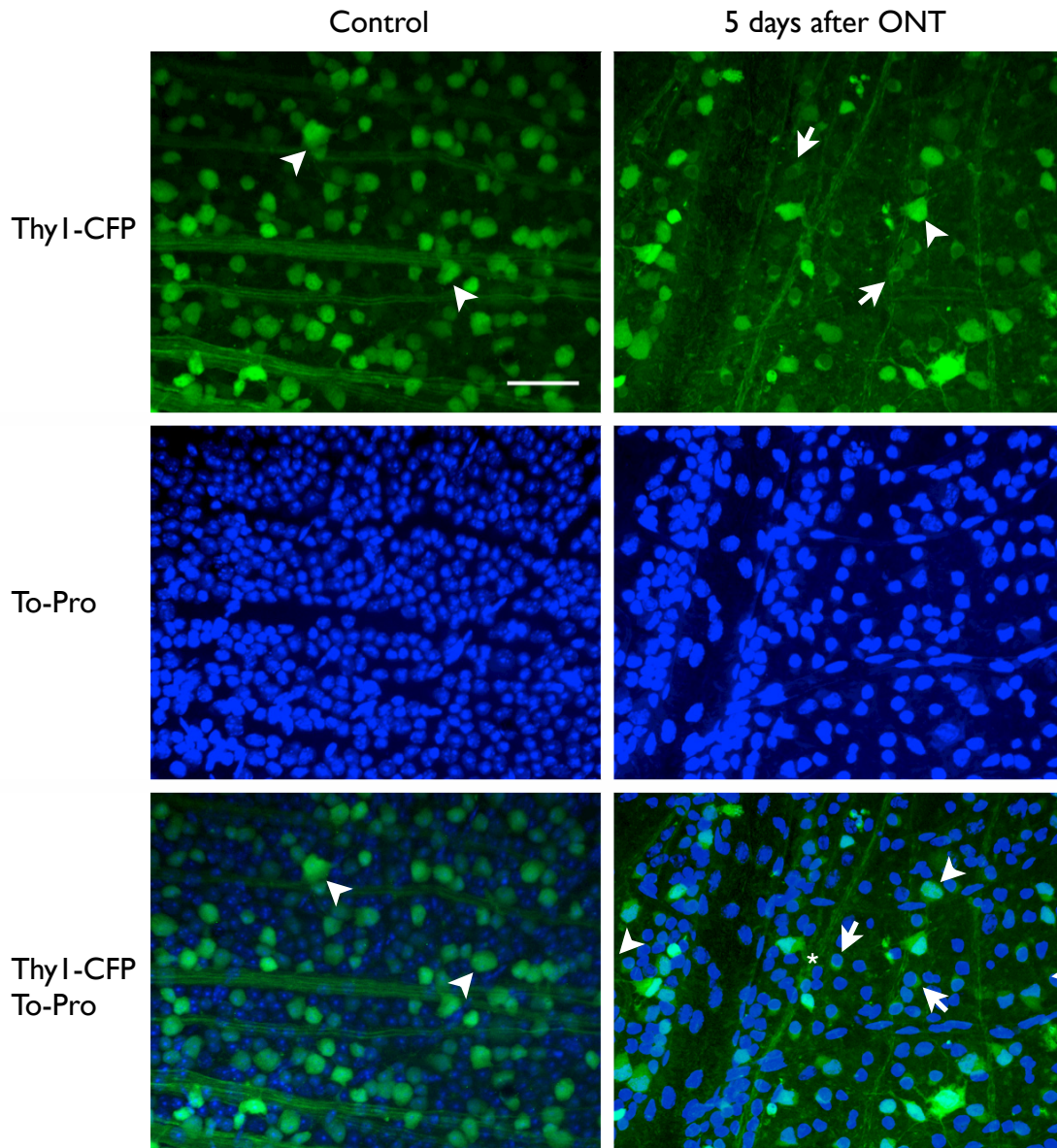


Figure 3.13 - Wholemout images of Thy1-CFP⁺ in control and ON injured retinas

Thy1-CFP is expressed in the cytoplasm and nucleus of cells (arrow head) since Thy1-CFP expression co-localizes with To-Pro staining and contours the nucleus of cells in control mice. In ON injured mice, Thy1-CFP labels the nucleus and cytoplasm of some cells (arrow head) while only labeling the cytoplasm of others since Thy1-CFP does not co-localize with To-Pro but instead contours the nucleus of cells (arrow). Thy1-CFP expression is found at all different intensities within the cytoplasm and nucleus of cells in both control and ON injured retinas. In ON injured mice, axonal blebbing could also be observed (star). Scale bar = 50 μm

Table 3.3 - RITC⁺ and ThyI-CFP⁺ cell densities after ONC and ONT ThyI-CFP transgenic mouse retinas

Control (n=4)					
RITC ⁺ RGCs	2989 ± 201				
ThyI-CFP ⁺ cells	1881 ± 163 [†]				
ONC	Day 3 (n=4)	Day 5 (n=4)	Day 7 (n=4)	Day 14 (n=4)	
RITC ⁺ RGCs	2252 ± 110*	1636 ± 432*	828 ± 203*	733 ± 181*	
ThyI-CFP ⁺ cells	1992 ± 184 [†]	1701 ± 318	1579 ± 152 ^{†*}	1286 ± 116 ^{†*}	
ONT	Day 3 (n=4)	Day 5 (n=4)	Day 7 (n=4)	Day 14 (n=4)	
RITC ⁺ RGCs	2556 ± 608	2017 ± 248*	1024 ± 388*	458 ± 208*	
ThyI-CFP ⁺ cells	2013 ± 216	1654 ± 180	1441 ± 163*	1064 ± 94 ^{†*}	

Cell densities (mean ± SD) of ThyI-CFP⁺ expressing cells and RITC⁺ labeled cells of the GCL. All cell densities were determined by manual counting of retinal images of whole-mounted retinas.

* Statistically significant when compared to the control group. MANOVA $P < 0.05$

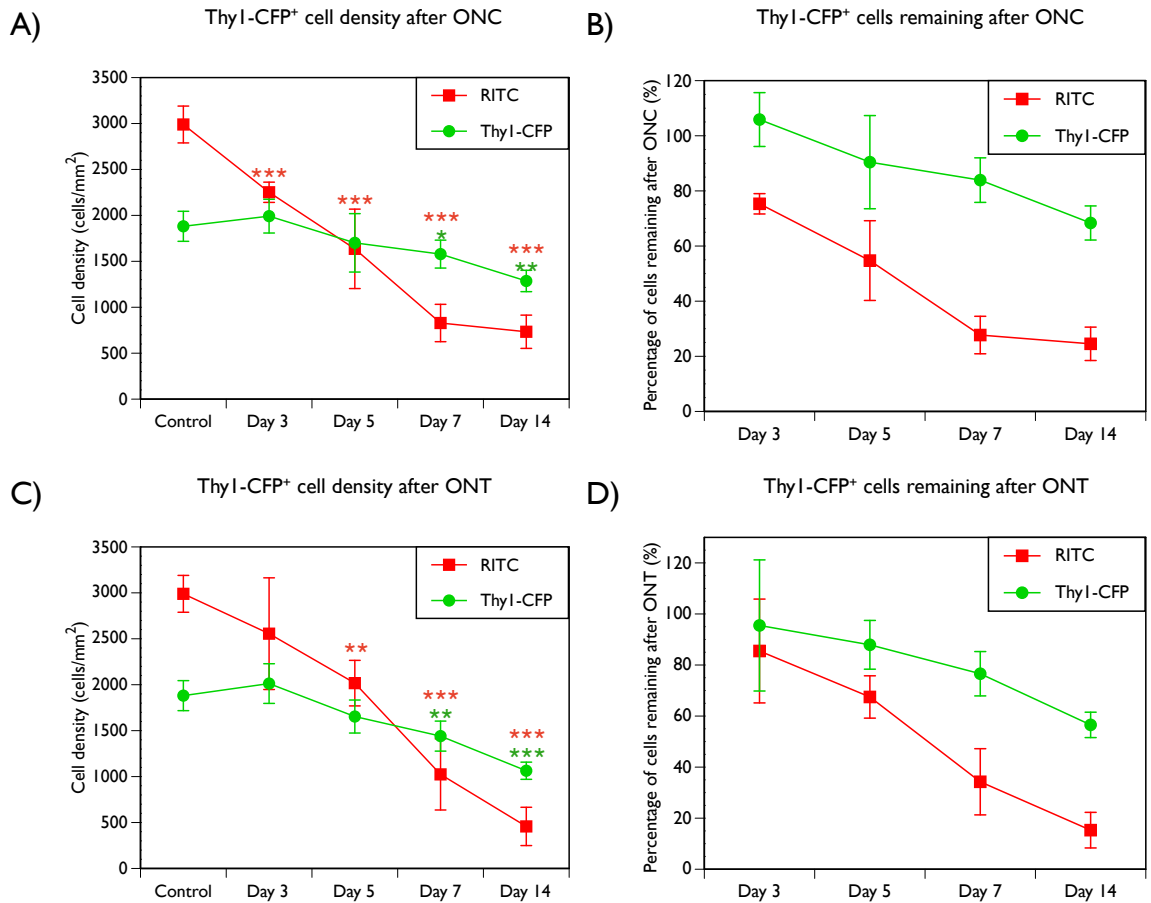


Figure 3.14- Thy1-CFP⁺ cell density after ON injury in Thy1-CFP transgenic mice

Thy1-CFP⁺ cell density significantly decreases 7 days after A) ONC and C) ONT. Thy1-CFP⁺ cell density is significantly lower than RITC⁺ cell density in control mice and Thy1-CFP⁺ cell density is significantly higher than RITC⁺ 14 days after ONC and ONT. Thy1-CFP⁺ cell density only decreases ~40% after B) ONC and D) ONT while RITC decreases ~80%.

Statistically significant when compared to the control group. MANOVA test * $P < 0.05$, ** $P < 0.005$, *** $P < 0.005$

3.5 Thy1-CFP⁺/RITC⁺ cells in control and ON injured mice

In retinas of control and ON injured mice, some cells were Thy1-CFP⁺/RITC⁻, some cells were only Thy1-CFP⁻/RITC⁺ while some cells were Thy1-CFP⁺/RITC⁺. Over time, there was a notable difference in the quantity of Thy1-CFP⁺/RITC⁻ that could be qualitatively observed after ONC and ONT (Fig. 3.15 and 3.16).

The cell density of Thy1-CFP⁺/RITC⁺ cell population was tabulated to identify whether Thy1-CFP expression was unique to RGCs after injury (Table 3.4 and Fig. 3.17 A and C). In control mice, the Thy1-CFP⁺/RITC⁺ cell density of 1403 ± 69 cells/mm² was significantly less than the individual RITC⁺ and Thy1-CFP⁺ cell densities (paired-sample t-test, $P < 0.05$). Throughout every time point after ON injury, the Thy1-CFP⁺/RITC⁺ cell density was significantly less than the RITC⁺ and Thy1-CFP⁺ cell densities (paired-sample t-test, $P < 0.05$).

The rate of cell death of Thy1-CFP⁺/RITC⁺ cells was similar to the rate of cell death of RITC⁺ cells (Fig. 3.17 B and D). In ON injured mice, the percentage of cells that remained was approximately the same at every time point; three days after ON injury, ~80% of Thy1-CFP⁺/RITC⁺ and RITC⁺ cells remained while by 14 days after ON injury, ~20% of Thy1-CFP⁺/RITC⁺ and RITC⁺ cells remained.

In control mice, ~47% of RITC⁺ cells were Thy1-CFP⁺/RITC⁺ (Fig. 3.18). Approximately 56% and ~50% of RITC⁺ cells were Thy1-CFP⁺/RITC⁺ at all time points after ONC and ONT, respectively.

In control mice, ~75% of Thy1-CFP⁺ cells were Thy1-CFP⁺/RITC⁺ (Fig. 3.19). The portion of Thy1-CFP⁺ cells that were Thy1-CFP⁺/RITC⁺ cells decreased from ~63% to ~32% between 3 to 14 days after ONC. After ONT, cell density of Thy1-CFP⁺ cells are co-identified with RITC decreased from ~65% to ~22% between 3 and 14 days after ON injury.

Thy1-CFP was detected in ChAT positive cells in control and 7 day ONT, thus confirming that Thy1-CFP is expressed in other cells of the GCL in control and after ONT. Thy1-CFP was expressed in very few cells in the INL in control mice while after ONT many cells of the INL expressed Thy1-CFP (Fig. 3.20).

In summary, Thy1-CFP⁺/RITC⁺ and RITC⁺ cell densities follow a similar rate of cell loss. The proportion of Thy1-CFP⁺/RITC⁺ cells decreases after injury while Thy1-CFP⁺ cell density remains relatively the same until 7 days after ON injury. Approximately 50% of all RITC⁺ cells express Thy1-CFP in all control and ON injured retinas. Thy1-CFP labels ChAT positive cells in the GCL after ON injury along with RGCs.

Table 3.4 - ThyI-CFP⁺/RITC⁺ cell densities of control, ONC and ONT ThyI-CFP transgenic mouse retinas

Control (n=4)				
ThyI-CFP ⁺ /RITC ⁺	1403 ± 69			
ThyI-CFP ⁻ /RITC ⁺	1586 ± 174			
ThyI-CFP ⁺ /RITC ⁻	478 ± 126			
ONC	Day 3 (n=4)	Day 5 (n=4)	Day 7 (n=4)	Day 14 (n=4)
ThyI-CFP ⁺ /RITC ⁺	1259 ± 125	956 ± 273*	488 ± 100*	408 ± 69*
ThyI-CFP ⁻ /RITC ⁺	993 ± 31	680 ± 160	340 ± 108	325 ± 114
ThyI-CFP ⁺ /RITC ⁻	733 ± 72	745 ± 56	1091 ± 138	878 ± 144
ONT	Day 3 (n=4)	Day 5 (n=4)	Day 7 (n=4)	Day 14 (n=4)
ThyI-CFP ⁺ /RITC ⁺	1317 ± 296	964 ± 46*	563 ± 183*	234 ± 99*
ThyI-CFP ⁻ /RITC ⁺	1239 ± 823	1053 ± 240	461 ± 205	224 ± 112
ThyI-CFP ⁺ /RITC ⁻	695 ± 146	689 ± 199	878 ± 155	830 ± 96

ThyI-CFP⁺/RITC⁺, ThyI-CFP⁻/RITC⁺ and ThyI-CFP⁺/RITC⁻ cell densities (mean ± SD) in control and ON injured mice. All cell densities were determined by manual counting of retinal images of whole mounted retinas.

* Statistically significant when compared to the control group. MANOVA test $P < 0.05$

Optic Nerve Crush

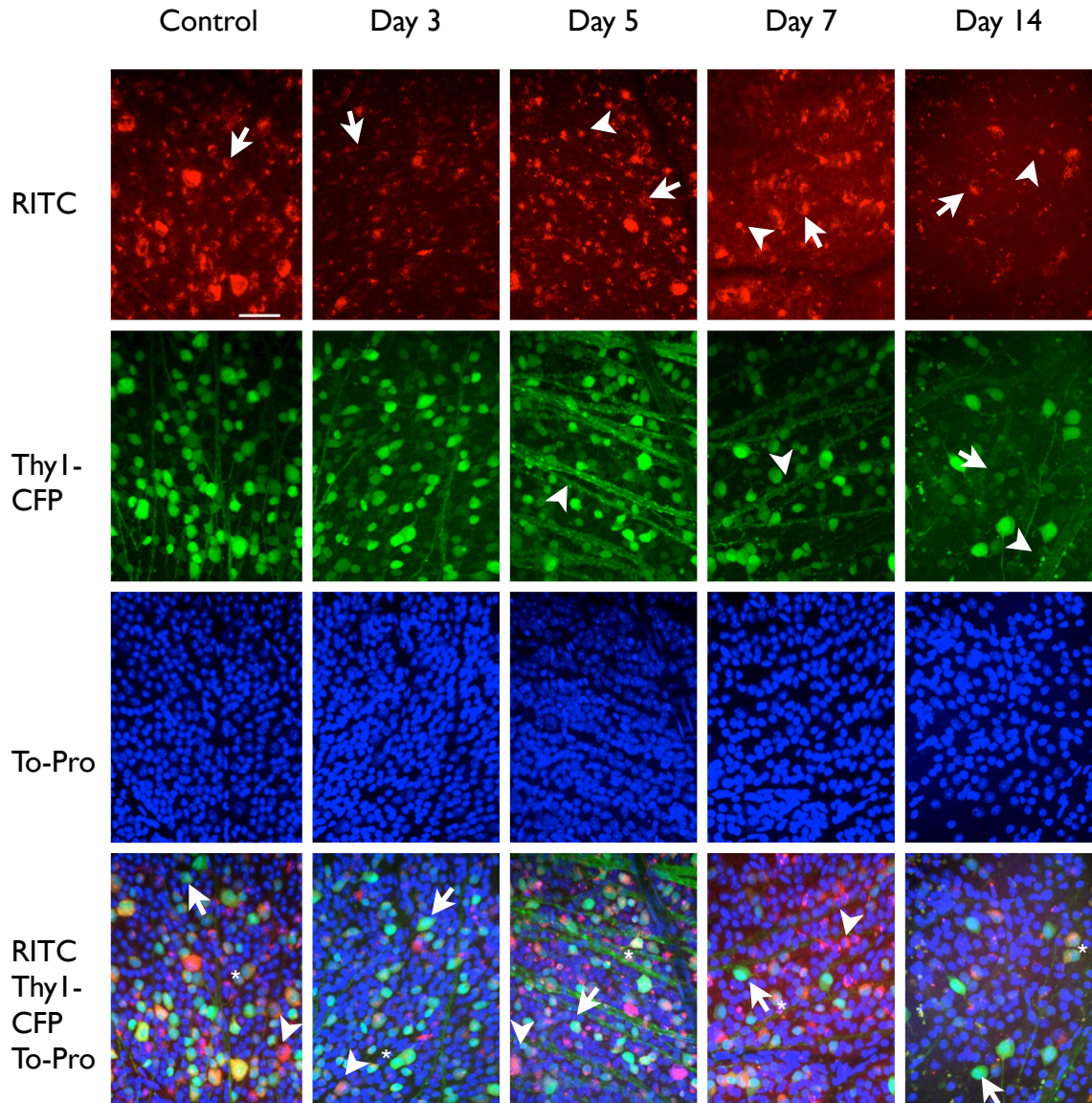


Figure 3.15 - Thy1-CFP⁺/RITC⁺ retinal wholemount images of control and ONC Thy1-CFP transgenic mice

RITC labeling of cells decreases after ONC. In healthy cells RITC appears in vesicles within the cytoplasm (arrow) while after injury RITC may appear as debris (arrow head). Thy1-CFP can be found in the cytoplasm of cells after injury (arrow) and axonal blebbing can be observed (arrowhead). In triple labeled images, some cells were Thy1-CFP⁺/RITC⁺ (star), while others were Thy1-CFP⁺/RITC⁻ (arrow) and Thy1-CFP⁻/RITC⁺ (arrow head). Scale bar = 50 μ m

Optic Nerve Transection

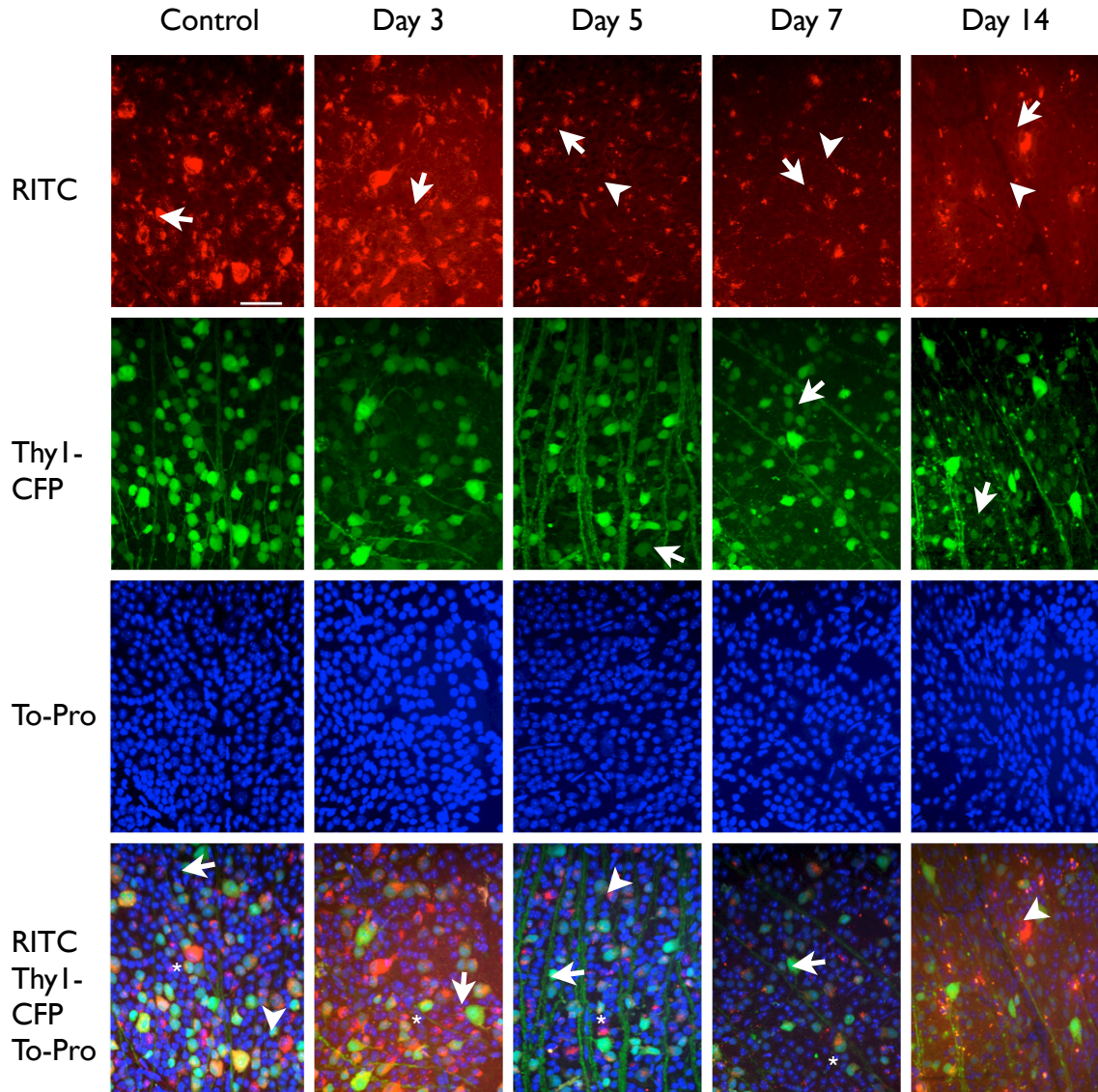


Figure 3.16 - Thy1-CFP⁺/RITC⁺ retinal wholemount images of control and ONT Thy1-CFP transgenic mice

RITC appears in vesicles within the cytoplasm (arrow) while after ONT RITC may appear as debris (arrow head) in dead and dying cells. Thy1-CFP expression changes from nuclear/cytoplasmic to solely cytoplasmic in some cells after ONT (arrow). In triple labeled images, some cells were Thy1-CFP⁺/RITC⁺ (star), while others were Thy1-CFP⁺/RITC⁻ (arrow) and Thy1-CFP⁻/RITC⁺ (arrow head). Scale bar = 50 μ m

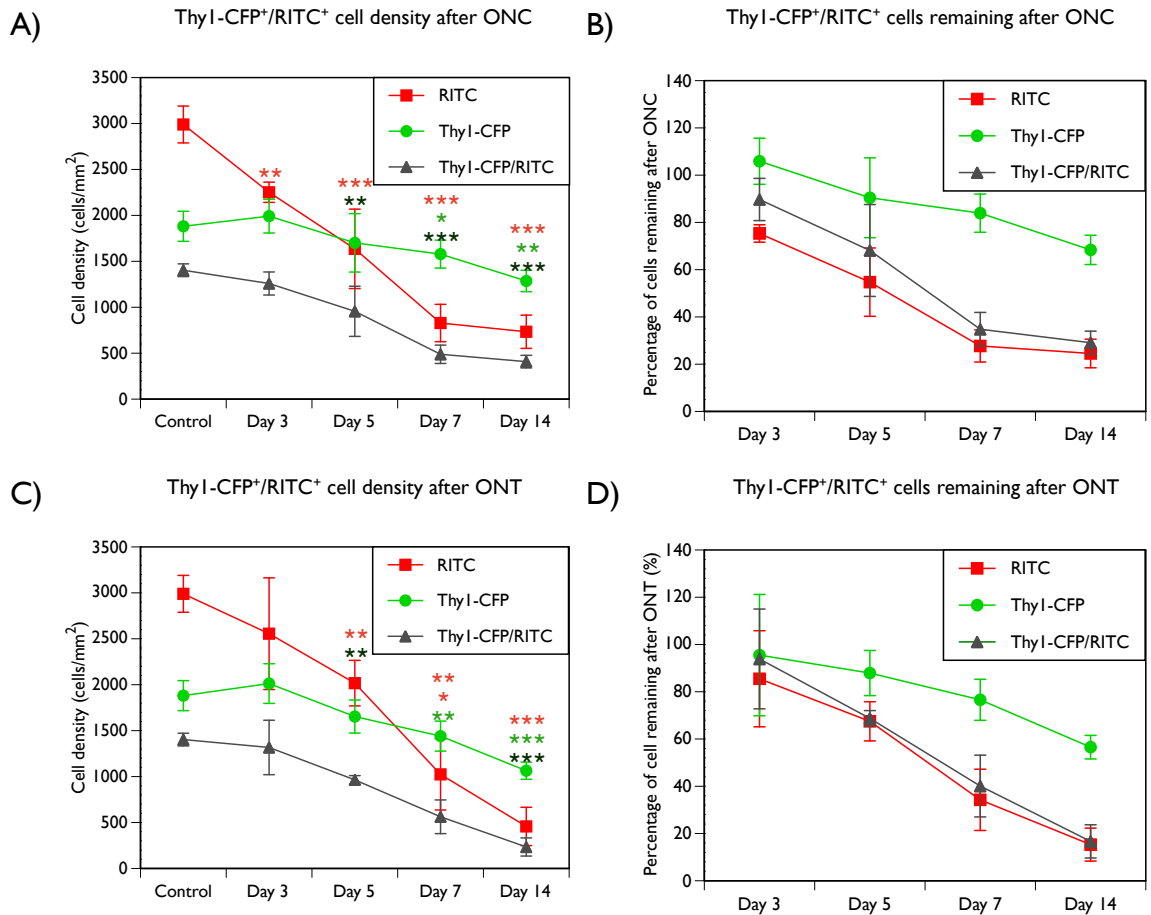
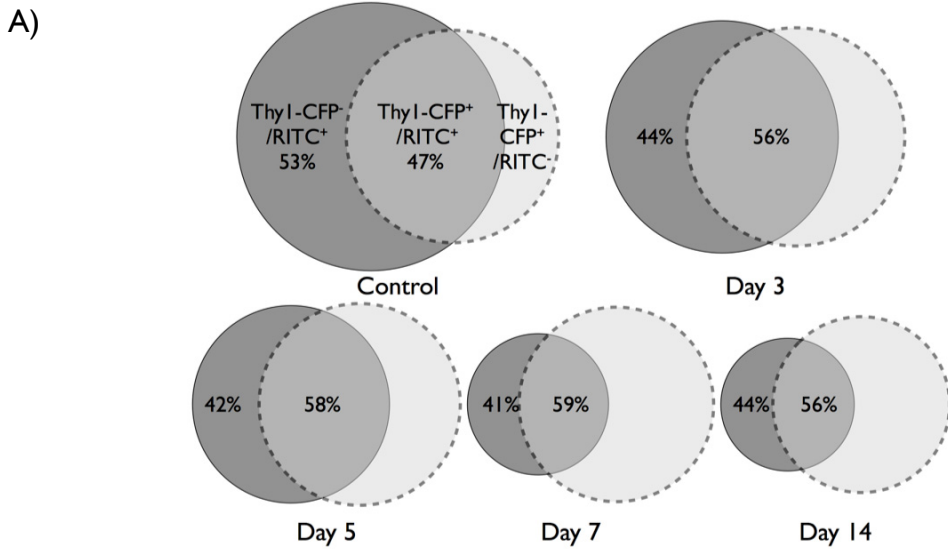


Figure 3.17 - Thy1-CFP⁺/RITC⁺ cell density after ON injury in Thy1-CFP transgenic mice

Thy1-CFP⁺/RITC⁺ cell density decreases in a time dependent manner after A) ONC and C) ONT in the Thy1-CFP transgenic mouse. Thy1-CFP⁺/RITC⁺ cell density decreases at a similar rate as RITC⁺ cell density after B) ONC and D) ONT.

Statistically significant when compared to the control group. MANOVA test * $P < 0.05$, ** $P < 0.005$, *** $P < 0.005$

Optic Nerve Crush



Optic Nerve Transection

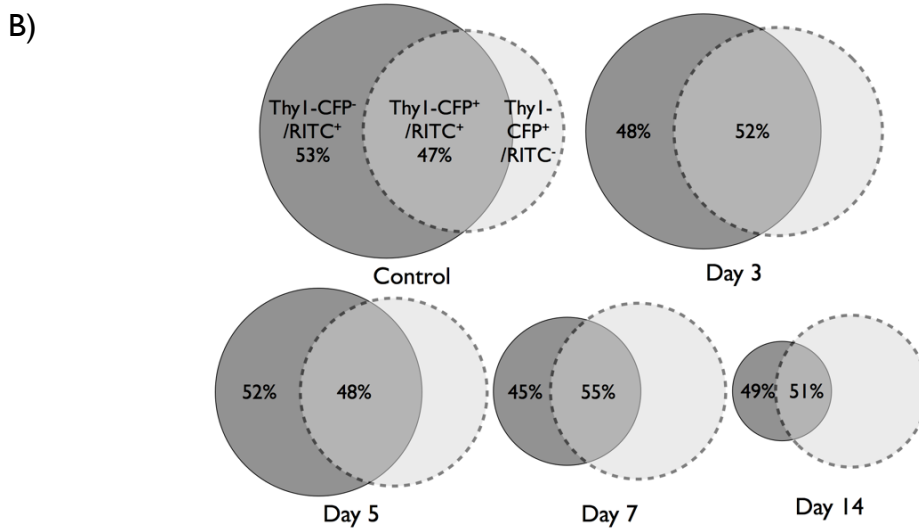
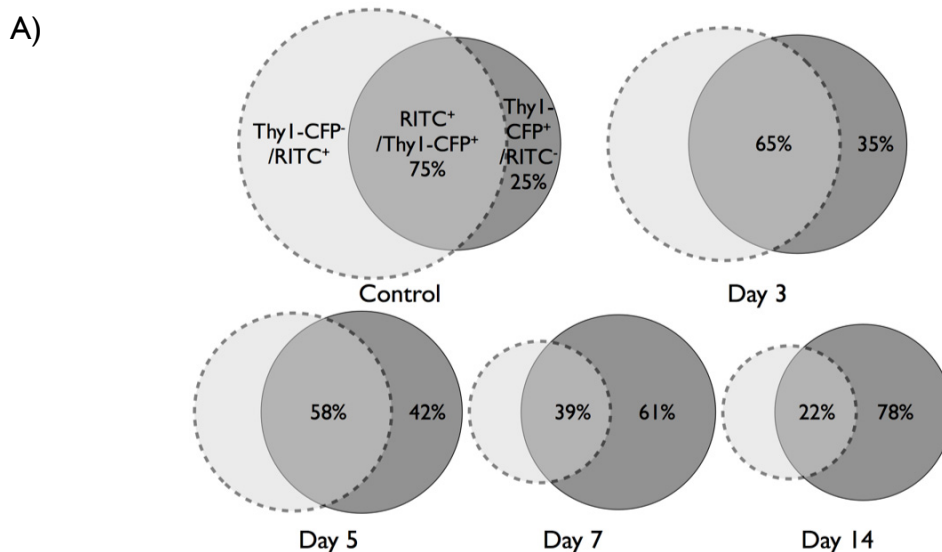


Figure 3.18 - Venn diagrams of Thy1-CFP expressing RGCs

These Venn diagrams are representative of the total cell population labeled by RITC (dark circles) and Thy1-CFP (light circles). The overlap between RITC⁺ and Thy1-CFP⁺ cell density is representative of the Thy1-CFP⁺/RITC⁺ cell density. As cell density decreases, the Venn diagrams also decrease proportionally when compared to the control cell population. After A) ONC and B) ONT, the proportion of RITC⁺ cells that express Thy1-CFP⁺ remains relatively the same.

Optic Nerve Crush



Optic Nerve Transection

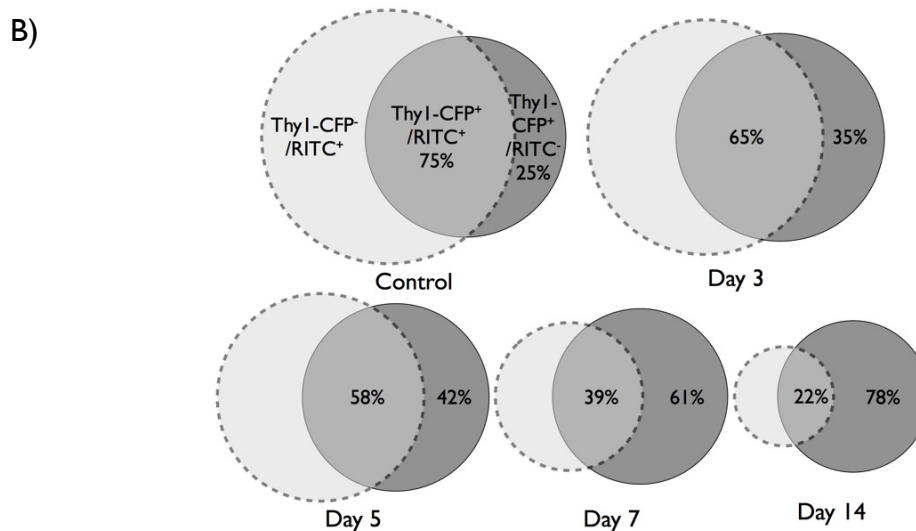


Figure 3.19 - Venn diagrams of Thy1-CFP confirmed RGCs

These Venn diagrams are representative of the total cell population labeled by RITC (light circle) and Thy1-CFP (dark circle). The overlap between RITC⁺ and Thy1-CFP⁺ cell density is representative of the Thy1-CFP⁺/RITC⁺ cell density. As cell density decreases, the Venn diagrams also decrease proportionally when compared to the control cell population. After A) ONC and B) ONT, proportion of Thy1-CFP⁺ cells that are confirmed RGCs labeled by RITC decreases.

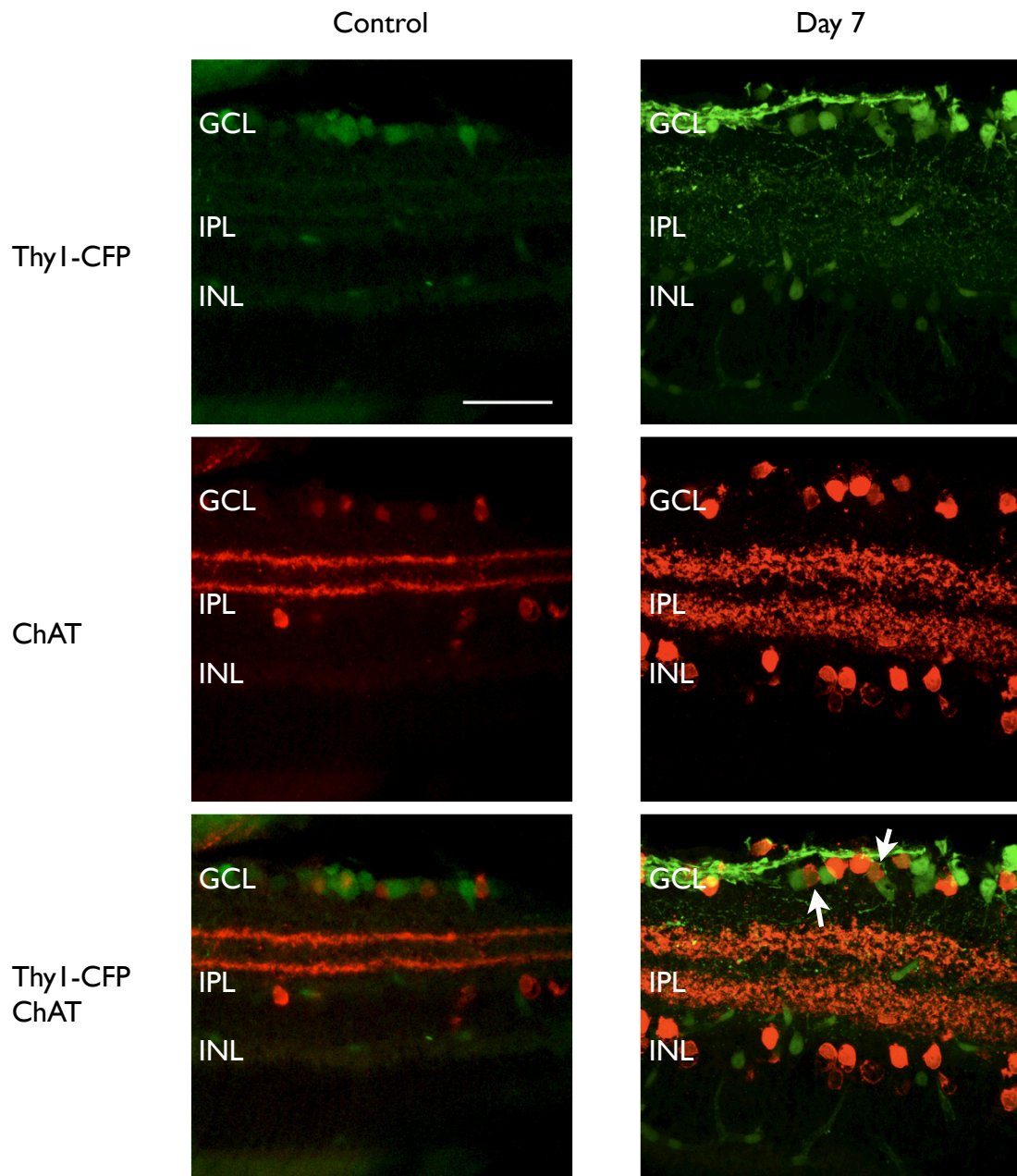


Figure 3.20 - Cross sections of Thy1-CFP mouse retinas labeled with ChAT

Thy1-CFP is mostly expressed in the GCL in control mice and few cells co-localize with ChAT. After ONT, Thy1-CFP is expressed in the GCL and INL.

Thy1-CFP co-localizes with ChAT in cells within the GCL (arrow), this co-localization is mostly seen in weakly expressing Thy1-CFP⁺ cells. Scale bar = 50 μ m

CHAPTER 4: DISCUSSION

Currently, one of the most common methods of RGC identification is by surgically labeling the SC, where ~96% of mouse RGCs project.⁸⁹ This method of retrograde labeling has its challenges, since it requires the surgical application of the neuronal tracer to the SC and prolonged time for transport of the label to RGCs.²⁵ Fading, leakage or degradation of the tracer can occur once in RGCs and the label can be transported through gap junctions into cells within the INL, thus identifying cells in a non-RGC specific manner.^{27, 30} Therefore, new markers and methods of identifying RGCs in a better way has been at the forefront of retinal research for many years.

Every type of neuron, including RGCs, has a specific set of proteins that is expressed within it, thus creating specialized cells with unique functions. This protein expression varies throughout the lifetime of the cell, during development,⁵⁶ survival,⁹⁰ immune response⁹¹ and death.⁹² Immunohistochemistry and transgenic mice has been utilized as tools to identify certain cell types including RGCs.^{23, 53, 57, 93, 94} The use of proteins such as Brn3a and Thy1-CFP to identify RGCs has the potential to be an ideal marker that can clearly and reliably label only and all RGCs in uninjured and ON injured mice, making the search of a viable RGC protein marker a desirable goal for many retinal research laboratories.

The goal of this project was to assess the use of Brn3a and Thy1-CFP expression as potential markers of RGCs in uninjured and ON injured retinas. The Brn3a protein is currently used as an RGC marker in rats¹⁹ and mice.⁵⁷ However the analysis of Brn3a as an RGC marker in mice by co-localization of a neuronal tracer to identify if Brn3a is solely labeling RGCs has yet to be done. Thy1-CFP is expressed in a transgenic mouse line that transcribes the fluorophore CFP under a modified Thy1 promoter.⁶⁵ Thy1-CFP transgenic mice are currently being used in *in vivo* longitudinal studies of RGCs.⁵⁹ However the effects of ON injury on Thy1-CFP⁺ cell density has yet to be fully analyzed. We wanted to assess the expression of these proteins in both control and ON injured

mice. The ON injuries, ONC and ONT, are both well documented and result in loss of RGCs.

4.1 RITC as a neuronal tracer of RGCs

4.1.1 - RITC labeling in uninjured control mice

Not all neuronal tracers have the same function or utility. FG is a neuronal tracer with a low molecular weight which can be easily transported to the cell soma of RGCs.²⁵ However it is also diffused through gap junctions into cells within the INL.²⁷ DiI is a heavy molecular weight neuronal tracer which is slowly transported to the cell soma and diffuses throughout the cytoplasm.²⁵ Diffusion of DiI is an advantage since it clearly fills cells making them easy to count. However, it can also be a disadvantage since DiI can diffuse in fixed tissue resulting in high background and labeling of other cells.³¹

We have used RITC as our neuronal tracer. RITC had to be analyzed in uninjured animals and for the duration of the timeline to assure that it was a viable neuronal tracer for the parameters of this study. By analyzing RITC in uninjured animals we were able to identify the characteristics of RITC labeling in healthy cells. Since ON injury disrupts transport, it is important to identify the required time for the retrograde transport of the tracer to reach the RGCs that

project to the SC. Therefore if any cells were not labeled prior to the injury, they would remain unlabeled after the injury.

We have shown in uninjured mice that RITC can be used as a neuronal tracer at 7 days after SC labeling. By 7 days after SC surgery, RITC⁺ cell densities were similar to other published RGC cell densities using neuronal tracers.^{7, 57} With these results, we determined that most RGCs were labeled with RITC by 7 days after SC labeling.

Since we caused an injury at 7 days after SC labeling and the last post-ON injury time point was 14 days after ON injury, the SC labeling must remain in RGCs for a total duration of 21 days after SC labeling. We speculated that RITC remains within the cell and would not fade for the duration of the experimental timeline since RITC has been shown to remain in RGCs of rats for 30 days.²⁰

To prove this, we have shown that the cell density of RITC at 7 and 21 days post-SC labeling surgery are similar. If RITC was being transported into other cells or fading over time we would expect a change, either an increase or decrease, in RITC⁺ cell density. This was not observed with these control experiments. RITC is qualitatively characterized by vesicular labeling within the cytoplasm of RGCs at both 7 and 21 day time points. If fading or a change in the labeling was present we would have expected the qualitative characteristics of RITC labeling to change over time and the quantitative cell densities to be

different at 7 and 21 day time points which was not observed in our RITC control experiments.

Therefore, we believe that RITC labels RGCs that project to the SC by 7 days after labeling surgery and remains within all cells until 21 days after labeling.

4.1.2 - RITC labeling after ON injury

We wanted to further assess RITC by analyzing the cell density of RITC labeled retinas in ON injured mice to assure that RITC labeling continued to label RGCs in a similar manner as uninjured mice. Because RITC⁺ cell density in uninjured control mice was similar to published densities, we postulate that RITC⁺ cell density would be similar to those previously published after ONC and ONT.

We have demonstrated that RITC⁺ cell density decreases after ONC and ONT in both C57BL/6 mice and Thy1-CFP transgenic mice. We have shown that RITC⁺ cell density decreases from 100% to 7% cell survival in C57BL/6 and from 100% to 25% cell survival in Thy1-CFP transgenic mice 14 days after ONC. ONC can vary from experimenter to experimenter since the force used to crush the nerve can change the amount of damage caused to the ON. Higashide et al. reported 70% and 30% of cell survival 7 and 28 days after ONC respectively⁹⁵

while Levkovitch-Verbin et al. reported 20% cell survival 14 days after ONC.⁹⁶

Our results are in agreement with those found by Levkovitch-Verbin *et al.*.

We have also shown that RITC⁺ cell density significantly decreases from 100% to 8% cell survival in C57BL/6 mice and from 100% to 15% cell survival in Thy1-CPF transgenic mice 14 days after ONT. Since ONT is performed by completely severing the ON, this technique is repeatable from experimenter to experimenter. Our ONT values are in agreement with other published results that have shown ~95%, ~50%, ~30%, 20% and ~15% cells survived respectively 2, 5, 7, 9, and 14 days after ONT by manual count of the OHSt⁺ cells, a neuronal tracer derivative of FG.⁵⁷ These results suggests that RITC is a reliable neuronal tracer that can be used for labeling of RGCs after ONT.

Further analysis of RITC labeling after ON injury has shown vesicularized RITC within healthy cells while appearing with condensed cytoplasm in damaged and dying cells. It has been demonstrated that dying RGCs become phagocytosed by microglial cells.⁸⁹ We have shown RITC labeled spindle-like shaped cells, microglial cells, after ON injury within the GCL. We suggest that RITC debris represents somal atrophy prior to being phagocytosed by microglial cells and that these RITC labeled microglial cells could be identified by their spindle-like shaped and non-vesicularized RITC labeling.

4.2 Brn3a labeling of cells in the GCL

4.2.1 Brn3a⁺ cell density in control retinas

In order to validate Brn3a as a potential RGC marker, we wanted to determine the effectiveness of Brn3a labeling in control mice. We have shown with manual cell counting that Brn3a⁺ cell density in control mice is ~30% less than RITC⁺ cell density. Brn3a⁺ cell density in the mouse retina was first analyzed by Xiang *et al.* who demonstrated that Brn3a is expressed in ~35% of cells in the GCL.⁹⁷ With this finding, we can approximate the quantity of RGCs that express Brn3a. If we assume that Brn3a is only expressed in RGCs and ~50% of the GCL are RGCs, we can approximate that 70% of RGCs express Brn3a. Conversely, Galindo *et al.* estimated 85% of the RGC population expresses Brn3a in mice using whole cell population and automated cell counting.⁵⁷ Recently published results have shown Brn3a⁺ cell densities of ~2100 cells/mm² which is similar to our findings in control mice.⁹⁸ Our results have shown that ~70% of RGCs express Brn3a if we assume that Brn3a is uniquely expressed in RGCs and that our RITC⁺ cell density represents all RGCs. Our result is in agreement with the estimation by Xiang *et al.* stated above therefore we speculate that Brn3a is expressed in a sub-population of RGCs in control mice.

This theory was analyzed by comparing the proportion of RITC⁺/Brn3a⁺ cells to the individual Brn3a⁺ and RITC⁺ cell densities. If Brn3a is labeling a subpopulation of RGCs then we would expect 100% of Brn3a⁺ cells to be labeled by RITC in control mice. If Brn3a is expressed in other cells then we would expect a portion of Brn3a⁺ cells not to be labeled by RITC. With the analysis of RITC⁺/Brn3a⁺ cells in control retinas we have shown that of all Brn3a⁺ cells, ~76% of cells are RITC⁺. This means that 24% of Brn3a⁺ cells are not labeled by RITC and therefore could be either RGCs that do not project to the SC or other cells of the GCL, for example, amacrine cells. We have also shown that 54% of RITC⁺ cells express Brn3a. This means that when uniquely using Brn3a immunohistochemistry as an RGC marker, approximately half of all RGCs express Brn3a while the remainder is unaccounted for. These were contrasting results from Galindo-Romero who found approximately 85% of all Brn3a⁺ cells co-localized with the neuronal tracer OHSt. Our results may have been different due to our blinded method of double labeling cell counting or our image sampling method.

4.2.2 Brn3a⁺ cell density in ON injured mice

We have demonstrated that RITC⁺ cell density significantly decreases at all time points after ONC and ONT. However, Brn3a⁺ cell density remains relatively

the same in control and the day 3 time point and begins to significantly decrease 5 days after ON injury. Brn3a⁺ cell density does not immediately decrease after injury, Brn3a⁺ and RITC⁺ cell density between 5 and 14 days after ON injury are very similar. RITC⁺ cell density may be decreasing at a faster rate because a portion of RGCs are more vulnerable to ONC and ONT and these cells do not express Brn3a and therefore die before Brn3a⁺ cells die. Our Brn3a⁺ cell densities are similar to published results of Brn3a⁺ cell densities after ONT in mice.⁵⁷ Published data has also shown that Brn3a⁺ cell density significantly decreased 5 days after ONT. However, when using OHSt⁺ as the neuronal tracer it was found that the Brn3a⁺ cell density was significantly lower than OHSt⁺ cell densities at all time points post-lesion.⁵⁷

Brn3a protein expression showed a significant decrease 3 days after ONT which suggests that although Brn3a is expressed in the same quantity of cells in uninjured and day 3 ON injured retinas, the quantity of Brn3a protein within each cell has already reduced from the uninjured state 3 days after ONT.

Cumulatively, the cell density tabulated from RGCs that express Brn3a suggest the following three possibilities: (1) Brn3a is expressed in a subpopulation of RGCs that are pro-survival and consequently have a delayed reaction to the ON injury (2) Brn3a expression may change after ON injury and begin to be expressed in different cells of the GCL, for example, amacrine cells (3)

Brn3a is expressed in RGCs that do not project to the SC and these RGCs have a higher survival rate than RGCs that project to the SC.

(1) In control mice we found ~24% of Brn3a⁺ cells were not labeled by RITC. However, our Brn3a⁺/RITC⁺ data represent healthy RGCs that express Brn3a. Therefore, is it possible that some Brn3a⁺ cells had condensed RITC appearing as debris and were not counted as a Brn3a⁺/RITC⁺ cells. The identification of a dying cell solely using Brn3a was not possible since the Brn3a⁺ cells always had nuclear expression of the protein in control and ON injured mice therefore, cell morphology could not be observed. However, Brn3a expression was also identified in cells with condensed RITC labeled somas and in cells with condensed chromatin which was observed with To-Pro staining. Transgenic mouse studies of knockout Brn3a mice were used to study the function of Brn3a expression and its role as a transcription factor for neurotrophic tyrosine kinase receptor type 1 (TrkA), the receptor for nerve growth factor (NGF).⁹⁹ These studies have shown that loss of Brn3a results in reduced transcription of TrkA consequently resulting is less TrkA/NGF interactions.¹⁰⁰ In rats, intraocular injection of NGF was found to promote the survival of RGCs after ONT for at least 7 weeks after the injury.¹⁰¹ A normal response to a change in homeostasis, such as ONT, could be an up regulation

or conservation of the transcription of TrkA receptor in order to increase the likelihood of receptor-ligand binding of NGF at the cell surface. This possibility is further supported by our qualitative evidence showing Brn3a expression in cells that have condensed RITC labeling. This may suggest that Brn3a is a pro survival protein that can be expressed in dying cells.

(2) If Brn3a expression remains only in RGCs after ON injury, we would expect 100% of Brn3a⁺ cells to be labeled by RITC. However we have already shown in control mice that 76% of Brn3a⁺ cells are RITC⁺ while the remaining 24% are cells that are Brn3a⁺ but not labeled by RITC. Therefore we suggest that Brn3a may be labeling RGCs and other cells after ON injury.

We have shown that the RITC⁺ cell density decreases at a slower rate than the Brn3a⁺ cell density after ON injury. Five days after ON injury ~60% of Brn3a⁺ cells had survived while ~40% of RITC⁺ cells had survived. We believe that the cause of this difference in cell death rates between the Brn3a⁺ and RITC⁺ cell densities may be due to Brn3a⁺ cells that are amacrine cells since amacrine cells die at a slower rate than RGCs after ON injury.¹⁰² If amacrine cells are being labeled by Brn3a, then these cells would not be labeled by RITC. Therefore the analysis of the rate of cell loss of cells that are both Brn3a⁺ and RITC⁺ may indicate whether Brn3a is labeling other cells after ON injury. We

have shown that the cell population that were both Brn3a⁺ and RITC⁺ had a rate of cell loss after ON injury that was very similar to RITC⁺ rate since by 5 days after ON injury, ~40% of Brn3a⁺/RITC⁺ had survived. This suggests that the Brn3a⁺/RITC⁺ cells are comprised of a similarly heterogeneous population of RGCs as the RITC⁺ cells and that the Brn3a⁺ cells that were not labeled by RITC were the cause of the difference in rates of cell death between the total RITC⁺ and Brn3a⁺ cell densities.

We also found that the proportion of RITC⁺ cells that are also Brn3a⁺ gradually decreases after ON injury from 54% in control retinas to ~30% 14 days after ON injury. This means that of all RGCs, the quantity of Brn3a⁺ expressing RGCs decreases over time after ON injury. We have also shown that the proportion of Brn3a⁺ cells that are RITC⁺ decreases after ON injury from 76% in control retinas to ~20% 14 days after ON injury. This means that Brn3a is expressed in an increasing population of cells that are not labeled with RITC after ON injury. Therefore, when performing immunohistochemistry to identify Brn3a⁺ cells after ON injury, Brn3a is gradually labeling less RGCs and proportionally more cells that are not RITC⁺. Even though Brn3a expression has not been identified in the INL, together these novel findings suggest that Brn3a is expressed in RGCs and potentially other cells after injury.

(3) Brn3a has been found in RGCs that project to the SC and the thalamus,⁵⁶ therefore it is possible that the RGCs that are surviving after ONC and ONT at the 3 day time point could be the RGCs that project to the thalamus. We found that of the RITC⁺ cell population, ~78% and ~62% of cells were RITC⁺ and did not express Brn3a 14 days after ONC and ONT, respectively. Approximately 4% of RGCs from the retina project to other areas of the brain.¹³ Although Brn3a could be expressed in RGCs that are not labeled with RITC, the proportion of these RGCs should be much smaller than the discrepancy found between RITC⁺ and Brn3a⁺ cell densities and Brn3a⁺/RITC⁺ cell density.

In brief, although Brn3a may label RGCs that are unlabeled by RITC, the discrepancy is most likely due to a combination of factors. However the most notable factor is that Brn3a may be labeling cells other than RGCs after injury.

4.3 Thy1-CFP expression in cells of the GCL

4.3.1 Thy1-CFP⁺ cell density in control retinas

In control retinas of Thy1-CFP transgenic mice, Thy1-CFP⁺ cell density was ~37% lower than RITC⁺ cell density. Therefore, in the control retina

Thy1-CFP⁺ cell density is significantly lower than RITC⁺ cell density. If Thy1-CFP was used as the sole RGC cell density marker, Thy1-CFP would give a significantly lower cell density than the true RGC cell density in control retinas. The effectiveness of Thy1-CFP to label 100% of RGCs within the GCL layer can be further analyzed by assessing the proportion of RITC⁺ cells that express Thy1-CFP, which indicates how many RGCs express Thy1-CFP. Our results showed that ~50% of RITC⁺ cells expressed Thy1-CFP in control Thy1-CFP transgenic retinas which means that Thy1-CFP is not expressed in all RGCs. These are contrasting results to Raymond *et al.* who estimated approximately 80% of RGCs in control retinas were Thy1-CFP⁺ cells.¹⁰³ However, Raymond *et al.* did not use a neuronal tracer as an RGC marker and there is no known immunohistochemical marker that can be used to solely and reliably identify all RGCs.

We have already shown that Thy1-CFP is not expressed in all RGCs. Since the Thy1 protein has been found in Müller cells¹⁰⁴ and amacrine cells,⁴⁸ we speculate that Thy1-CFP may not be uniquely expressed in RGCs. This deduction was analyzed by looking at the proportion of cells that are Thy1-CFP⁺ cells and are labeled by RITC. This showed the proportion of Thy1-CFP⁺ cells that are RGCs and the proportion of cells that are not confirmed RGCs. If Thy1-CFP is solely expressed in RGCs, we would expect 100% of Thy1-CFP⁺ cells to be RITC⁺.

We have shown that 75% of Thy1-CFP⁺ cells are RITC⁺ in control retinas of Thy1-CFP transgenic mice, therefore 25% of cells are not RGCs that project to the SC. This means that 25% of Thy1-CFP⁺ cells in control mice are either (1) a portion of RGCs that project to other areas of the brain or (2) other cells of the GCL, for example, amacrine cells, thus supporting our previous theory stated above. This can be further analyzed by assessing Thy1-CFP expression after ON injury.

4.3.2 Thy1-CFP⁺ cell density in ON injured retinas

After an injury, an immune response is inevitable. Consequently, a change in protein expression is not uncommon. Due to the ubiquitous nature of Thy1, any perturbation of homeostasis may trigger a change in the expression of Thy1 and thus the potential up regulation of Thy1-CFP. It has been demonstrated that Thy1 mRNA is down regulated after ONC or N-Methyl-D-Aspartic acid (NMDA) injection.⁵⁰ Cumulatively, we hypothesize that Thy1-CFP expression pattern changes after injury.

We have also demonstrated that Thy1-CFP cell morphology changes after ON injury. In control mice Thy1-CFP is expressed in both the cytoplasm and nucleus while in the injured retina, some cells solely express Thy1-CFP in the cytoplasm suggesting that Thy1-CFP expression changes after ON injury. This

argument is further supported by our quantitative data of the individual Thy1-CFP⁺ and RITC⁺ cell densities. If Thy1-CFP is expressed in amacrine cells, we would expect the Thy1-CFP cell density to decrease at a slower rate than RITC since amacrine cells die at a slower rate than RGCs after ON injury.¹⁰² After ON injury, the RITC⁺ cell density begins to gradually decrease almost immediately after insult while the Thy1-CFP⁺ cell density remains relatively unchanged until 7 days after ON injury. The Thy1-CFP⁺ cell density after ON injury is markedly different from RITC⁺ cell density. In uninjured control retina, Thy1-CFP⁺ cell density is ~37% lower than RITC⁺ cell density and by 14 days after ON injury Thy1-CFP⁺ cell density is ~43% higher than RITC⁺ cell density. Therefore, Thy1-CFP⁺ cells have a much slower rate of cell loss than RITC⁺ cells.

Cumulatively these novel findings suggest that Thy1-CFP is either expressed in an increasingly heterogeneous population of cells after ON injury or CFP is taken up by either gap junction or transcytosis in a non-RGC specific manner. This was further analyzed by looking at the proportion of Thy1-CFP⁺ cells that were also RITC⁺. If all Thy1-CFP⁺ cells are RGCs after injury we would expect nearly 100% of Thy1-CFP⁺ cells to be RITC⁺.

We have shown that Thy1-CFP⁺/RITC⁺ cell density gradually decreases after ON injury. Thy1-CFP⁺/RITC⁺ cell density was significantly lower than the individual RITC⁺ and Thy1-CFP⁺ cell densities. Approximately 50% of

Thy1-CFP⁺ cells were RITC⁺ at every time point after ON injury. This indicated that Thy1-CFP is expressed in a subpopulation of RGCs however we have shown that Thy1-CFP is also expressed in an increasing population of Thy1-CFP⁺ cells that are not labeled by RITC⁺. This means that after ON injury there was an increasing number of cells that express Thy1-CFP that were not RGCs that project to the SC. Qualitative analysis of retinal cross sections also demonstrated a marked change in Thy1-CFP expression. In uninjured control retinal sections, Thy1-CFP⁺ cells were mainly found in the GCL while after ON injury, Thy1-CFP⁺ cells were found in both the INL and the GCL.

Collectively, we postulate that Thy1-CFP is expressed in amacrine cells after injury since the population of Thy1-CFP⁺ cells that were not labeled by RITC increased after injury.

With ChAT immunohistochemistry, we detected cholinergic amacrine cells co-localized with Thy1-CFP⁺ cells in 7 day ONT retinal cross sections. This finding confirmed our belief that Thy1-CFP is expressed in amacrine cells after injury. These findings were in agreement with previously published data from Raymond *et al.*¹⁰³

In summary, these results demonstrate that Thy1-CFP is only expressed in ~50% of all RGCs. Thy1-CFP expression changes after ON injury and is expressed in cholinergic amacrine cells in ON injured mice. Thy1-CFP⁺ cell

density does not reflect the RGC cell density identified with the neuronal tracer RITC and should not be used as a marker of RGCs in uninjured or ON injured mice.

4.4 Limitations

4.4.1 Cell counting

The entirety of the quantitative data for this project was obtained by manual cell counting of images. Although this method is used by many researchers, manual cell counting can be subjective which may skew some cell counts. The subjectivity of the manual cell counting was limited by masking the images to the experimenter which meant that the degree of damage of the retina was unknown. We also used a sampling method to obtain our images used for cell counting, thus not counting all cells of the retina but resulting in an estimation of the cell density of the retina. This meant that a large portion of the retina remained uncounted and therefore the cell density measurements are an estimate of the total cell density of the retina.

4.4.2 ON injury

In both the ONC and ONT, the distance at which the injury is made can affect the speed at which RGCs will die.^{69, 105} The further the injury is made from the eye, the longer it will take for RGCs to die. With ONT, the ON was completely severed however with ONC, the damage to the ON can have more variability since the amount of time the crush lasts may vary slightly, resulting in varying degrees of damage between mice. The variability of the ONC injury may account for the larger standard deviations in cell densities found for ONC mice.

4.4.3 Retrograde labeling

Retrograde labeling is the standard method of labeling RGCs, however it can be a technically challenging surgery. In order to properly label the SC, the entire area must be completely exposed. A blood clot or remaining cortex could impede the transport of the neuronal tracer to RGC cell bodies in the retina. If transport is impeded, the neuronal tracer may only label a portion of RGCs which can be observed as patchy labeling. These technical limitations can affect the transport of RITC thus making it appear that the RITC⁺ cell density is lower than it truly is. If patchy labeling was identified in this study, these retinas were discarded.

4.4.4 Animal variance

The Thy1-CFP mouse is a transgenic mouse line that was bred within the Carlton Animal Care Facility at Dalhousie University. When breeding transgenic mice, there can be some variability between first generation animals and last generation animals which can result in animal variability within this study.

The Thy1-CFP transgenic mouse retinas express Thy1-CFP in cells within the GCL however they also express CFP in axons. In the retina, axons are densely packed around the ON head, where RGC cell density is greatest. These fluorescent axons may have impeded the cell counting of images where axons were predominant. However, to aid in the visualization of cells where axons were obstructing the view of cells, a z-stack of the area counted was taken in order to better visualize images at different levels below the NFL.

4.5 Future work

With this thesis, we have demonstrated that Brn3a is only expressed in ~54% of RGCs in uninjured mice and this proportion gradually decreases to ~30% 14 days after ON injury. This suggest that Brn3a is only expressed in a small proportion of RGCs. We have also demonstrated that of all Brn3a⁺ cells, ~76% are RGCs in uninjured mice however this proportion gradually decreases to ~20% by 14 days after ON injury. This suggests that after injury the quantity of

Brn3a⁺ cells that are RGCs significantly decreases and that Brn3a may be expressed in other cells such as amacrine cells. Further research could examine if Brn3a co-localizes with other cell markers, for example, amacrine cell markers. We have also demonstrated that Brn3a cell density remains relatively unchanged until 5 days after ON injury which we have speculated may be due to a possible pro-survival property of the Brn3a protein. Further research could try to identify if Brn3a has a pro-survival role via TrkA expression after ON injury in the C57BL/6 mouse. This may help to further understand the functional role of Brn3a in ON injured mice.

Further research using the Thy1-CFP mouse may assess the function of Thy1 in the retina after injury, since Thy1 is not a well understood protein. More research may also be done to assess if Thy1 is expressed in other amacrine cells or Müller cells after ON injury.

4.6 Significance

The measure of RGC cell density remains one of the most useful tools in retinal research to measure damage and vision loss in a laboratory setting. By analyzing Brn3a⁺ and Thy1-CFP⁺ cell density and comparing to a neuronal tracer such as RITC, we were able to assess the cell specificity of these markers in control and ON injured mice making this work novel. With this work, we were

able to provide a better insight of Brn3a and Thy1-CFP expression patterns after ON injury.

An ideal RGC marker would be minimally invasive, label most RGCs, would not label other cells within the GCL, remain solely in RGCs after retinal injury and only identify viable RGCs. An ideal marker may be an immunohistochemical marker since there is no fading of the marker over time and labeling does not need to be performed prior to injury. However, our findings have shown that Brn3a is expressed in a small portion of RGCs, its expression pattern changes after ON injury and its cell density changes after ON injury in mice.

These novel findings will allow others to have a better understanding of what cells are visualized when using Thy1-CFP transgenic mice for *in vivo* retinal research. Protein expression patterns can change after insult resulting in protein expression in cells that were not previously labeled. Therefore caution should be used when using immunohistochemical markers to identify RGCs.

4.7 Conclusion

Brn3a⁺ labels only ~54% of RGCs in uninjured mice. It is believed that it may label other cells after injury since the proportion of cells that are Brn3a⁺ and not labeled by RITC increases after ON injury which means that the population

of cells that are not confirmed RGCs increases after ON injury. Although Brn3a may be expressed in cells that project to other areas of the brain, the quantity of cells that are Brn3a⁺ but not RITC⁺ is too great to be solely RGCs that project to other areas of the brain. These results suggest that further use of Brn3a as an RGC marker in injured retinas should be used with caution since Brn3a does not appear to be unique to RGCs.

Brn3a expression at cellular level is down regulated immediately after ON injury. However it remains expressed in the same quantity of cells for a long period of time before cells die possibly indicating that Brn3a may have a pro-survival effect in cells of the GCL.

Thy1-CFP⁺ cell density was significantly lower than RITC⁺ cell density in uninjured retinas. Thy1-CPF transgenic mice express Thy1-CFP in ~50% of RITC⁺ cells however it is also expressed in an increasing population of other cells after ON injury. Thy1-CPF is not a useful tool in quantifying RGC cell density and should only be used as a tool to observe all cells within the GCL since its expression is non-specific, particularly after ON injury.

Based on these findings, labeling of the SC with a neuronal tracer remains the most accurate method of identifying RGCs in uninjured and ON injured mice.

BIBLIOGRAPHY

1. The cost of vision loss in Canada. Report by Access Economics Pty Limited for the CNIB and the Canadian Ophthalmological Society; 2009.
2. Quigley HA. Neuronal death in glaucoma. *Prog Retin Eye Res* 1999;18:39-57.
3. Kuehn MH, Fingert JH, Kwon YH. Retinal ganglion cell death in glaucoma: mechanisms and neuroprotective strategies. *Ophthalmol Clin North Am* 2005;18:383-395, vi.
4. Levin LA, Louhab A. Apoptosis of retinal ganglion cells in anterior ischemic optic neuropathy. *Arch Ophthalmol* 1996;114:488-491.
5. Farkas RH, Grosskreutz CL. Apoptosis, neuroprotection, and retinal ganglion cell death: an overview. *Int Ophthalmol Clin* 2001;41:111-130.
6. Soto I, Oglesby E, Buckingham BP, et al. Retinal ganglion cells downregulate gene expression and lose their axons within the optic nerve head in a mouse glaucoma model. *J Neurosci* 2008;28:548-561.
7. Wang X, Archibald ML, Stevens K, Baldrige WH, Chauhan BC. Cyan fluorescent protein (CFP) expressing cells in the retina of Thy1-CFP transgenic mice before and after optic nerve injury. *Neurosci Lett* 2010;468:110-114.

8. Chalupa LM, Williams, R. M. *Eye, retina and visual system of the mouse*: the mit press; 2008.
9. Murata H, Aihara M, Chen YN, Ota T, Numaga J, Araie M. Imaging mouse retinal ganglion cells and their loss in vivo by a fundus camera in the normal and ischemia-reperfusion model. *Invest Ophthalmol Vis Sci* 2008;49:5546-5552.
10. Neilsen GJT, MT. Principles of human anatomy. Wiley; 2009:702-710.
11. Kaufman PL, Alm, A. *Adler's physiology of the eye*. 10th ed: Mosby; 2003.
12. Plump AS, Erskine L, Sabatier C, et al. Slit1 and Slit2 cooperate to prevent premature midline crossing of retinal axons in the mouse visual system. *Neuron* 2002;33:219-232.
13. Salinas-Navarro M, Jimenez-Lopez M, Valiente-Soriano FJ, et al. Retinal ganglion cell population in adult albino and pigmented mice: a computerized analysis of the entire population and its spatial distribution. *Vision Res* 2009;49:637-647.
14. Hattar S, Liao HW, Takao M, Berson DM, Yau KW. Melanopsin-containing retinal ganglion cells: architecture, projections, and intrinsic photosensitivity. *Science* 2002;295:1065-1070.

15. Hattar S, Kumar M, Park A, et al. Central projections of melanopsin-expressing retinal ganglion cells in the mouse. *J Comp Neurol* 2006;497:326-349.
16. Nelson R. Visual Responses of Ganglion Cells. 1995.
17. Chiu K, Lau WM, Yeung SC, Chang RC, So KF. Retrograde labeling of retinal ganglion cells by application of fluoro-gold on the surface of superior colliculus. *J Vis Exp* 2008.
18. Salinas-Navarro M, Mayor-Torroglosa S, Jimenez-Lopez M, et al. A computerized analysis of the entire retinal ganglion cell population and its spatial distribution in adult rats. *Vision Res* 2009;49:115-126.
19. Nadal-Nicolas FM, Jimenez-Lopez M, Sobrado-Calvo P, et al. Brn3a as a marker of retinal ganglion cells: qualitative and quantitative time course studies in naive and optic nerve-injured retinas. *Invest Ophthalmol Vis Sci* 2009;50:3860-3868.
20. Thanos S, Vidal-Sanz M, Aguayo AJ. The use of rhodamine-B-isothiocyanate (RITC) as an anterograde and retrograde tracer in the adult rat visual system. *Brain Res* 1987;406:317-321.
21. Vidal-Sanz M, Villegas-Perez MP, Bray GM, Aguayo AJ. Persistent retrograde labeling of adult rat retinal ganglion cells with the carbocyanine dye diI. *Exp Neurol* 1988;102:92-101.

22. Selles-Navarro I, Villegas-Perez MP, Salvador-Silva M, Ruiz-Gomez JM, Vidal-Sanz M. Retinal ganglion cell death after different transient periods of pressure-induced ischemia and survival intervals. A quantitative in vivo study. *Invest Ophthalmol Vis Sci* 1996;37:2002-2014.
23. Kwong JM, Caprioli J, Piri N. RNA binding protein with multiple splicing: a new marker for retinal ganglion cells. *Invest Ophthalmol Vis Sci* 2010;51:1052-1058.
24. Wessendorf MW. Fluoro-Gold: composition, and mechanism of uptake. *Brain Res* 1991;553:135-148.
25. Kobbert C, Apps R, Bechmann I, Lanciego JL, Mey J, Thanos S. Current concepts in neuroanatomical tracing. *Prog Neurobiol* 2000;62:327-351.
26. Thanos S, Pavlidis C, Mey J, Thiel HJ. Specific transcellular staining of microglia in the adult rat after traumatic degeneration of carbocyanine-filled retinal ganglion cells. *Exp Eye Res* 1992;55:101-117.
27. Abdel-Majid RM, Archibald ML, Tremblay F, Baldrige WH. Tracer coupling of neurons in the rat retina inner nuclear layer labeled by Fluorogold. *Brain Res* 2005;1063:114-120.
28. Schmued LC, Fallon JH. Fluoro-Gold: a new fluorescent retrograde axonal tracer with numerous unique properties. *Brain Res* 1986;377:147-154.

29. Schmued L, Kyriakidis K, Heimer L. In vivo anterograde and retrograde axonal transport of the fluorescent rhodamine-dextran-amine, Fluoro-Ruby, within the CNS. *Brain Res* 1990;526:127-134.
30. Novikova L, Novikov L, Kellerth JO. Persistent neuronal labeling by retrograde fluorescent tracers: a comparison between Fast Blue, Fluoro-Gold and various dextran conjugates. *Journal of Neuroscience Methods* 1997;74:9-15.
31. Godement P, Vanselow J, Thanos S, Bonhoeffer F. A study in developing visual systems with a new method of staining neurones and their processes in fixed tissue. *Development* 1987;101:697-713.
32. Thanos S, Bonhoeffer F. Investigations on the development and topographic order of retinotectal axons: anterograde and retrograde staining of axons and perikarya with rhodamine in vivo. *J Comp Neurol* 1983;219:420-430.
33. Thanos S, Bonhoeffer F. Axonal arborization in the developing chick retinotectal system. *J Comp Neurol* 1987;261:155-164.
34. Surguchov A, McMahan B, Masliah E, Surgucheva I. Synucleins in ocular tissues. *J Neurosci Res* 2001;65:68-77.

35. Lavedan C, Leroy E, Dehejia A, et al. Identification, localization and characterization of the human gamma-synuclein gene. *Hum Genet* 1998;103:106-112.
36. George JM. The synucleins. *Genome Biol* 2002;3:REVIEWS3002.
37. Ji H, Liu YE, Jia T, et al. Identification of a breast cancer-specific gene, BCSG1, by direct differential cDNA sequencing. *Cancer Res* 1997;57:759-764.
38. Buchman VL, Adu J, Pinon LG, Ninkina NN, Davies AM. Persyn, a member of the synuclein family, influences neurofilament network integrity. *Nat Neurosci* 1998;1:101-103.
39. Duda JE, Shah U, Arnold SE, Lee VM, Trojanowski JQ. The expression of alpha-, beta-, and gamma-synucleins in olfactory mucosa from patients with and without neurodegenerative diseases. *Exp Neurol* 1999;160:515-522.
40. Jiang Y, Liu YE, Goldberg ID, Shi YE. Gamma synuclein, a novel heat-shock protein-associated chaperone, stimulates ligand-dependent estrogen receptor alpha signaling and mammary tumorigenesis. *Cancer Res* 2004;64:4539-4546.

41. Surgucheva I, Weisman AD, Goldberg JL, Shnyra A, Surguchov A. Gamma-synuclein as a marker of retinal ganglion cells. *Mol Vis* 2008;14:1540-1548.
42. Mu X, Beremand PD, Zhao S, et al. Discrete gene sets depend on POU domain transcription factor Brn3b/Brn-3.2/POU4f2 for their expression in the mouse embryonic retina. *Development* 2004;131:1197-1210.
43. Kwong JM, Quan A, Kyung H, Piri N, Caprioli J. Quantitative analysis of retinal ganglion cell survival with Rbpms immunolabeling in animal models of optic neuropathies. *Invest Ophthalmol Vis Sci* 2011;52:9694-9702.
44. Huang W, Fileta J, Guo Y, Grosskreutz CL. Downregulation of Thy1 in retinal ganglion cells in experimental glaucoma. *Curr Eye Res* 2006;31:265-271.
45. Schnitzer J, Schachner M. Expression of Thy-1, H-2, and NS-4 cell surface antigens and tetanus toxin receptors in early postnatal and adult mouse cerebellum. *J Neuroimmunol* 1981;1:429-456.
46. McKenzie JL, Fabre JW. Distribution of Thy-1 in human brain: immunofluorescence and absorption analyses with a monoclonal antibody. *Brain Res* 1981;230:307-316.

47. Barclay AN. Localization of the Thy-1 antigen in the cerebellar cortex of rat brain by immunofluorescence during postnatal development. *J Neurochem* 1979;32:1249-1257.
48. Pruss RM. Thy-1 antigen on astrocytes in long-term cultures of rat central nervous system. *Nature* 1979;280:688-690.
49. Perry VH, Morris RJ, Raisman G. Is Thy-1 expressed only by ganglion cells and their axons in the retina and optic nerve? *J Neurocytol* 1984;13:809-824.
50. Schlamp CL, Johnson EC, Li Y, Morrison JC, Nickells RW. Changes in Thy1 gene expression associated with damaged retinal ganglion cells. *Mol Vis* 2001;7:192-201.
51. Osborne NN, Larsen AK. Antigens associated with specific retinal cells are affected by ischaemia caused by raised intraocular pressure: effect of glutamate antagonists. *Neurochem Int* 1996;29:263-270.
52. Nash MS, Osborne NN. Assessment of Thy-1 mRNA levels as an index of retinal ganglion cell damage. *Invest Ophthalmol Vis Sci* 1999;40:1293-1298.
53. Barnstable CJ, Drager UC. Thy-1 antigen: a ganglion cell specific marker in rodent retina. *Neuroscience* 1984;11:847-855.
54. Xiang M, Zhou L, Macke JP, et al. The Brn-3 family of POU-domain factors: primary structure, binding specificity, and expression in subsets of

- retinal ganglion cells and somatosensory neurons. *J Neurosci* 1995;15:4762-4785.
55. Badea TC, Cahill H, Ecker J, Hattar S, Nathans J. Distinct roles of transcription factors brn3a and brn3b in controlling the development, morphology, and function of retinal ganglion cells. *Neuron* 2009;61:852-864.
 56. Quina LA, Pak W, Lanier J, et al. Brn3a-expressing retinal ganglion cells project specifically to thalamocortical and collicular visual pathways. *J Neurosci* 2005;25:11595-11604.
 57. Galindo-Romero C, Aviles-Trigueros M, Jimenez-Lopez M, et al. Axotomy-induced retinal ganglion cell death in adult mice: quantitative and topographic time course analyses. *Exp Eye Res* 2011;92:377-387.
 58. Chauhan BC, Stevens KT, Levesque JM, et al. Longitudinal in vivo imaging of retinal ganglion cells and retinal thickness changes following optic nerve injury in mice. *PLoS One* 2012;7:e40352.
 59. Leung CK, Lindsey JD, Crowston JG, Lijia C, Chiang S, Weinreb RN. Longitudinal profile of retinal ganglion cell damage after optic nerve crush with blue-light confocal scanning laser ophthalmoscopy. *Invest Ophthalmol Vis Sci* 2008;49:4898-4902.

60. Leung CK, Weinreb RN, Li ZW, et al. Long-term in vivo imaging and measurement of dendritic shrinkage of retinal ganglion cells. *Invest Ophthalmol Vis Sci* 2011;52:1539-1547.
61. Liu X, Grishanin RN, Tolwani RJ, et al. Brain-derived neurotrophic factor and TrkB modulate visual experience-dependent refinement of neuronal pathways in retina. *J Neurosci* 2007;27:7256-7267.
62. Chalupa LM. Developing dendrites demonstrate unexpected specificity. *Neuron* 2006;52:567-568.
63. Morgan J, Huckfeldt R, Wong RO. Imaging techniques in retinal research. *Exp Eye Res* 2005;80:297-306.
64. Walsh MK, Quigley HA. In vivo time-lapse fluorescence imaging of individual retinal ganglion cells in mice. *J Neurosci Methods* 2008;169:214-221.
65. Feng G, Mellor RH, Bernstein M, et al. Imaging neuronal subsets in transgenic mice expressing multiple spectral variants of GFP. *Neuron* 2000;28:41-51.
66. Leung CK, Lindsey JD, Crowston JG, et al. In vivo imaging of murine retinal ganglion cells. *J Neurosci Methods* 2008;168:475-478.

67. Raymond ID, Pool AL, Vila A, Brecha NC. A Thy1-CFP DBA/2J mouse line with cyan fluorescent protein expression in retinal ganglion cells. *Vis Neurosci* 2009;26:453-465.
68. Berkelaar M, Clarke DB, Wang YC, Bray GM, Aguayo AJ. Axotomy results in delayed death and apoptosis of retinal ganglion cells in adult rats. *J Neurosci* 1994;14:4368-4374.
69. Villegas-Perez MP, Vidal-Sanz M, Rasminsky M, Bray GM, Aguayo AJ. Rapid and protracted phases of retinal ganglion cell loss follow axotomy in the optic nerve of adult rats. *J Neurobiol* 1993;24:23-36.
70. Xu HP, Tian N. Retinal ganglion cell dendrites undergo a visual activity-dependent redistribution after eye opening. *J Comp Neurol* 2007;503:244-259.
71. Dijk F, Kraal-Muller E, Kamphuis W. Ischemia-induced changes of AMPA-type glutamate receptor subunit expression pattern in the rat retina: a real-time quantitative PCR study. *Invest Ophthalmol Vis Sci* 2004;45:330-341.
72. Chauhan BC, LeVatte TL, Jollimore CA, et al. Model of endothelin-1-induced chronic optic neuropathy in rat. *Invest Ophthalmol Vis Sci* 2004;45:144-152.

73. Samsel PA, Kisiswa L, Erichsen JT, Cross SD, Morgan JE. A novel method for the induction of experimental glaucoma using magnetic microspheres. *Invest Ophthalmol Vis Sci* 2011;52:1671-1675.
74. Levkovitch-Verbin H, Quigley HA, Martin KR, Valenta D, Baumrind LA, Pease ME. Translimbal laser photocoagulation to the trabecular meshwork as a model of glaucoma in rats. *Invest Ophthalmol Vis Sci* 2002;43:402-410.
75. Morrison JC, Moore CG, Deppmeier LM, Gold BG, Meshul CK, Johnson EC. A rat model of chronic pressure-induced optic nerve damage. *Exp Eye Res* 1997;64:85-96.
76. Agudo M, Perez-Marin MC, Lonngren U, et al. Time course profiling of the retinal transcriptome after optic nerve transection and optic nerve crush. *Mol Vis* 2008;14:1050-1063.
77. Chierzi S, Strettoi E, Cenni MC, Maffei L. Optic nerve crush: axonal responses in wild-type and bcl-2 transgenic mice. *J Neurosci* 1999;19:8367-8376.
78. Vidal-Sanz M, Lafuente M, Sobrado-Calvo P, et al. Death and neuroprotection of retinal ganglion cells after different types of injury. *Neurotox Res* 2000;2:215-227.

79. Osborne NN, Ugarte M, Chao M, et al. Neuroprotection in relation to retinal ischemia and relevance to glaucoma. *Surv Ophthalmol* 1999;43 Suppl 1:S102-128.
80. Dreyer EB, Zurakowski D, Schumer RA, Podos SM, Lipton SA. Elevated glutamate levels in the vitreous body of humans and monkeys with glaucoma. *Arch Ophthalmol* 1996;114:299-305.
81. Luo X, Heidinger V, Picaud S, et al. Selective excitotoxic degeneration of adult pig retinal ganglion cells in vitro. *Invest Ophthalmol Vis Sci* 2001;42:1096-1106.
82. Sucher NJ, Lipton SA, Dreyer EB. Molecular basis of glutamate toxicity in retinal ganglion cells. *Vision Res* 1997;37:3483-3493.
83. Georgiou AL, Guo L, Cordeiro MF, Salt TE. Changes in NMDA receptor contribution to synaptic transmission in the brain in a rat model of glaucoma. *Neurobiol Dis* 2010;39:344-351.
84. Fournier AE, Beer J, Arregui CO, Essagian C, Aguayo AJ, McKerracher L. Brain-derived neurotrophic factor modulates GAP-43 but not T alpha1 expression in injured retinal ganglion cells of adult rats. *J Neurosci Res* 1997;47:561-572.
85. Nickells RW. Retinal ganglion cell death in glaucoma: the how, the why, and the maybe. *J Glaucoma* 1996;5:345-356.

86. Cui Q, Harvey AR. At least two mechanisms are involved in the death of retinal ganglion cells following target ablation in neonatal rats. *J Neurosci* 1995;15:8143-8155.
87. Mansour-Robaey S, Clarke DB, Wang YC, Bray GM, Aguayo AJ. Effects of ocular injury and administration of brain-derived neurotrophic factor on survival and regrowth of axotomized retinal ganglion cells. *Proc Natl Acad Sci U S A* 1994;91:1632-1636.
88. Gao H, Qiao X, Hefti F, Hollyfield JG, Knusel B. Elevated mRNA expression of brain-derived neurotrophic factor in retinal ganglion cell layer after optic nerve injury. *Invest Ophthalmol Vis Sci* 1997;38:1840-1847.
89. Bodeutsch N, Thanos S. Migration of phagocytotic cells and development of the murine intraretinal microglial network: an in vivo study using fluorescent dyes. *Glia* 2000;32:91-101.
90. Cheng L, Sapielha P, Kittlerova P, Hauswirth WW, Di Polo A. TrkB gene transfer protects retinal ganglion cells from axotomy-induced death in vivo. *J Neurosci* 2002;22:3977-3986.
91. Holtkamp GM, Kijlstra A, Peek R, de Vos AF. Retinal pigment epithelium-immune system interactions: cytokine production and cytokine-induced changes. *Prog Retin Eye Res* 2001;20:29-48.

92. Nickells RW. Apoptosis of retinal ganglion cells in glaucoma: an update of the molecular pathways involved in cell death. *Surv Ophthalmol* 1999;43 Suppl 1:S151-161.
93. Gastinger MJ, Singh RS, Barber AJ. Loss of cholinergic and dopaminergic amacrine cells in streptozotocin-diabetic rat and Ins2Akita-diabetic mouse retinas. *Invest Ophthalmol Vis Sci* 2006;47:3143-3150.
94. Heck MM, Earnshaw WC. Topoisomerase II: A specific marker for cell proliferation. *J Cell Biol* 1986;103:2569-2581.
95. Higashide T, Kawaguchi I, Ohkubo S, Takeda H, Sugiyama K. In vivo imaging and counting of rat retinal ganglion cells using a scanning laser ophthalmoscope. *Invest Ophthalmol Vis Sci* 2006;47:2943-2950.
96. Levkovitch-Verbin H, Harris-Cerruti C, Groner Y, Wheeler LA, Schwartz M, Yoles E. RGC death in mice after optic nerve crush injury: oxidative stress and neuroprotection. *Invest Ophthalmol Vis Sci* 2000;41:4169-4174.
97. Xiang M, Zhou H, Nathans J. Molecular biology of retinal ganglion cells. *Proc Natl Acad Sci U S A* 1996;93:596-601.
98. Galindo-Romero C, Valiente-Soriano FJ, Jimenez-Lopez M, et al. Effect of brain-derived neurotrophic factor on mouse axotomized retinal ganglion cells and phagocytic microglia. *Invest Ophthalmol Vis Sci* 2013;54:974-985.

99. Chao M, Casaccia-Bonnel P, Carter B, Chittka A, Kong H, Yoon SO. Neurotrophin receptors: mediators of life and death. *Brain Res Brain Res Rev* 1998;26:295-301.
100. Ma L, Lei L, Eng SR, Turner E, Parada LF. Brn3a regulation of TrkA/NGF receptor expression in developing sensory neurons. *Development* 2003;130:3525-3534.
101. Carmignoto G, Maffei L, Candeo P, Canella R, Comelli C. Effect of NGF on the survival of rat retinal ganglion cells following optic nerve section. *J Neurosci* 1989;9:1263-1272.
102. Kielczewski JL, Pease ME, Quigley HA. The effect of experimental glaucoma and optic nerve transection on amacrine cells in the rat retina. *Invest Ophthalmol Vis Sci* 2005;46:3188-3196.
103. Raymond ID, Vila A, Huynh UC, Brecha NC. Cyan fluorescent protein expression in ganglion and amacrine cells in a thy1-CFP transgenic mouse retina. *Mol Vis* 2008;14:1559-1574.
104. Dabin I, Barnstable CJ. Rat retinal Muller cells express Thy-1 following neuronal cell death. *Glia* 1995;14:23-32.
105. Chaudhary P, Ahmed F, Quebada P, Sharma SC. Caspase inhibitors block the retinal ganglion cell death following optic nerve transection. *Brain Res Mol Brain Res* 1999;67:36-45.

APPENDIX A : SUPPLEMENTARY FIGURE

After ON injury Thy1-CFP expression changes from both cytoplasmic and nuclear to solely cytoplasmic in some cells. This can be viewed in supplementary figure A.1. Thy1-CFP expression contours the nucleus of cells which are stained with To-Pro and is not expressed in the nucleus.

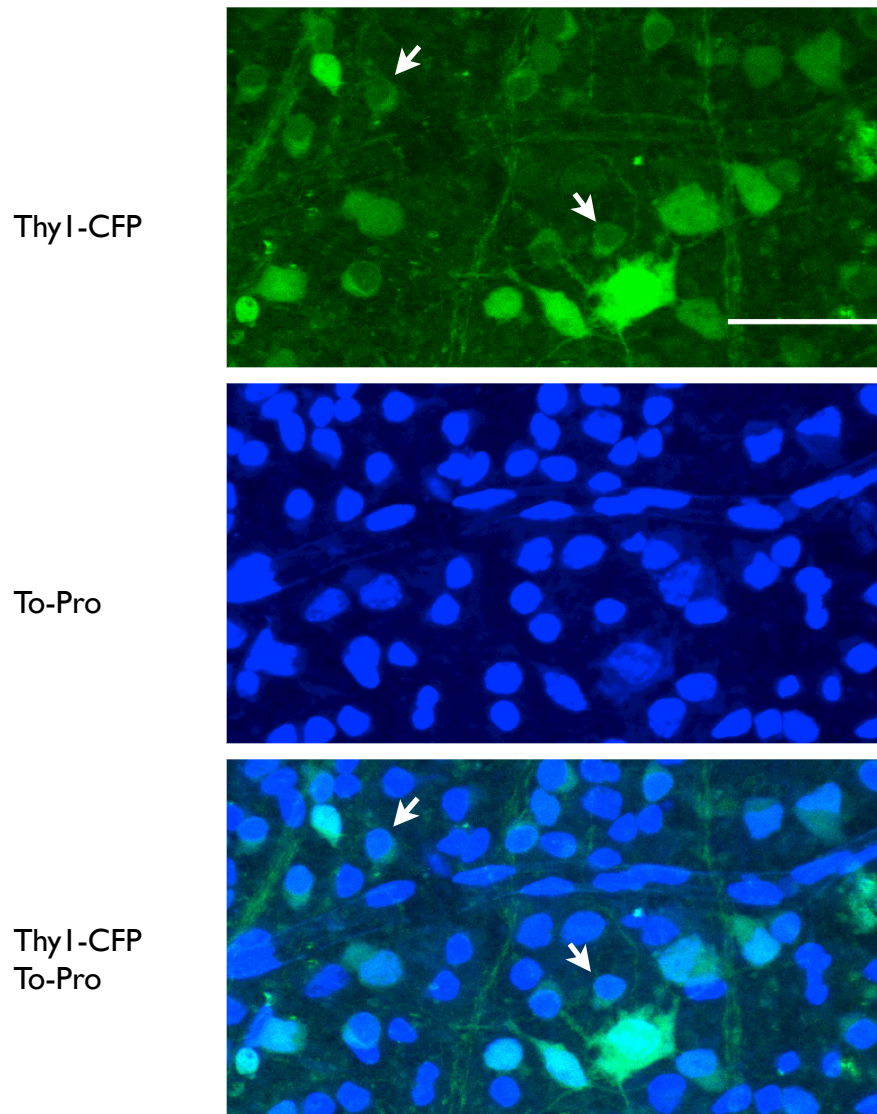


Figure A.1 - Cytoplasmic expression of Thy1-CFP in Thy1-CFP transgenic wholemount retina

Thy1-CFP is expressed solely in the cytoplasm of some cells (arrow) of 5 day ONT wholemount retina.

APPENDIX B : COPYRIGHT PERMISSIONS

1. Image shown in figure 1.1 B of this thesis was modified and appears courtesy of GLIA:

Bodeutsch N, Thanos S. Migration of phagocytotic cells and development of the murine intraretinal microglial network: An in vivo study using fluorescent dyes. *GLIA* 2000;32:91-101.

John Wiley and Sons have granted permission for use of this figure.

2. Image shown in figure 1.2 was obtained from Neuroscience:

Purves et al. Neuroscience 2ed. p.229 figure 11.4 B

Sinauer Associate, Inc. have granted permission for the use of this figure.

JOHN WILEY AND SONS LICENSE TERMS AND CONDITIONS

This is a License Agreement between Julie M Levesque ("You") and John Wiley and Sons ("John Wiley and Sons") provided by Copyright Clearance Center ("CCC"). The license consists of your order details, the terms and conditions provided by John Wiley and Sons, and the payment terms and conditions.

All payments must be made in full to CCC. For payment instructions, please see information listed at the bottom of this form.

License Number	3171410116027
License date	Jun 17, 2013
Licensed content publisher	John Wiley and Sons
Licensed content publication	GLIA
Licensed content title	Migration of phagocytotic cells and development of the murine intraretinal microglial network: An in vivo study using fluorescent dyes
Licensed copyright line	Copyright © 2000 Wiley-Liss, Inc.
Licensed content author	Nicole Bodeutsch,Solon Thanos
Licensed content date	Aug 31, 2000
Start page	91
End page	101
Type of use	Dissertation/Thesis

Requestor type	University / Academic
Format	Print and electronic
Portion	Figure / table
Number of figures / tables	1
Original Wiley figure / table number(s)	I would like to use Figure 1 A found on page 93 of the journal article "Migration of phagocytotic cells and development of the murine intraretinal microglial network: An in vivo study using fluorescent dyes" in my thesis
Will you be translating?	No
Total	0.00 USD

Terms and Conditions

TERMS AND CONDITIONS

This copyrighted material is owned by or exclusively licensed to John Wiley & Sons, Inc. or one of its group companies (each a "Wiley Company") or a society for whom a Wiley Company has exclusive publishing rights in relation to a particular journal (collectively "WILEY"). By clicking "accept" in connection with completing this licensing transaction, you agree that the following terms and conditions apply to this transaction (along with the billing and payment terms and conditions established by the Copyright Clearance Center Inc., ("CCC's Billing and Payment terms and conditions"), at the time that you opened your RightsLink account (these are available at any time at <http://myaccount.copyright.com>).

Terms and Conditions

1. The materials you have requested permission to reproduce (the "Materials") are protected by copyright.
2. You are hereby granted a personal, non-exclusive, non-sublicensable, non-transferable, worldwide, limited license to reproduce the Materials for the purpose specified in the licensing process. This license is for a one-time use only with a maximum distribution equal to the number that you identified in the licensing process. Any form of republication granted by this license must be completed within two years of the date of the grant of this license (although copies prepared before may be distributed thereafter). The Materials shall not be used in any other manner or for any other purpose. Permission is granted subject to an appropriate acknowledgement given to the author, title of the material/book/journal and the publisher. You shall also duplicate the copyright notice that appears in the Wiley publication in your use of the Material. Permission is also granted on the understanding that nowhere in the text is a previously published source acknowledged for all or part of this Material. Any third party material is expressly excluded from this permission.
3. With respect to the Materials, all rights are reserved. Except as expressly granted by the terms of the license, no part of the Materials may be copied, modified, adapted (except for minor reformatting required by the new Publication), translated, reproduced, transferred or distributed, in any form or by any means, and no derivative works may be made based on the Materials without the prior permission of the respective copyright owner. You may not alter, remove or suppress in any manner any copyright, trademark or other notices displayed by the Materials. You may not license, rent, sell, loan, lease, pledge, offer as security, transfer or assign the Materials, or any of the rights granted to you hereunder to any other person.
4. The Materials and all of the intellectual property rights therein shall at all times remain the exclusive property of John Wiley & Sons Inc or one of its related companies (WILEY) or their respective licensors, and your interest therein is only that of having possession of and the right to reproduce the Materials pursuant to Section 2 herein during the continuance of this Agreement. You agree that you own no right, title or interest in or to the Materials or any of the intellectual property rights therein. You shall have no rights hereunder other than the license as provided for above in Section 2. No right, license or interest to any trademark, trade name, service mark or other branding ("Marks") of WILEY or its licensors is granted hereunder, and you agree that you shall not assert any such right, license or interest with respect thereto.

If you would like to pay for this license now, please remit this license along with your payment made payable to "COPYRIGHT CLEARANCE CENTER" otherwise you will be invoiced within 48 hours of the license date. Payment should be in the form of a check or money order referencing your account number and this invoice number RLNK501044757.

Once you receive your invoice for this order, you may pay your invoice by credit card. Please follow instructions provided at that time.

Make Payment To:
Copyright Clearance Center
Dept 001
P.O. Box 843006
Boston, MA 02284-3006

For suggestions or comments regarding this order, contact RightsLink Customer Support: customercare@copyright.com or +1-877-622-5543 (toll free in the US) or +1-978-646-2777.

Gratis licenses (referencing \$0 in the Total field) are free. Please retain this printable license for your reference. No payment is required.



SINAUER ASSOCIATES, Inc. • Publishers • P.O. Box 407 • Sunderland, MA 01375-0407

Telephone: (413) 549-4300
Fax: (413) 549-1118
E-mail: orders@sinauer.com

PERMISSIONS AGREEMENT

June 24, 2013

Permission granted to:
Julie Levesque
Dalhousie University
Physiology and Biophysics
5850 College Street
Halifax, NS
CANADA

FAX: 902-494-6309

Material to be reproduced:
Purves et al: *Neuroscience, Second Edition*
Figure 11.4 B, page 229

To be reproduced in the work:
Julie Levesque's Master of Science Thesis entitled "The Analysis of Brn3a and Thy1-CFP as Potential Markers of Retinal Ganglion Cells after Optic Nerve Injury in Mice" to be published by the Library and Archives of Canada (print and electronic)

Sinauer Associates owns copyright to the material described above and hereby grants permission for the one-time use of the material as specified, and for nonexclusive world rights provided that full and appropriate credit is given to the original source and that the work is for NON-COMMERCIAL use only. Please request permission for further use in subsequent editions, translations, or revisions of the work.

[Redacted Signature]

Sherri L. Ellsworth
Permissions Coordinator

[Redacted Date]

Date

Please acknowledge your acceptance of these terms by signing one copy of this form and returning it to Sinauer Associates. Permission Agreement is not valid until signed by applicant and received by Sinauer Associates.

[Redacted Signature]

Signature of Applicant

[Redacted Date]

Date